CHAPTER 10

# Time-Frequency Signal Transforms

Time-frequency signal transforms combine traditional Fourier transform signal spectrum information with a time location variable. There results a two-dimensional transformed signal having an independent frequency variable and an independent time variable. Such a signal operation consititutes the first example of a *mixed-domain signal transform*.

Earlier discussions, many applications, and indeed our entire theoretical approach considered signal analysis strategies based upon time, frequency, or scale. *Time-domain* methods are adequate for tasks such as edge detection, elementary segmentation, correlation-based shape recognition, and some texture analysis problems. But in many situations, the inherent periodicity within signal regions pushes us toward a decomposition of the signal according to its *frequency content*.

Frequency—or *spectral*—analysis enters the picture as a tool for discovering a signal's sinusoidal behavior. But this is an inherently global approach. Standard spectral analysis methods, which the Fourier transform in both its analog and discrete guises completely typifies, suffer signal interpretation difficulties when oscillations of interest exist only within a limited signal region. As we discovered in the previous chapter, windowing the signal improves local spectral estimates.

Another approach takes a standard signal shape element, shrinks or expands it into a library of local signal forms, and then considers how well different regions of the signal match one or another such local prototypes. This is an analysis based on *signal scale*. The first chapter provided tutorial sketches of all three approaches. Later chapters built up theoretical tools, demonstrated their applications, and discovered some limitations. So far we have worked out much theory and many applications involving time- and frequency-domain techniques, but we have not formalized the notion of a scale-based analysis.

We now have a sufficient theoretical foundation and practical motivation to explore combined methods. The idea is to mix time-domain methods with either the frequency- or the scale-domain approach. Both combinations provide avenues for structural signal decomposition. The theory is rich and powerful. It has developed rapidly in the last few years. We elect to start with the methods that are most intuitive and, in fact, historically prior: the time-frequency transform techniques.

*Signal Analysis: Time, Frequency, Scale, and Structure*, by Ronald L. Allen and Duncan W. Mills
ISBN: 0-471-23441-9 

The Fourier transform is the fundamental tool for frequency-domain signal analysis. It does allow us to solve some problems that confound time-domain techniques. The mapping $X(\omega) = \mathcal{F}[x(t)]$ lays out the frequency content of a signal $x(t)$, albeit in complex values, and its large magnitude $|X(\omega)|$ indicates the presence of a strong sinusoidal component of frequency $\omega$ radians per second in $x(t)$. We can construct filters and assemble them into filter banks in order to search for spectral components in frequency ranges of interest. All such strategies stem from the convolution theorem, which identifies time-domain convolution—and hence linear, time-invariant processing—with frequency-domain multiplication. The caveat is that standard Fourier techniques depend on a knowledge of the entire time-domain extent of a signal. Even the filter bank highlights ranges of frequencies that existed in the signal for all time: past, present, and future.

But many signals have salient periodic features only over limited time intervals. Although a global analysis is theoretically possible, it may not be practical or efficient. Consider, for example, an orchestra that must play a two-hour symphony, and let us fancy that the composer employs a Fourier transform music style that assigns each instrument just one tone for the entire duration of the performance. The superposition of the various tones, each constantly emitted for two hours by the musicians, does indeed produce the composer's envisioned piece. Of course, the orchestra has but a finite number of musicians, so what is in effect here is really a Fourier series music synthesis. The conductor's job is greatly simplified, perhaps reducing to a few minor pre-concert modifications to the chosen tones. Concert hall owners could well be drawn to encourage such an artform; it would allow them to hire low-paid, unskilled musicians and cut the conductor's hours. The problem of course is that it would be nearly impossible to get the right tonal mix to compose a Fourier symphony. A few hertz too far in this or that direction generates not a symphony but a cacophany instead. Localizing the tones works much better. The composer uses a local frequency synthesis, assigning tones to moments in time; the musicians—they must be artists of supreme skill and dedication—read the musical notation and effect the appropriate, time-limited tones; and the conductor orchestrates the entire ensemble, settting the tempo and issuing direction as the performance proceeds. The composition of the signal in terms of time-localized tones is far easier to understand, communicate, replicate, and modify.[1]

## 10.1 GABOR TRANSFORMS

The previous chapter studied the strategy of time-limiting, or windowing, a signal before calculating its spectrum. This technique—of which there are many variants—furnishes better estimates of the signal's spectrum, because it restricts the signal

[1]Interestingly enough, there is a musical composition style that combines long-term tones to produce desired harmonies: "spectral music." Its resonances evolve slowly, retain a distinctly synthetic character, and thereby differ greatly from traditional 12-tone music. French composer Gérard Grisey (1946–1998), winner of the Rome prize, pioneered this form.

values to those over which the relevant oscillatory signal features should appear. The spectrogram of the signal $x(t)$ relative to the window function $w(t)$ is the squared magnitude of the Fourier transform of the product $s(t) = x(t)w(t)$: $|\mathcal{F}[s(t)]|^2 = |\mathcal{F}[x(t)w(t)]|^2 \geq 0$. Applications can therefore compare or threshold spectrogram values in order to decide whether one frequency is more significant than another or whether an individual frequency is significant, respectively. With the spectrogram, of course, the application design may need to search through possible time locations as well as through possible frequency ranges when seeking local spectral components. That is, Fourier applications tend to be one-dimensional, in contrast to short-time Fourier applications, which are inherently two-dimensional in nature.

We first explore the basic ideas of the transform, working with its original analog formulation. Section 10.1.2 develops the idea of the time-frequency plane. The Gabor transform partitions the $(t, \omega)$-plane into equally sized regions, which Gabor dubbed "logons," from the ancient Greek word *logos*, meaning *word* or *account*. Logons are now generally called *time-frequency windows* or *atoms*. These time-frequency cells contain the signal's local frequency information, and their derivation provides a structural interpretation. Time-frequency windows with smaller $t$-dimensions provide higher signal time resolution, and those with tighter $\omega$-dimensions have better signal frequency resolution. So small time-frequency cells are good, but we will eventually discover that a lower limit on cell size exists.

We generalize the Gabor transform further in Section 10.2 to include general window functions. It is proven, however, that among the many short-time Fourier techniques, the Gabor transform has smallest time-frequency windows. A Gaussian window, therefore, provides a joint time and frequency resolution superior to all other window functions: Hanning, Hamming, Kaiser, Bartlett, and so on. Finally, we derive the discretization of the Gabor transform in Section 10.3.

The Gabor transform uses a Gaussian window to create a window of time from which the spectrum of the local signal values are computed. Gaussian signals possess a magic property: Their Fourier transform is also a Gaussian. And this fact imparts an utterly elegant mathematical development to the study of the transform. But elegance is not the only reason for starting our study of short-time Fourier methods with the Gabor transform. In a sense that we will make precise momentarily, the Gabor transform is in fact the optimal short-time Fourier transform.

Carefully note that the width of the Gaussian window, as measured by its variance, is fixed throughout the transformation. Allowing it to vary has proven useful in many applications, but doing so undermines the essence of the transform as a time-frequency tool. It could indeed be argued that varying the window width makes it more like a time-scale transform. The location of the time-domain window, on the other hand, does change and becomes a variable of the two-dimensional, complex valued, Gabor transform function.

After Gabor's original paper [1], occasional research contributions related to Gabor transforms appeared sporadically in the scientific and engineering literature over the next 30 years. Interest in mixed-domain transforms accelerated with the discovery of the wavelet transform in the mid-1980s. There are now a variety of tutorial articles [2–4] on time-frequency transforms. Books devoted to Gabor analysis and

the broader category of time-frequency transforms include Refs. 5–9. Their introductory chapters and those concentrating on the short-time Fourier transforms—of which the Gabor transform, by using a Gaussian window, is a particular case—are the most accessible. Treatments of time-scale transforms, or wavelets, often contain material introducing time-frequency transforms; we have found the material in Refs. 10–13 to be particularly useful.

### 10.1.1 Introduction

The Gabor transform picks a particular time-limiting window—the Gaussian—and generalizes the windowed spectrum computation into a full signal transform. The goal is to capture both the frequency components of a signal and their time locality in the transform equation. Of course, a Gaussian window is not truly finite in extent; its decay is so fast, however, that as a practical computation matter it serves the purpose of localizing signal values. Finite windows are possible with species [14–18].

**Definition (Gabor Transform).** Let $g(t)$ be some Gaussian of zero mean:

$$g(t) = Ae^{-Bt^2}, \tag{10.1}$$

where $A, B > 0$. If $x(t) \in L^2(\mathbb{R})$ is an analog signal, then its *Gabor transform*, written $X_g(\mu, \omega)$, is the radial Fourier transform of the product $x(t)g(t - \mu)$:

$$X_g(\mu, \omega) = \int_{-\infty}^{\infty} x(t) e^{-\frac{(t-\mu)^2}{2\sigma^2}} e^{-j\omega t} dt. \tag{10.2}$$

We will occasionally use the "fancy $G$" notation for the Gabor transform: $X_g(\mu, \omega) = \mathcal{G}_g[x(t)](\mu, \omega)$. The windowing function $g(t)$ in (10.1) remains fixed for the transform. If its parameters are understood—for instance, it may be the Gaussian of zero mean and standard deviation $\sigma > 0$—then we may drop the subscript $g$ for the windowing function.

No reader can have overlooked the fact that we define the Gabor transform for $L^2(\mathbb{R})$ signals. Analog Fourier analysis (Chapter 5) shows that square-integrable signals have Fourier transforms which are also in $L^2(\mathbb{R})$. Thus, if $x(t) \in L^2(\mathbb{R})$ and $g(t)$ is a Gaussian, then $x(t)g(t - \mu) \in L^2(\mathbb{R})$ also, and the Fourier transform integral (10.2) therefore exists. Now for each $\mu$, $\mathcal{F}[x(t)g(t - \mu)](\omega) \in L^2(\mathbb{R})$, and this will therefore enable us to find a Gabor inverse transform, or synthesis formula.

It is possible to specify a particular normalization for the Gaussian window used in the Gabor transform. For example, we might choose $\|g(t)\|_1 = 1$ or $\|g(t)\|_2 = 1$, where $\|\cdot\|_p$ is the norm in the Banach space $L^p(\mathbb{R})$ of Chapter 3. Gaussian signals belong to both spaces. Either choice makes some Gabor transform properties look

nice but not others. We generally normalize the window with respect to the $L^1(\mathbb{R})$ norm, so that our windowing functions are zero-mean Gaussians of standard deviation $\sigma > 0$, $g_{0,\sigma}(t)$:

$$X_g(\mu, \omega) = \frac{1}{\sigma\sqrt{2\pi}} \int_{-\infty}^{\infty} x(t) e^{-\frac{(t-\mu)^2}{2\sigma^2}} e^{-j\omega t} dt . \tag{10.3}$$

The exercises explore how these alternative Gabor transform normalizations affect various transform properties.

Observe that the Gabor transform, unlike the analog Fourier transform, is a function of two variables. There is a time-domain variable $\mu$, which is the center or mean of the window function, and a frequency-domain variable, $\omega$. Since a time-domain variable—namely the location of the window's center, $\mu$—is a parameter of the transform, the inverse Gabor transform involves a two-dimensional, or iterated integral. Figure 10.1 shows the Gabor transform scheme.

It is also possible to vary the width of the window, which is determined by $\sigma$, the standard deviation of the Gaussian. However, this changes the fundamental analytical nature of the transform operation, and our theory endeavors to avoid this. If $\sigma$ changes while $\omega$ remains fixed, then the effect of the transform is to find oscillatory components of radial frequency $\omega$ over signal regions of varying width. But this is the defining characteristic of a scale-based signal analysis. The size of the prototype signal changes. When $\omega$ and $\sigma$ both vary, we lapse into a hybrid scale and frequency approach. This does aid some applications. But our present purpose is to reveal the strengths and weaknesses of pure time-frequency methods, and therefore we fix $\sigma$ for each particular Gabor transform formulation.

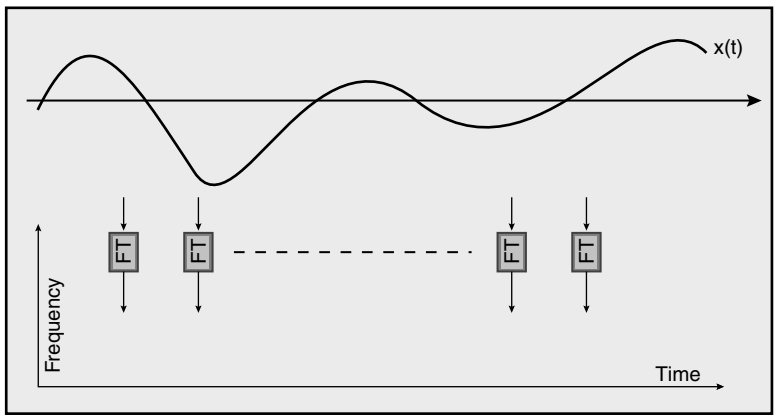


**Fig. 10.1.** The Gabor transform finds the spectral content of $x(t)$ within a Gaussian window $g(t - \mu)$. The two-dimensional transform function takes parameters $\mu$, the window's center, and $\omega$, the frequency of the exponential $\exp(j\omega t)$.

### 10.1.2 Interpretations

There are several fruitful ways to interpret the resulting Gabor transform:

- The most immediate way to visualize $X_g(\mu, \omega)$ is to see it as the Fourier transform of the windowed—and therefore essentially time-limited—signal $x(t)g(t - \mu)$.
- Secondly, in resonance with our physical concept of the Fourier transform, we can think of $X_g(\mu, \omega)$ as an inner product relation that measures the similarity of $x(t)$ to the pulse $g(t)\exp(j\omega t)$, a Gabor elementary function (GEF).
- Parseval's theorem provides yet a third interpretation: an inner product measure of the similarity of the Fourier transforms of $x(t)$ and $g(t)\exp(j\omega t)$.
- Finally, the Fourier transform's convolution theorem shows that the Gabor transform is a filtering operation on $X(\omega)$, the Fourier transform of $x(t)$.

So the idea of windowing a signal $x(t)$ with a Gaussian and making the location of the window a parameter of the transform richly interconnects concepts in signal spaces and transforms. In fact, we encounter two more interpretations of this many-faceted transform later in the chapter! But these first four carry us a long ways, so let us further investigate them.

The most immediate observation is that the Gaussian function $g(t)$ windows signal values of $x(t)$ in a neighborhood of around the point $t = \mu$. This springs right out of the definiton. The windowing effect suppresses oscillatory components of $x(t)$ distant from $t = \mu$. The Gabor transform of $x(t)$, $X_g(\mu, \omega)$, is thus the frequency content of $x(t)$ in this Gaussian-trimmed region.

Another perspective on the Gabor transform follows, if we recall that the product $g(t)\exp(-j\omega t)$ in the integrand (10.2) is the complex conjugate of a Gabor elementary function,[2] introduced in Chapter 1. Thus, if $x(t) \in L^2(\mathbb{R})$, then for each $\omega \in \mathbb{R}$, the Gabor transform integral is an inner product: $\langle x(t), g(t - \mu)\exp(j\omega t)\rangle$. Or, if the Gaussian has zero mean and standard deviation $\sigma > 0$, then $X_g(\mu, \omega) = \langle x(t), g_{\mu,\sigma}(t)\exp(j\omega t)\rangle$. Beginning with elementary vector spaces, through abstract inner product spaces, and finally with Hilbert spaces, the inner product relation continues to serve as our yardstick for establishing signal similarity. Hence, the Gabor transform $X_g(\mu, \omega)$ measures the similarity between $x(t)$ and the Gabor elementary function $g(t - \mu)\exp(j\omega t)$—an important idea which leads directly to the next point and figures prominently in the sequel.

Our third view of the Gabor transform follows from applying Parseval's formula to inner product relation:

$$\langle x(t), g(t-\mu)e^{j\omega t}\rangle = \frac{1}{2\pi}\langle X(\theta), \mathcal{F}[g(t)e^{j\omega t}]\rangle = X_g(\mu, \omega). \tag{10.4}$$

[2]Gabor actually used the Hertz formulation of the Fourier transform in his landmark 1946 paper. He applied the results to human hearing, observing that, up to about 1 kHz and independent of pulse width, we can distinguish some 50% of audible GEFs. Above that frequency, our sense rapidly deteriorates; Gabor concluded that cheaper means of transmission—although perhaps hampered by a poorer frequency, response—might replace more faithful and expensive systems [19].

Note that we are fixing ω so that the Gabor elementary function $g(t)\exp(j\omega t)$ is a pure function of t. The dummy variable for $\mathcal{F}[x(t)](\theta) = X(\theta)$ in (10.4) changes from the usual ω to avoid a conflict. Thus, the Gabor transform is a (scaled) similarity measure between the Fourier transforms of $x(t)$ and the GEF $g(t-\mu)\exp(j\omega t)$.

The convolution theorem for the radial Fourier transform provides a fourth insight into the Gabor transform. Convolution in time is equivalent to multiplication in frequency. And, reversing the transform direction, convolution in frequency corresponds to termwise multiplication in time. Therefore, if $y(t) = g(t)\exp(j\omega t)$, it follows that

$$X_g(\mu, \omega) = \langle x(t), g(t-\mu)e^{j\omega t} \rangle = \frac{1}{2\pi}(\mathrm{X}^*\mathrm{Y})(\theta) = \frac{1}{2\pi}\int_{-\infty}^{\infty} X(\zeta)Y(\theta-\zeta)\, d\zeta. \tag{10.5}$$

Gabor transforming a signal $x(t)$ is the same as filtering $X(\theta)$ with the Fourier transform of the Gabor elementary function $y(t) = g(t-\mu)\exp(j\omega t)$.

These several interpretations lead us to further study the Gaussian, the GEFs, inner products, and convolution operations in both the time and frequency domains.

### 10.1.3 Gabor Elementary Functions

By now, Gabor elementary functions $y(t) = g(t-\mu)\exp(j\omega t)$ are quite familiar. We introduced them as early as Chapter 1, noted their applicability to spectral analysis of signal texture in Chapter 4, and considered them as amplitude-modulated sinusoidal carrier signals in Chapter 5. They have other names, too: Gabor atoms or windowed Fourier atoms. Now we have seen that $y(t)$ is a signal *model*—or *prototype*—to which the Gabor transform compares $x(t)$. This section continues our investigation of these important signal prototypes.

In the time domain, $y(t) = g(t)\exp(j\omega t)$ is a complex exponential that is amplitude modulated by a Gaussian $g(t)$. The Gaussian envelope—let us say it has mean μ and standard deviation σ—$g_{\mu,\sigma}(t)$ amplitude modulates the real and imaginary parts of exp(jωt). From a communications theory standpoint, the latter are sinusoidal carrier signals. The real part of $y(t)$ is cos(ω$t$)-modulated by $g_{\mu,\sigma}(t)$; hence, Real$[g_{\mu,\sigma}(t)\exp(j\omega t)]$ is even. And its imaginary part is sin(ωt) inside the same envelope, making Imag$[g_{\mu,\sigma}(t)\exp(j\omega t)]$ an odd signal. The GEFs exhibit more or less oscillations as the frequency of the exponential carrier signal increases or decreases, respectively, under a modulating Gaussian pulse of constant width. This changes the shape of the model signal as in Figure 10.2.

Altering the spread of the Gaussian envelope (given by its width parameter σ) while leaving ω constant also produces prototype signals of different shapes. The large sinusoidal oscillations persist over a wider time-domain region (Figure 10.3). This behavior typifies time-scale analysis methods, which depend upon comparing source signals with models of variable time-domain extent, but similar shape. Unless we tie the frequency ω to the Gaussian's standard deviation σ, then the Gabor elementary functions will exhibit different basic shapes as σ changes. This

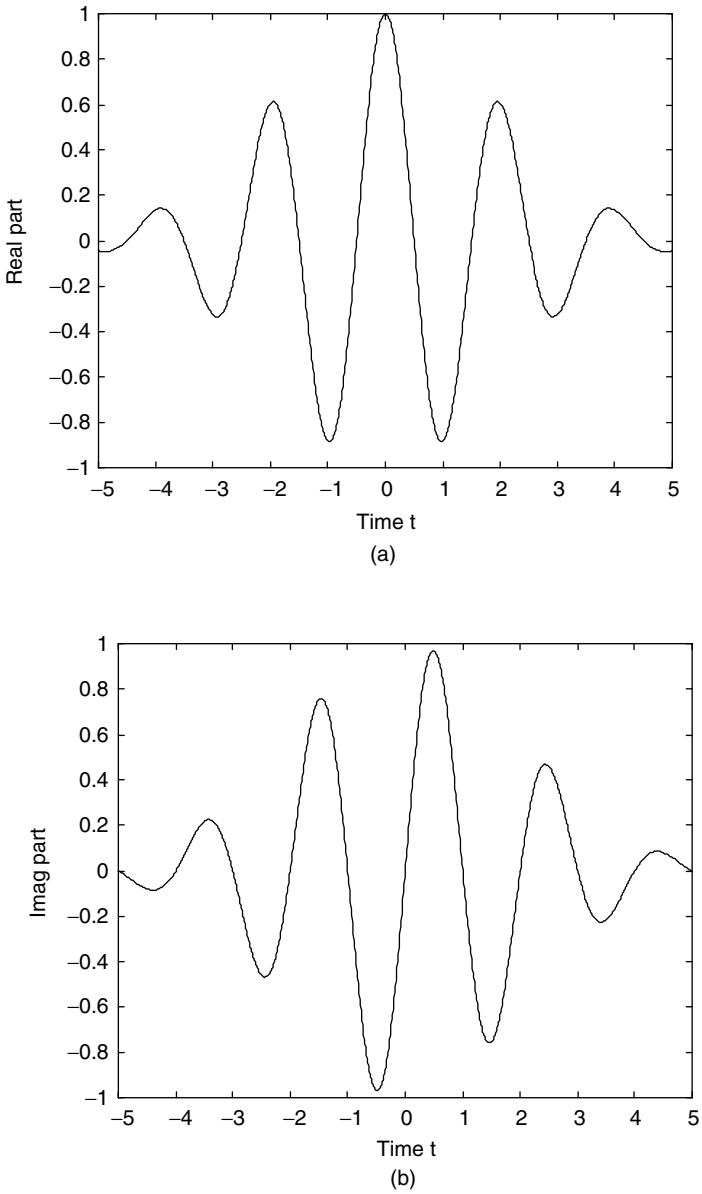


**Fig. 10.2.** Gabor elementary functions. The cosine term (a) represents the real part of a GEF and is an even signal. The sine term represents the imaginary part and is an odd signal (b). Panels (c) and (d) show the effect of frequency doubling.

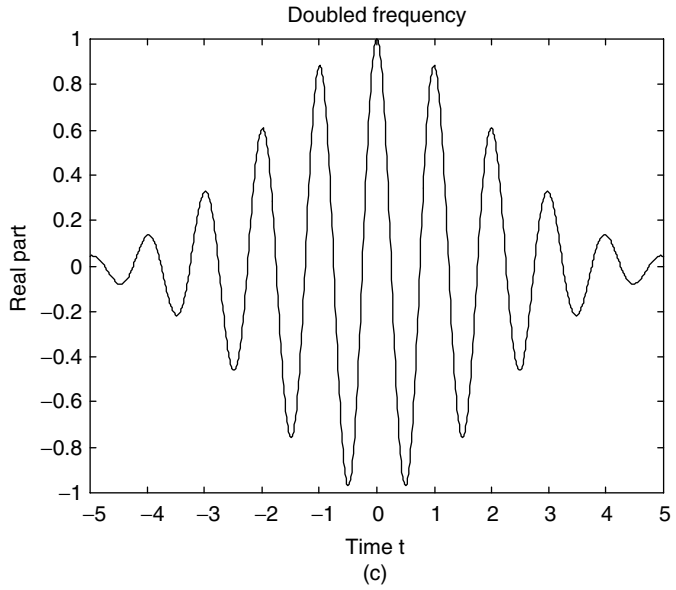


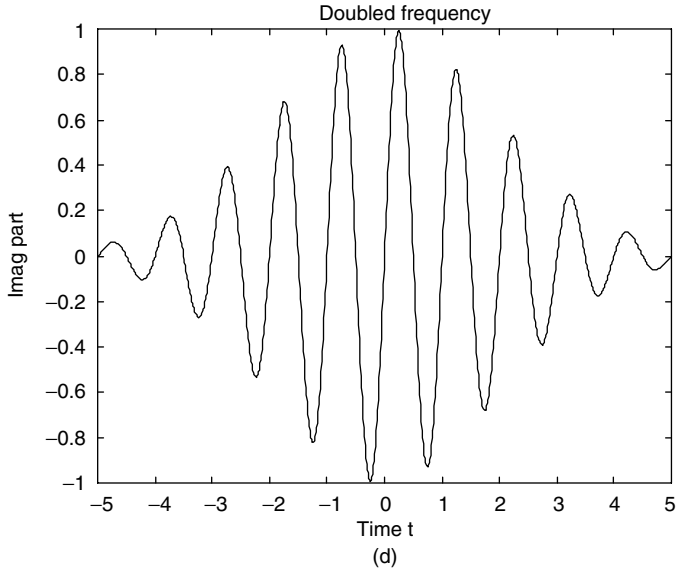


**Fig. 10.2** (*Continued*)

technique is often called the *adaptive Gabor transform*. But a bona fide time-frequency transform should be able to reveal all frequencies within a local signal region; we cannot mathematically link $\omega$ and $\sigma$. Consequently, to preserve the time-frequency nature of the Gabor transform and short-time Fourier tools in general, we avoid flexible windows. Time-scale transforms (Chapter 11) use dilation to

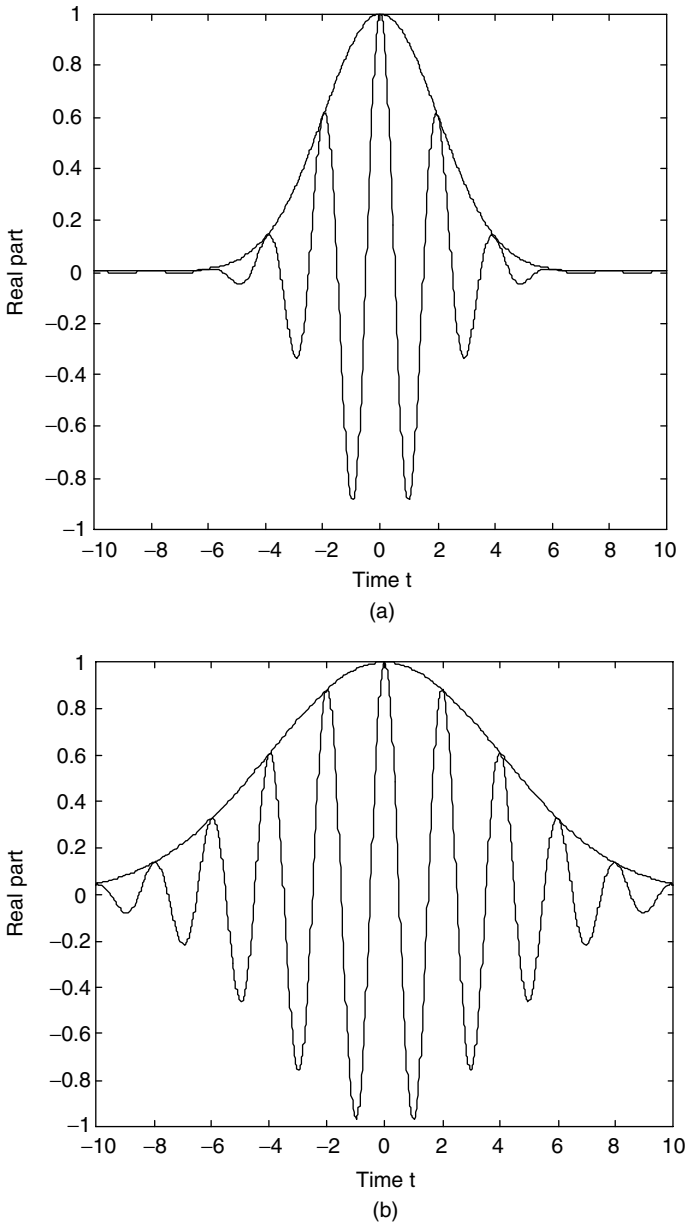


**Fig. 10.3.** Window size variation. With the radial frequency ω fixed, the shape of a Gabor elementary function signal (*a*) changes as the window expands (*b*).

maintain a basic shape while changing the size of a prototype signal. This chapter's exercises preview this idea.

Now let us consider the frequency-domain representation of Gabor elementary functions. The formula for the Fourier transform of $y(t) = g_{\mu,\sigma}(t)\exp(j\omega_0 t)$ derives from the radial Fourier transform's properties (Chapter 5).

**Proposition (Fourier Transform of Gabor Elementary Function).** Let $\sigma > 0$ and suppose $g(t) = g_{\mu,\sigma}(t)$ is the Gaussian with mean $\mu$ and standard deviation $\sigma$. Let $y(t) = g(t)\exp(j\omega_0 t)$ be a Gabor elementary function with envelope $g(t)$ and radial frequency $\omega_0$. Then

$$Y(\omega) = \frac{1}{2\pi}\exp\left[-\frac{\sigma^2}{2}(\omega-\omega_0)^2 + j(\omega-\omega_0)\mu\right]. \tag{10.6}$$

***Proof:*** In Chapter 5 we calculated the radial Fourier transform of the Gaussian; there results a Gaussian once more: $\mathcal{F}[\exp(-t^2)](\omega) = \pi^{1/2}\exp(-\omega^2/4)$. The Fourier transform properties allow us to write out the Fourier transform for $g(t) = g_{\mu,\sigma}(t)$:

$$G(\omega) = \int_{-\infty}^{\infty} g(t)e^{-j\omega t}dt = \exp\left(-\left[\frac{\sigma^2\omega^2}{2} + j\omega\mu\right]\right) \tag{10.7}$$

whose magnitude $|G(\omega)|$ is a Gaussian centered at $\omega = 0$. Applying the generalized Fourier transform handles the exponential factor: $\mathcal{F}[\exp(j\omega_0 t)](\omega) = \delta(\omega - \omega_0)$. A termwise multiplication $y(t) = x_1(t)x_2(t)$ in time has Fourier transform $Y(\omega) = X_1(\omega)*X_2(\omega)/(2\pi)$. This implies $\mathcal{F}[g(t)\exp(j\omega_0 t)] = G(\omega)*\delta(\omega-\omega_0)/(2\pi)$, the convolution of a Gaussian with a shifted Dirac delta. Making $\theta$ the integration variable for continuous-domain convolution, we compute:

$$\begin{aligned} Y(\omega) &= \mathcal{F}[g(t)e^{j\omega_0 t}] = \frac{1}{2\pi}\int_{-\infty}^{\infty}\delta(\theta-\omega_0)e^{-[\sigma^2(\omega-\theta)^2 + j(\omega-\theta)\mu]}\,d\theta \\ &= \frac{1}{2\pi}e^{-(\sigma^2(\omega-\omega_0)^2 + j(\omega-\omega_0)\mu)}. \end{aligned} \tag{10.8}$$

We use the Sifting Property of the Dirac delta in (10.8), the last expression of which is precisely the value (10.6). ■

*Remarks.* In (10.8) observe that $|Y(\omega)|$ is a scaled (amplified or attenuated) Gaussian pulse centered at $\omega = \omega_0$ in the frequency domain (Figure 10.4). To find the Fourier transform of Real$[y(t)]$, we write $\cos(\omega_0 t) = [\exp(j\omega_0 t) + \exp(-j\omega_0 t)]/2$. Its spectrum is a pair of impulses at $|\omega| = \omega_0$; hence, a convolution like (10.8) produces a sum of two Gaussians. A similar procedure (exercises) works for the imaginary part of $\exp(j\omega_0 t)$ and gives us the Fourier transform of Imag$[y(t)]$.

Simple experiments demonstrate that for the Gabor elementary function a reciprocal relationship apparently exists between time- and frequency-domain window widths (Figure 10.4). Further elucidation requires us to formalize the concept of window width, which is a topic covered in Section 10.2.4.

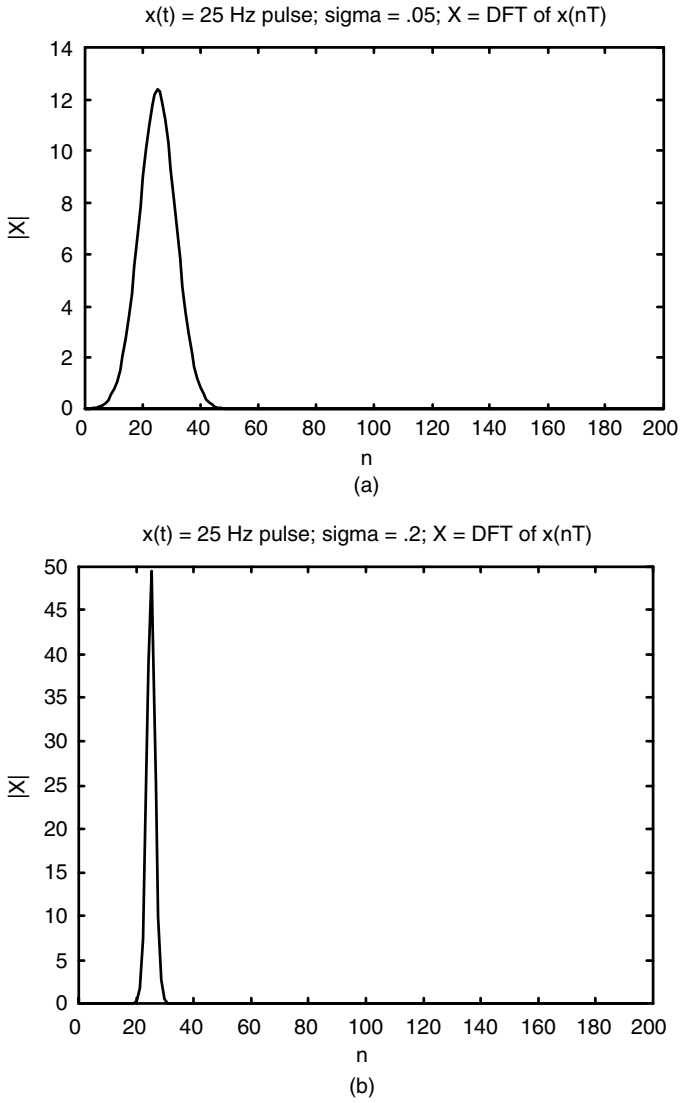


**Fig. 10.4.** Fourier transform of a Gabor elementary function. A narrow time-domain signal, $y(t) = g_{\mu,\sigma}(t)\exp(\, j\omega_0 t)$, has a wide magnitude spectrum (a). As the time-domain width of the Gaussian envelope grows, the frequency-domain window width shrinks (b).

### 10.1.4 Inversion

Recalling that all of the analog and discrete versions of the Fourier transform of Chapters 5 and 7 have inverse relations, let us consider the same problem for the Gabor transform. Suppose we transform with respect to a Gaussian window

$g(t) = g_{\mu,\sigma}(t)$. We call the forward transform relation, $X(\omega) = \mathcal{F}[x(t)]$, the *analysis equation*, and we call the inverse Fourier transform relation, $x(t) = \mathcal{F}^{-1}[X(\omega)]$, the *synthesis equation*. Of course, $X_g(\mu, \omega)$ is the radial Fourier transform of the windowed signal $x(t)g_{\mu,\sigma}(t)$, so its synthesis equation produces not $x(t)$, but $x(t)g_{\mu,s}(t)$ back again. How can we get $x(t)$ from $X_g(\mu, \omega)$? Because $X_g(\mu, \omega)$ is a function of two variables, we can integrate a second time, letting the Gaussian's location $\mu$ vary and using it as an integration variable.

We divide our efforts according to whether the Gabor transform of $x(t)$ is integrable. As with the Fourier transform development in Chapter 5, if $X_g(\mu, \omega) \in L^1(\mathbb{R})$, then we can freely interchange integration limits. If we assume $x(t) \in L^2(\mathbb{R})$ and nothing more, then a limiting argument is once again necessary.

***10.1.4.1 Assuming Transform Integrability.*** The following lemma is a direct consequence of our choice of $g_{\mu,\sigma}(t)$ for the Gabor transform windowing signal. It shows that, for each $\mu$, the Gabor transform $X_g(\mu, \omega)$ represents a local piece of $\mathcal{F}[x(t)]$. Independent variable $\omega$ corresponds to the spectral frequency, and $\mu$ represents the spectral fragment's time location. Indeed, when we integrate all of these pieces together (10.9), the result is the full signal spectrum $X(\omega)$.

**Lemma.** Suppose $x(t) \in L^2(\mathbb{R})$; $\mu, \sigma \in \mathbb{R}$, $\sigma > 0$; $g(t) = g_{\mu,\sigma}(t)$ is the Gaussian window with mean $\mu$ and standard deviation $\sigma$; and let $X_g(\mu, \omega) \in L^1(\mathbb{R})$ be the Gabor transform of $x(t)$. Then,

$$X(\omega) = \int_{-\infty}^{\infty} X_g(\mu, \sigma)\, d\mu. \tag{10.9}$$

***Proof:*** Let us expand the integrand in (10.9):

$$\int_{-\infty}^{\infty} X_g(\mu, \sigma)\, d\mu = \int_{-\infty}^{\infty} \left( \int_{-\infty}^{\infty} x(s) g(s) e^{-j\omega s} ds \right) d\mu = \int_{-\infty}^{\infty} x(s) e^{-j\omega s} \left( \int_{-\infty}^{\infty} g_{\mu,\sigma}(s)\, d\mu \right) ds. \tag{10.10a}$$

Fubini's theorem [11, 12] states that if an iterated integral's integrand is absolutely integrable, then it is identical to the double integral, and the order of iteration is irrelevant. The interchange of limits (10.10a) is possible by applying Fubini's theorem, which is possible because the integrand is absolutely integrable. The inner integrand is unity, since $\|g\|_1 = 1$. Consequently,

$$\int_{-\infty}^{\infty} X_g(\mu, \sigma)\, d\mu = \int_{-\infty}^{\infty} x(s) e^{-j\omega s} ds = X(\omega). \tag{10.10b}$$

■

Now we can prove an initial inverse Gabor transform relationship for the situation where $X_g(\mu, \omega)$ is integrable.

**Theorem (Inverse Gabor Transform or Synthesis Equation).** Suppose $\sigma > 0$; $x(t) \in L^2(\mathbb{R})$; $g(t) = g_{\mu,\sigma}(t)$ is the Gaussian window with mean $\mu$ and standard deviation $\sigma$; and let $X_g(\mu, \omega) \in L^1(\mathbb{R})$ be the Gabor transform of $x(t)$. Then,

$$x(t) = \frac{1}{2\pi} \int_{-\infty}^{\infty} \left( \int_{-\infty}^{\infty} X_g(\mu, \omega) e^{j\omega t} d\omega \right) d\mu \,. \tag{10.11}$$

***Proof:*** Using the definition of the Gabor transform for $x(t)$, we have

$$\frac{1}{2\pi} \int_{-\infty}^{\infty} \left( \int_{-\infty}^{\infty} X_g(\mu, \omega) e^{j\omega t} d\omega \right) d\mu = \frac{1}{2\pi} \int_{-\infty}^{\infty} e^{j\omega t} \left( \int_{-\infty}^{\infty} X_g(\mu, \omega)\, d\mu \right) d\omega \,. \tag{10.12}$$

We use the assumption that $X_g(\mu, \omega) \in L^1(\mathbb{R})$ to infer $X_g(\mu, \omega)\exp(j\omega t) \in L^1(\mathbb{R})$ as well; Fubini's theorem then implies (10.12). Using the lemma to evaluate the parenthesized integral on the right-hand side of (10.12) gives

$$\frac{1}{2\pi} \int_{-\infty}^{\infty} e^{j\omega t} \left( \int_{-\infty}^{\infty} X_g(\mu, \omega) d\mu \right) d\omega = \frac{1}{2\pi} \int_{-\infty}^{\infty} e^{j\omega t} X(\omega)\, d\omega = x(t) \tag{10.13}$$

as desired. ■

The next result is a time-frequency version of Plancherel's theorem. It shows that the Gabor transform preserves signal energy. We do not have a perfect proportion, since the equation depends on the $L^2(\mathbb{R})$ norm of the window function.

We interpose a lemma that shows how to compute the Fourier transform of a Gabor transform.

**Lemma (Fourier Transform of Gabor Transform).** Suppose $\sigma > 0$; $x(t) \in L^2(\mathbb{R})$; $g(t) = g_{\mu,\sigma}(t)$ is the Gaussian window with mean $\mu$ and standard deviation $\sigma$; and let $X_g(\mu, \omega) \in L^1(\mathbb{R})$ be the Gabor transform of $x(t)$. Then, for each $\omega \in \mathbb{R}$ we can Fourier transform the signal $X_g(\mu, \omega)$, viewing it as a function of $\mu$. So,

$$\int_{-\infty}^{\infty} X_g(\mu, \omega) e^{-j\mu\theta} d\mu = \frac{1}{2\pi} X(\omega + \theta) G(\theta) = \frac{1}{2\pi} X(\omega + \theta) e^{-\frac{\theta^2\sigma^2}{2}} , \tag{10.14}$$

where $G(\theta)$ is the radial Fourier transform of $g(t)$.

***Proof:*** Expanding $X_g(\mu, \omega)$ in the integrand (10.14) gives

$$\begin{aligned} \int_{-\infty}^{\infty} \left[ \int_{-\infty}^{\infty} x(t) g(t) e^{-j\omega t} dt \right] e^{-j\mu\theta} d\mu &= \int_{-\infty}^{\infty} \left( \left[ \int_{-\infty}^{\infty} x(t) g_{0,\sigma}(t-\mu) e^{-j\omega t} dt \right] \right) e^{-j\mu\theta}\, d\mu \\ &= \int_{-\infty}^{\infty} \left( \left[ \int_{-\infty}^{\infty} x(t) g_{0,\sigma}(t-\mu) e^{-j\omega t} e^{j\omega\mu} dt \right] \right) e^{-j\mu\theta} e^{-j\omega\mu} d\mu. \end{aligned} \tag{10.15}$$

The algebraic manipulations in (10.15) aim to change the expression's form into a convolution of $x(t)$ with the Gabor elementary function $y(s) = g_{0,\sigma}(s)\exp(j\omega s)$. Because $g_{0,\sigma}(t-\mu) = g_{0,\sigma}(\mu - t)$,

$$\int_{-\infty}^{\infty}\left[\int_{-\infty}^{\infty} x(t)g(t)e^{-j\omega t}dt\right]e^{-j\mu\theta}d\mu = \int_{-\infty}^{\infty}\left[\int_{-\infty}^{\infty} x(t)g_{0,\sigma}(\mu - t)e^{j\omega(\mu - t)}dt\right]e^{-j\mu\theta}e^{-j\omega\mu}d\mu$$

$$= \int_{-\infty}^{\infty}(x^{*}y)(\mu)e^{-j\mu(\theta+\omega)}d\mu, \tag{10.16}$$

which exposes a convolution integral, $(x * y)(\mu)$. But now the outer integral in  is evidently a radial Fourier transform; invoking the convolution theorem,

$$\int_{-\infty}^{\infty}\left[\int_{-\infty}^{\infty} x(t)g(t)e^{-j\omega t}dt\right]e^{-j\mu\theta}\,d\mu = \int_{-\infty}^{\infty}(x * y)(\mu)e^{-j\mu(\theta+\omega)}\,d\mu$$

$$= X(\omega+\theta)Y(\omega+\theta). \tag{10.17}$$

Now, $X(\omega + \theta)$ is the Fourier transform of $x(t)$ evaluated at $\omega + \theta$, as the lemma requires. $Y(\phi) = \mathcal{F}[y(s)](\phi) = \mathcal{F}[\,g_{0,\sigma}(s)\exp(\,j\omega s)](\phi)$ is the Fourier transform of a Gabor elementary function. In (10.8) we found $Y(\phi) = (2\pi)^{-1}\mathcal{F}[g_{0,\sigma}(s)](\phi - \omega)$. If $\mu = 0$, then $\mathcal{F}[\,g_{\mu,\sigma}(s)](\phi) = \exp(-\sigma^2\phi^2/2)$. So $Y(\omega + \theta) = (2\pi)^{-1}\mathcal{F}[g_{0,\sigma}(s)]([\omega + \theta] - \omega) = (2\pi)^{-1}[g_{0,\sigma}(s)](\theta)$. Finally,

$$X(\omega+\theta)Y(\omega+\theta) = X(\omega+\theta)\,\mathcal{F}[g_{0,\sigma}(t)e^{j\omega t}](\omega+\theta) = \frac{X(\omega+\theta)}{2\pi}e^{-\frac{\sigma^2\theta^2}{2}}, \tag{10.18}$$

and the proof is complete. ■

***10.1.4.2 Two-Dimensional Hilbert Spaces in Brief.*** Our next result is the time-frequency version of the Plancherel formula. Now, this theorem depends on the two-dimensional $L^2(\mathbb{R})$ norm. "You are so unaccustomed to speak in images," Adeimantus ironically remarks to Socrates in the Republic,[3] and we too have been—intentionally—so unaccustomed! The $L^2(\mathbb{R})$ norm applies to analog *images*, and up until now we have been deliberately partial to one-dimensional signal theory. Nonetheless, time-frequency methods, and mixed-domain techniques in general, often transgress into multidimensional or *image* analysis. This is to be expected, since the transforms do encode both time and frequency information as independent variables in the transformed signal. The theoretical extensions are gratefully straightforward. In fact, $L^2(\mathbb{R}\times\mathbb{R})$ is a Hilbert space also, and its theoretical development follows from our one-dimensional endeavors in Chapter 3. We do not need to spend a lot of time developing that multidimensional theory here; nevertheless, the concepts of the $L^2(\mathbb{R}^2)$ space and its norm are worth reviewing.

[3] *Republic*, vol. II, B. Jowett, translator, Oxford: Clarendon Press, 1964.

**Definition ($\mathbf{L^2(\mathbb{R}^2)}$).** A two-dimensional signal $x(s, t)$ is *square-integrable* or has *finite energy* if

$$\int_{-\infty}^{\infty}\int_{-\infty}^{-\infty} |x(s, t)|^2 \, ds dt < \infty. \tag{10.19}$$

We denote the set of all such signals by $L^2(\mathbb{R}^2)$ or $L^2(\mathbb{R} \times \mathbb{R})$. If $x(s, t) \in L^2(\mathbb{R}^2)$, then

$$\left[\int_{-\infty}^{\infty}\int_{-\infty}^{-\infty} |x(s, t)|^2 ds dt\right]^{\frac{1}{2}} = \|x\|_{2,\, L^2(d\mathbb{R}^2)} \tag{10.20}$$

is its $L^2(\mathbb{R}^2)$ norm. If the context is clear, then we omit the subscripted $L^2(\mathbb{R}^2)$ in (10.20). If $x(s, t)$ and $y(s, t)$ are in $L^2(\mathbb{R}^2)$, then we define their inner product by

$$\langle x, y\rangle_{L^2(\mathbb{R}^2)} = \int_{-\infty}^{\infty}\int_{-\infty}^{-\infty} x(s, t)\overline{y(s, t)} \, ds dt\,. \tag{10.21}$$

In a clear context, we drop the subscript and write (10.21) as $\langle x, y\rangle$. The exercises further cover the ideas of two-dimensional signal spaces.

**Theorem (Gabor Transform Plancherel's).** Suppose $\sigma > 0$; $x(t) \in L^2(\mathbb{R})$; $g(t) = g_{\mu,\sigma}(t)$ is the Gaussian with mean $\mu$ and standard deviation $\sigma$; and let $X_g(\mu, \omega) \in L^1(\mathbb{R})$ be the Gabor transform of $x(t)$. Then

$$\|x\|_2 = \sqrt{2\pi}\frac{\|X_g(\mu, \omega)\|_{2,\, L^2(\mathbb{R}^2)}}{\|g\|_2}\,. \tag{10.22}$$

***Proof:*** Fubini's theorem applies to the double integral that defines the $L^2(\mathbb{R}^2)$ norm:

$$\|X_g(\mu, \omega)\|^2_{2,\, L^2(\mathbb{R}^2)} = \int_{-\infty}^{\infty}\int_{-\infty}^{\infty} |X_g(\mu, \omega)|^2 d\mu \, d\omega = \int_{-\infty}^{\infty}\left[\int_{-\infty}^{\infty} |X_g(\mu, \omega)|^2 d\mu\right] d\omega. \tag{10.23}$$

Since the inner integral is a function of the time domain variable $\mu$, we can Fourier transform its integrand with respect to $\mu$. An application of the Fourier transform Plancherel formula is then feasible:

$$\|X_g(\mu, \omega)\|^2_{2,\, L^2(\mathbb{R}^2)} = \int_{-\infty}^{\infty}\frac{1}{2\pi}\left[\int_{-\infty}^{\infty} |\mathcal{F}[X_g(\mu, \omega)](\theta)|^2 d\theta\right] d\omega\,. \tag{10.24}$$

Let $H(\theta) = \mathcal{F}[g_{0,\sigma}(t)](\theta)$, so that by the Lemma we find

$$\left\|X_g(\mu, \omega)\right\|^2_{2,\, L^2(\mathbb{R}^2)} = \frac{1}{2\pi}\int_{-\infty}^{\infty}\left[\int_{-\infty}^{\infty}\left|\frac{1}{2\pi}X(\omega+\theta)H(\theta)\right|^2 d\theta\right] d\omega$$

$$= \frac{1}{2\pi}\int_{-\infty}^{\infty}\frac{1}{(2\pi)^2}\left[\int_{-\infty}^{\infty}|X(\omega+\theta)|^2|H(\theta)|^2 d\theta\right] d\omega. \qquad (10.25)$$

To evaluate the iterated integral (10.25), we swap the order of integration and use Plancherel two more times. The last expression above becomes

$$\left\|X_g(\mu, \omega)\right\|^2_{2,\, L^2(\mathbb{R}^2)} = \frac{1}{2\pi}\int_{-\infty}^{\infty}\frac{|H(\theta)|^2}{2\pi}\left[\int_{-\infty}^{\infty}\frac{|X(\omega+\theta)|^2}{2\pi}d\omega\right] d\theta$$

$$= \frac{\|x\|_2^2}{2\pi}\int_{-\infty}^{\infty}\frac{\left|H(\theta)^2\right|}{2\pi}d\theta = \frac{\|x\|_2^2}{2\pi}\left\|g_{0,\,\sigma}\right\|_2^2. \qquad (10.26)$$

■

***10.1.4.3 For General Square-Integrable Signals.*** This section develops the Plancherel and inverse results for square-integrable signals, dropping the assumption of integrability on the Gabor transform. We begin with a form of the Parseval theorem.

**Theorem (Gabor Transform Parseval's).** Suppose $\sigma > 0$; $x(t), y(t) \in L^2(\mathbb{R})$; $g(t) = g_{\mu,\sigma}(t)$ is the Gaussian window with mean $\mu$ and standard deviation $\sigma$; and let $X_g(\mu, \omega)$ and $Y_g(\mu, \omega)$ be the Gabor transforms of $x(t)$ and $y(t)$, respectively. Then

$$2\pi\|g\|_2^2\langle x, y\rangle = \int_{-\infty}^{\infty}\int_{-\infty}^{\infty} X_g(\mu, \omega)\overline{Y_g(\mu, \omega)}\, d\omega d\mu = \langle X_g, Y_g\rangle_{L^2(\mathbb{R}^2)}. \qquad (10.27)$$

***Proof:*** For fixed $\mu$, we can apply the Parseval theorem to find

$$\int_{-\infty}^{\infty} X_g(\mu, \omega)\overline{Y_g(\mu, \omega)}\, d\omega = 2\pi\int_{-\infty}^{\infty}\mathcal{F}^{-1}X_g(\mu, \omega)\mathcal{F}^{-1}\overline{Y_g(\mu, \omega)}\, d\omega, \qquad (10.28)$$

where $\mathcal{F}^{-1}$ is the inverse radial Fourier transform. Since the inverse Fourier transform of the Gabor transform $X_g(\mu, \omega)$ is the windowed signal $x(t)g_{\mu,\sigma}(t)$, we continue (10.28) as follows:

$$2\pi\int_{-\infty}^{\infty} x(t)g_{\mu,\,\sigma}(t)\overline{y(t)g_{\mu,\,\sigma}(t)}\, dt = 2\pi\int_{-\infty}^{\infty} x(t)\overline{y(t)}g^2{}_{\mu,\,\sigma}(t)\, dt. \qquad (10.29)$$

Integrating (10.29) with respect to $\mu$ produces

$$\begin{aligned}\int_{-\infty}^{\infty}\int_{-\infty}^{\infty} X_g(\mu,\omega)\overline{Y_g(\mu,\omega)}\,d\omega d\mu &= 2\pi\int_{-\infty}^{\infty}\int_{-\infty}^{\infty} x(t)\overline{y(t)}g^2_{\mu,\sigma}(t)\,dtd\mu \\ &= 2\pi\int_{-\infty}^{\infty} x(t)\overline{y(t)}\int_{-\infty}^{\infty} g^2_{\mu,\sigma}(t)\,d\mu dt \\ &= 2\pi\|g_{\mu,\sigma}\|_2^2\langle x, y\rangle. \end{aligned} \tag{10.30}$$

Fubini's theorem and the Schwarz inequality (applied to the inner integral on the top right-hand side of (10.30), which is itself an inner product) allow us to interchange the integration order. ■

The next result shows how to retrieve the original signal $x(t) \in L^2(\mathbb{R})$ from its Gabor transform $X_g(\mu, \omega)$. This is the Gabor transform inverse relation, but it has other names, too. It is sometimes called the *resolution of the identity* or simply the *synthesis equation* for the Gabor transform.

**Theorem (Inverse Gabor Transform).** Suppose $\sigma > 0$; $x(t) \in L^2(\mathbb{R})$; $g(t) = g_{\mu,\sigma}(t)$ is the Gaussian window with mean $\mu$ and standard deviation $\sigma$; and let $X_g(\mu, \omega)$ be the Gabor transform of $x(t)$. Then for all $s \in \mathbb{R}$, if $x(t)$ is continuous at $s$, then

$$x(a) = \frac{1}{(2\pi\|g\|_2^2)}\int_{-\infty}^{\infty} X_g(\mu,\omega)g_{\mu,\sigma}(a)e^{j\omega a}d\omega d\mu\,. \tag{10.31}$$

***Proof:*** Consider a family of Gaussians $h_{a,s}(t)$, where $s > 0$. As $s \to 0$, they approximate a delta function, and, informally, from the sifting property we expect that

$$\lim_{s\to 0}\langle x(t), h_{a,s}(t)\rangle = x(a) \tag{10.32}$$

when $x(t)$ is continuous at $t = a$. If we set $y(t) = h_{a,s}(t)$, then we can apply the prior Plancherel theorem to obtain

$$\langle x, h_{a,s}\rangle = \frac{1}{2\pi\|g\|_2^2}\int_{-\infty}^{\infty}\int_{-\infty}^{\infty} X_g(\mu,\omega)\overline{\left[\int_{-\infty}^{\infty} h_{a,s}(t)g_{\mu,\sigma}(t)e^{-j\omega t}dt\right]}\,d\omega d\mu\,. \tag{10.33}$$

We calculate the limit

$$\begin{aligned}\lim_{s\to 0}\overline{\int_{-\infty}^{\infty} h_{a,s}(t)g_{\mu,\sigma}(t)e^{-j\omega t}dt} &= \lim_{s\to 0}\int_{-\infty}^{\infty} h_{a,s}(t)g_{\mu,\sigma}(t)e^{j\omega t}dt \\ &= \int_{-\infty}^{\infty}\lim_{s\to 0} h_{a,s}(t)g_{\mu,\sigma}(t)e^{j\omega t}dt \\ &= \int_{-\infty}^{\infty}\delta(t-a)g_{\mu,\sigma}(t)e^{j\omega t}dt = g_{\mu,\sigma}(a)e^{j\omega a}. \end{aligned} \tag{10.34}$$

Taking the same limit $s \to 0$ on both sides of (10.33) and interchanging limit and integration operations gives

$$\lim_{s \to 0} \langle x, h_{a,s} \rangle = \frac{1}{2\pi \|g\|_2^2} \int_{-\infty}^{\infty} \int_{-\infty}^{\infty} X_g(\mu, \omega) g_{\mu,\sigma}(a) e^{j\omega a} d\omega d\mu = x(a). \quad (10.35)$$

■

### 10.1.5 Applications

Let us pause the theoretical development for a moment to explore two basic Gabor transform applications: a linear chirp and a pulsed tone. These illustrate the use and behavior of the transform on practical signals. Studying the transform coefficients as dependent on the width of the transform window function will also lead us to important ideas about the relation between the transform's time and frequency resolutions.

***10.1.5.1 Linear Chirp.*** This section discusses the Gabor transform for a linear chirp signal. A linear chirp is a sinusoidal function of a squared time variable $At^2$, where $A$ is constant. Thus, as $|t|$ increases, the signal oscillations bunch up. Signal frequency varies with time in a linear fashion, and we anticipate that the Gabor transform will expose this behavior.

Let us consider the analog signal

$$X_a(t) = \begin{cases} \cos(At^2), & t \in [0, L] \\ 0 & \text{otherwise.} \end{cases} \quad (10.36)$$

The Gabor transform of $x_a(t)$ is

$$\mathcal{G}[x_a(t)](\mu, \omega) = (X_a)_g(\mu, \omega) = \int_0^L x_a(t) g_{\mu,\sigma}(t) e^{-j\omega t} dt. \quad (10.37)$$

We need to decide upon an appropriate value for the spread of the Gaussian, which is given by its standard deviation $\sigma$. Also, $(X_a)_g$ is a two-dimensional function, so we seek an image representation of the Gabor transform for a range of values, $\mu$ and $\omega$.

We apply Section 7.1.2's ideas for approximating an analog transform with discrete samples. Recall that the discrete Fourier series (DFS) coefficients

$$c(k) = \frac{1}{N} \sum_{n=0}^{N-1} x(n) e^{\frac{-2\pi jnk}{N}}, \quad (10.38)$$

where $0 \le k \le N-1$, are a trapezoidal rule approximation to the Fourier series integral using the intervals $[0, T/N]$, $[T/N, 2T/N]$, …, $[(N-1)T/N, T]$. Recall as well from

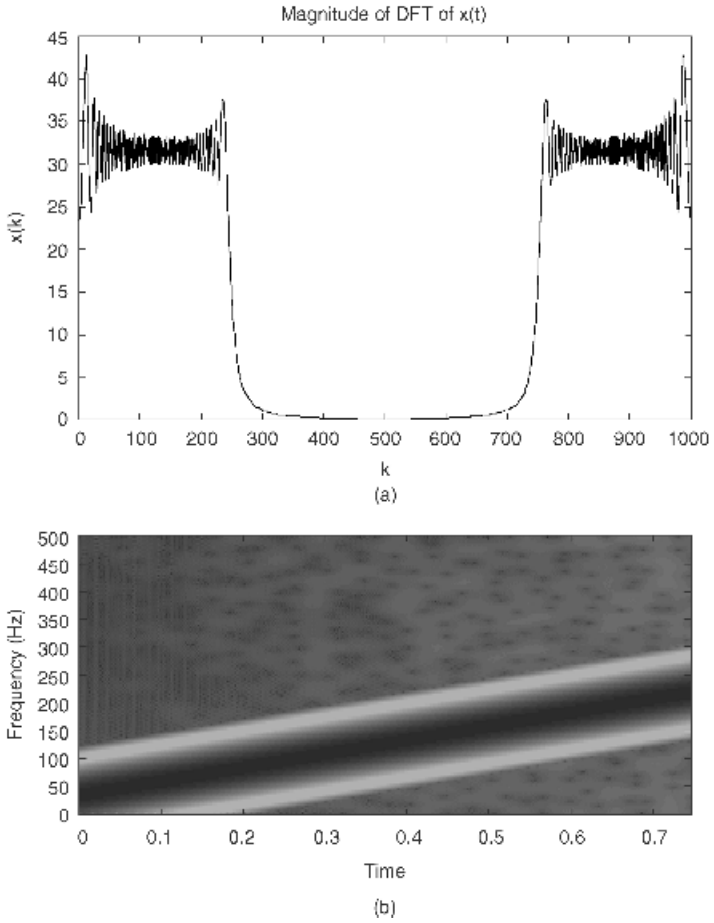


**Fig. 10.5.** Gabor transform of linear chirp, windowing with a Gaussian of $\sigma = 16$. The frequency of $x_a(t) = \cos(At^2)$ rises from 0 to 250 Hz over a 1–s time interval. Its magnitude spectrum $X(k)$ is shown in panel (a). Note the apparent presence of frequencies between 0 and 250 Hz, but that the time of a particular frequency is lost by the discrete Fourier transform (DFT). The Gabor transform reveals the time evolution of frequencies in $x(t)$, as shown in panel (b). Time values are shown along the bottom over the interval [0, 1], which represents samples $n$ from 0 to 255. Image intensities represent Gabor magnitude spectral values $|\mathcal{G}[x_a](\mu, \omega)|$; darker values indicate larger magnitudes.

Chapter 7 that if $x(n)$ has discrete Fourier transform (DFT) coefficients $X(k)$ and DFS coefficients $c(k)$ on $[0, N-1]$, then $X(k) = Nc(k)$. Since we have to perform a discrete transform on $N$ samples over an array of points, we choose that $N = 2^m$, for some $m$, so that the efficient fast Fourier transform (FFT) algorithm applies. We transform the windowed signal $x_a(t)g_{\mu,\sigma}(t)$ sampled at $t = 0, T/N, 2T/N, \ldots, (N-1)T/N$. Finally,

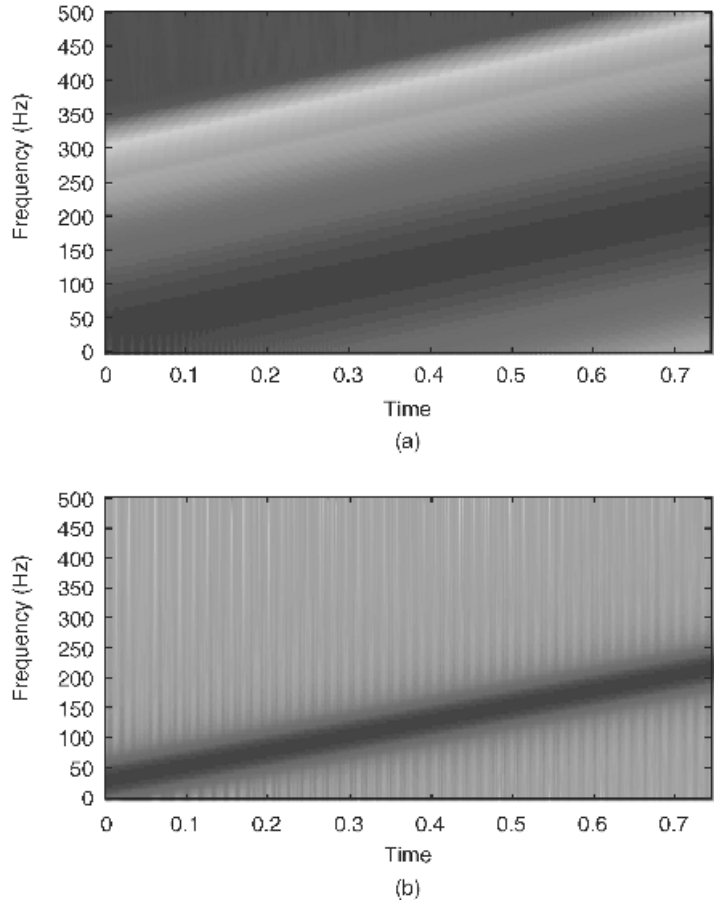


**Fig. 10.6.** Window width effects in the Gabor transform of a linear chirp. Windowing with a Gaussian of $\sigma = 4$ is shown in panel (a). Panel (b) shows the case of $\sigma = 64$.

we select $\sigma = 16$ as the standard deviation of the Gaussian window function for the transform (Figure 10.5).

What effect does the decision $\sigma = 16$ play for the transform? If $\sigma$ increases, then the band of large transform coefficients shrinks. And decreasing the width of the transform's window function causes the sloping region of large magnitude coefficients to expand.

Carefully note in Figure 10.6 that broadening the time-domain window functions narrows the region of large magnitude values in the transformed signal. Indeed a reciprocal relation is manifest. This is an important characteristic. The next section further explores the link between time- and frequency-domain resolution under Gabor signal transformation.

***10.1.5.2 Pulsed Tone.*** Now suppose that we begin with a time-domain pulse:

$$x_a(t) = \exp(-Bt^2)\cos(At). \tag{10.39}$$

We shall suppose that the pulse frequency is 50 Hz and consider different time-domain durations of $x_a(t)$, which are governed by stretching the Gaussian envelope, $\exp(-Bt^2)$. (Figures 10.7 and 10.8).

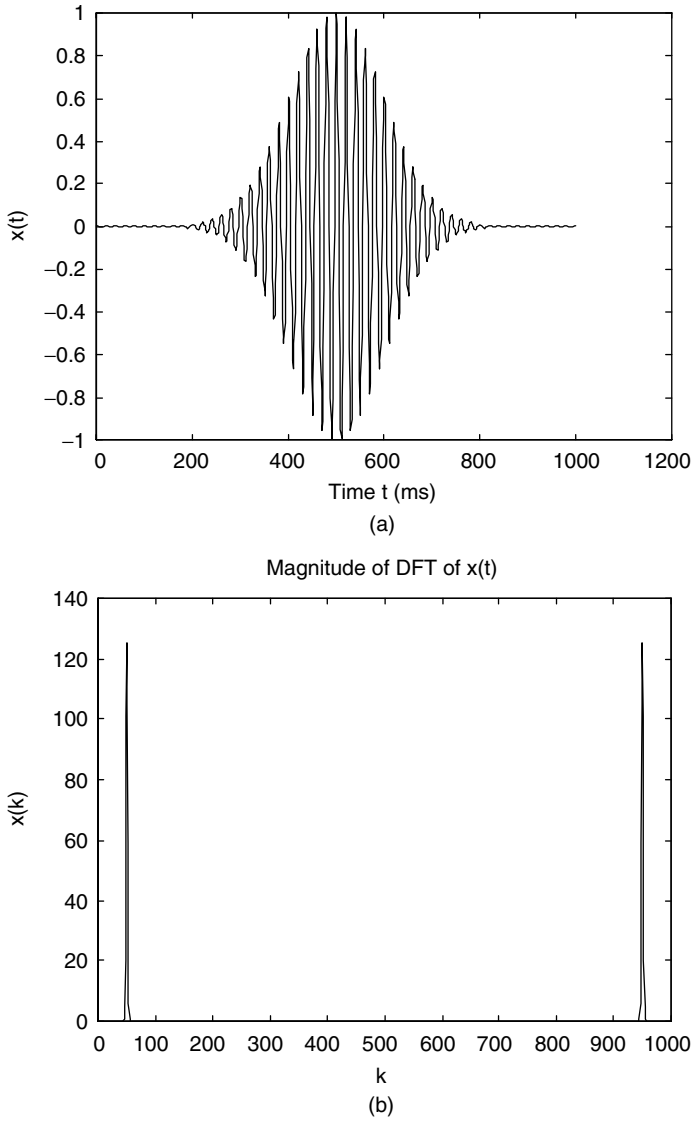


**Fig. 10.7.** Time-frequency localization tradeoff for a pulse tone. (a) The 50-Hz tone pulse rising and decaying in a 600-ms interval about $t = 0.5$ *s*. (b) Its Fourier spectrum shows the frequencies present but provides no time information. (c) The Gabor transform.

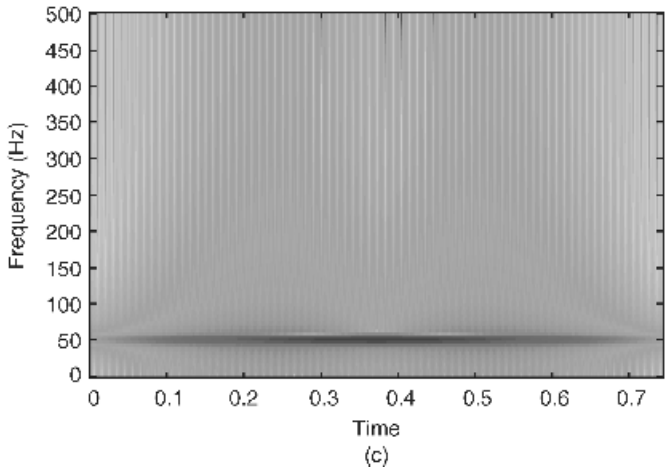


**Fig. 10.7** (*Continued*)

This elementary experiment reveals that as the time-domain locality of the pulse increases, the frequency-domain locality decreases. In other words, it seems that as we gain a better knowledge of the time span a signal's frequencies occupy, then we lose knowledge of the specific frequencies it contains. This points to a fundamental tradeoff

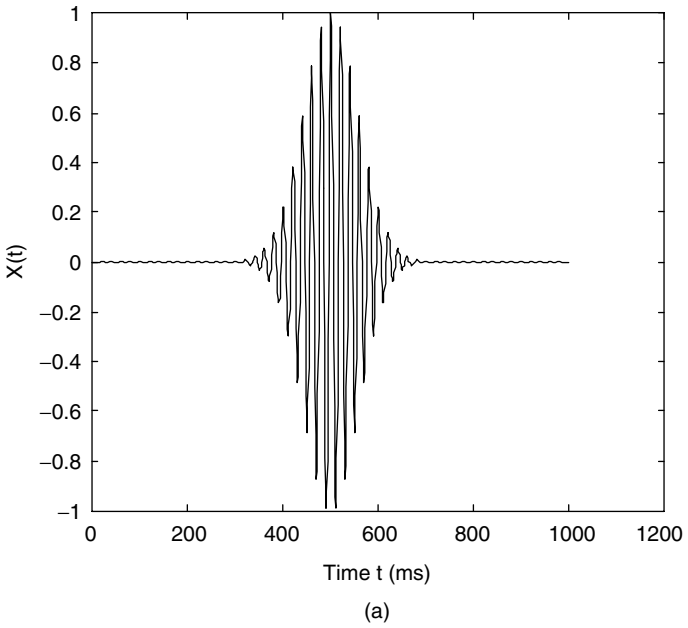


**Fig. 10.8.** Time-frequency localization tradeoff for a pulse tone. Panel (a) shows the 50-Hz tone pulse rising and decaying in a 300-ms interval about $t = 0.5$ *s*; (b) the more tightly localized pulse has a Gabor transform that is correspondingly dispersed.

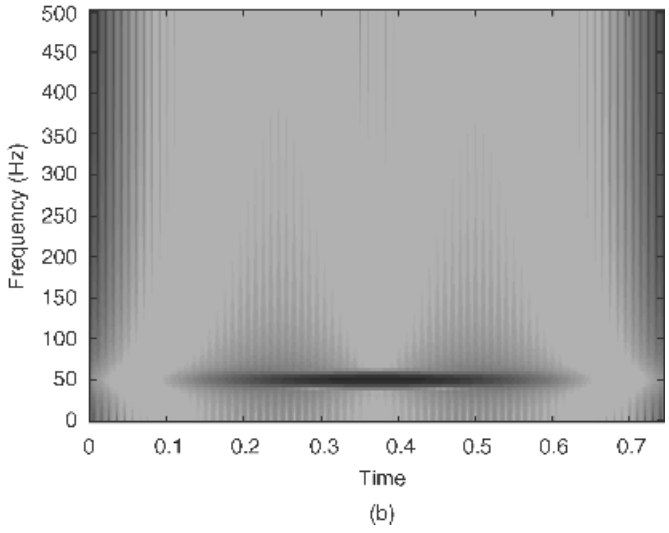


**Fig. 10.8** (*Continued*)

in time-frequency analysis. It is also closely related to the Heisenberg Uncertaintly Principle, which we touched upon in our treatment of frequency-domain analysis.

### 10.1.6 Properties

Table 10.1 summarizes properties of the Gabor transformation, some of which are left as exercises.

**TABLE 10.1. Gabor Transform Properties**[a]

| Signal Expression | Gabor Transform or Property |
|---|---|
| $x(t)$ | $X_g(\mu, \omega)$ |
| $ax(t) + by(t)$ | $aX_g(\mu, \omega) + bY_g(\mu, \omega)$ |
| $x(t-a)$ | $e^{-j\omega a}X_g(\mu - a, \omega)$ |
| $x(t)\exp(j\theta t)$ | $X_g(\mu, \omega - \theta)$ |
| $\|x\|_2 = \sqrt{2\pi}\dfrac{\|X_g(\mu, \omega)\|_{2, L^2(R^2)}}{\|g\|_2}$ | Plancherel's theorem |
| $\langle x, y\rangle = \dfrac{1}{2\pi\|g\|_2^2}\langle X_g, Y_g\rangle$ | Parseval's theorem |
| $x(t) = \dfrac{1}{(2\pi\|g\|_2^2)}\int_{-\infty}^{\infty} X_g(\mu, \omega)g_{\mu, \sigma}(t)e^{j\omega t}d\omega d\mu$ | Inverse, resolution of the identity, or synthesis equation |

[a]In the table, $x(t)$ is square-integrable, and $g(t)$ is a Gaussian of mean $\mu$ and standard deviation $\sigma$.

## 10.2 SHORT-TIME FOURIER TRANSFORMS

A *short-time Fourier transform* (STFT) generalizes the Gabor transform by allowing a general window function. For the supporting mathematics to work, the theory requires constraints on the window functions. These we will elaborate in a moment. Once these theoretical details are taken care of, though, the general transform enjoys many of the same properties as the Gabor transform.

One might well ask whether a window shape other than the Gaussian can provide a better time-frequency transform. The answer is affirmative, but qualified. If the window shape matches the shape of signal regions to be analyzed, then an alternative window function offers somewhat better numerical results in signal detection applications. Thus, choosing the window to have roughly the same shape as the signals to be analyzed improves detection performance. These benefits are usually slight, however.

We know from the experiments with pulses and chirps at the end of the previous section that there is a tradeoff between time and frequency localization when using the Gabor transform. How does the selection of a transform window affect this behavior? It turns out that there is a hard lower limit on the joint time-frequency resolution of windowed Fourier transforms. Constricting the time-domain window so as to sharpen the time domain resolution results in a proportionately broader, more imprecise frequency-domain localization. This is a fundamental limitation on windowed Fourier methods. Its practical import is that signals with both low and high frequencies or with abrupt transients are difficult to analyze with this transform family. In fact, this limitation—which is a manifestation of the famous Heisenberg Uncertainty Principle—stimulated the search for alternative mixed domain transforms and was an impetus behind the discovery of the wavelet transform (Chapter 11).

Among all possible window functions, there is one signal in particular that shows the best performance in this regard: the Gaussian. Thus, the Gabor transform is the short-time Fourier transform with the best joint time-frequency resolution. So despite the benefits a special window may have, the Gabor transform prevails in all but certain specialized STFT-based signal analysis applications.

### 10.2.1 Window Functions

This section specifies those functions that may serve as the basis for a windowed transform. We formally define window functions and the resulting general window transform. We also develop some window function properties. This leads to a criterion for measuring joint time-frequency resolution. We prove the uncertainty principle, and the optimality of the Gabor transform follows as a corollary.

We should note right away that exponential signals modulated by window functions will play the role of structuring elements for signal analysis purposes. The short-time Fourier transform applies this structuring element at different time locations to obtain a set of time-ordered snapshots of the signal at a given frequency. When we later discretize the STFT, this idea will become clearer.

**Definition (Window Function).** If $x(t) \in L^2(\mathbb{R})$, $\|x(t)\|_2 \neq 0$, and $tx(t) \in L^2(\mathbb{R})$, then $x(t)$ is called a *window function*.

So, $x(t)$ is a window function when its squared magnitude, $|x(t)|^2$, has a second order moment. This technical condition is necessary for many of the properties of the windowed transform. Of course, the familiar functions we have used to improve signal spectra in Chapter 9 satisfy this definition.

**Example (Gaussian).** The Gaussian $g(t) = A\exp(-Bt^2)$, where $A \neq 0$ and $B > 0$, is a window function. The Gaussian has moments of all orders, as we can check by integrating by parts:

$$\int_{-\infty}^{\infty} |tg(t)|^2 dt = A \int_{-\infty}^{\infty} t^2 e^{-2Bt^2} dt = \left( \frac{Ate^{-2Bt^2}}{-4B} \Big|_{-\infty}^{\infty} + \left(\frac{A}{4B}\right) \int_{-\infty}^{\infty} e^{-2Bt^2} dt \right)$$

$$= \left(\frac{A}{4B}\right) \int_{-\infty}^{\infty} e^{-2Bt^2} dt. \tag{10.40}$$

The Fourier transform of a Gaussian is still a Gaussian, and therefore $G(\omega)$ is a window function in the frequency domain too. But many window functions have Fourier transforms that are not window functions by our definition.

**Example (Square Pulse).** The square pulse of width $2T > 0$, $w(t) = u(t + T) - u(t - T)$, is a window function. Indeed any non-trivial compactly supported $L^2(\mathbb{R})$ signal is a window function. The Fourier transform of $w(t)$, $W(\omega) = 2T\text{sinc}(T\omega)$, decays like $\omega^{-1}$ in the frequency domain. Thus, $\omega W(\omega) = 2\sin(T\omega) \notin L^2(\mathbb{R})$. So a window function does not necessarily have a Fourier transform that is a window function as well. Indeed, this occurs rarely, as the next result shows.

**Lemma (Integrability).** If $x(t)$ is a windowing function, then $x(t) \in L^1(\mathbb{R})$.

***Proof:*** (A Schwarz Inequality exercise). ■

**Proposition.** If $x(t)$ is a discontinuous window function, then $X(\omega)$ cannot also be a window function.

***Proof:*** If $X(\omega)$ is a window function, then it is absolutely integrable by the lemma, and its inverse Fourier transform $\mathcal{F}^{-1}[X(\omega)] = x(t)$ is continuous. But this is a contradiciton. ■

So constructing double pane windows requires some care. To do so we must find window functions that are continuous, decay quickly, and have Fourier transforms which are continuous with fast decay. Later, we will define the concept of the center and size of a window function. These definitions will lead to the uncertainty principle and the

result that, among the short-time Fourier transforms, the Gabor transform alone possesses a window function with optimal time- and frequency-domain resolution.

### 10.2.2 Transforming with a General Window

It is not hard to generalize the Gabor transform to work with a general window, now that we have introduced the moment condition that a window function must satisfy. We will define the windowed transform for window functions and make the additional assuption that the Fourier transform of the window is also a window function for some of the properties. Drawing inspiration from the Gabor transform formalizations, we can easily draft a definition for a general windowed transform.

**Definition (Short-Time Fourier Transform).** Let $w(t)$ be a window function and $x(t) \in L^2(\mathbb{R})$. The *short-time Fourier transform (STFT) with respect to w(t)*, written $X_w(\mu, \omega)$, is the radial Fourier transform of the product $x(t)w(t-\mu)$:

$$X_w(\mu, \omega) = \int_{-\infty}^{\infty} x(t)w(t-\mu)e^{-j\omega t}dt\,. \tag{10.41}$$

The STFT is also known as the *windowed Fourier transform*. There is a "fancy $W$" notation for the short-time Fourier transform: $X_w(\mu, \omega) = (\mathcal{W}_w)[x(t)](\mu, \omega)$.

*Remarks.* The windowing function $w(t)$ in (10.41) remains fixed for the transform, as does the Gaussian in a Gabor transform. Indeed, our definition generalizes the Gabor transform: If $w(t)$ is a Gaussian, then the short-time Fourier transform with respect to $w(t)$ of $x(t)$ is precisely the Gabor transform of $x(t)$ using the Gaussian $w(t)$. We do not demand that the Fourier transform $(\mathcal{F}w)(\omega) = W(\omega)$ must also be a window function; when we turn to study time-frequency localization using the transform, however, we make this qualification.

***10.2.2.1 Standard Windows.*** We can define an STFT for any of the windowing functions used to improve local spectra estimates in Chapter 9. We recall that windowing a signal $x(t)$ with a tapered window function reduces the size of Gibbs phenomenon sidelobes. Table 10.2 summarizes possible standard analog windows: rectangle, Bartlett (triangle), Hamming, Hanning, and Blackman functions.

Each of the standard window functions above has a discontinuity in a time-domain derivative of some order. We can develop the STFT using $B$-splines, however, and achieve smooth time-domain derivatives of arbitrarily high orders.

***10.2.2.2 B-spline Windows.*** Another window function appropriate for the STFT involves $B$-splines, which we introduced in Section 3.2.5. Splines are popular in applied mathematics [14], computer graphics [15], and signal processing and analysis [16–18]. We recall the definition.

**TABLE 10.2. Short-Time Fourier Transform Window Functions**[a]

| Name | Definition |
|---|---|
| Rectangle | $w(t) = \begin{cases} b & \text{if } (\lvert t\rvert \le \text{a}) \\ 0 & \text{otherwise.} \end{cases}$ |
| Bartlett (triangle) | $w(t) = \begin{cases} \frac{b}{a}t + b & \text{if } -a \le t \le 0, \\ -\frac{b}{a}t + b & \text{if } 0 \le t \le a, \\ 0 & \text{otherwise.} \end{cases}$ |
| Hanning (von Hann) | $w(t) = \begin{cases} b\cos^2\left(\frac{\pi t}{2a}\right) & \text{if } \lvert t\rvert \le a \\ 0 & \text{otherwise.} \end{cases}$ |
| Hamming | $w(t) = \begin{cases} 0.54\text{b} + 0.46\text{b}\cos\left(\frac{\pi t}{a}\right) & \text{if } \lvert t\rvert \le a \\ 0 & \text{otherwise.} \end{cases}$ |
| Blackman | $w(t) = \begin{cases} 0.42b + 0.5b\cos\left(\frac{\pi t}{a}\right) + 0.08b\cos\left(\frac{2\pi t}{a}\right) & \text{if } \lvert t\rvert \le a \\ 0 & \text{otherwise.} \end{cases}$ |

[a]Adjust parameter $a > 0$ for a window width appropriate to the signal features of interest. Adjust parameter $b > 0$ in order to normalize the window function.

**Definition (B-spline).** The B-spline of order zero is

$$\beta_0(t) = \begin{cases} 1 & \text{if } -\frac{1}{2} < t < \frac{1}{2} \\ \frac{1}{2} & \text{if } \lvert t\rvert = \frac{1}{2} \\ 0 & \text{if otherwise.} \end{cases} \tag{10.42}$$

and higher-order B-splines are found by successive convolution:

$$\beta_n(t) = \underbrace{\beta_0(t) * \beta_0(t) * \ldots \beta_0(t)}_{n+1 \text{ times}}. \tag{10.43}$$

The B-splines are clearly window functions; $\beta_n(t)$ has compact support. Now let us examine the Fourier transform of $\beta_n(t)$. Let $B_n(\omega) = \mathcal{F}(\beta_n)(\omega)$. The Fourier transform convolution theorem implies

$$B_n(\omega) = \left[ \frac{\sin\left(\frac{\omega}{2}\right)}{\frac{\omega}{2}} \right]^{n+1} . \tag{10.44}$$

So the denominator of (10.44) is $\omega^{n+1}$; in case $n \geq 1$, we see $\omega B_n(\omega) \in L^2(\mathbb{R})$, so that $B_n(\omega)$ is indeed a window function.

In Section 10.2.4 we formulate, refine, and quantify the concept of the a windowed Fourier transform's time-frequency localization. A crucial precondition for frequency-domain locality is that the window function's Fourier transform must also be a window function. Note that both the Gabor transform and the B-spline windowed STFT enjoy this condition. Before addressing the idea of joint localization, however, let us cover some STFT properties.

### 10.2.3 Properties

Many of the properties of the Gabor transform carry over directly to the short-time Fourier transform. Like the specialized Gabor transform, the STFT obeys basic properties of linearity, time shift, and frequency shift. We state and leave as exercises the STFT Plancherel, Parseval, and inverse results.

**Theorem (Short-Time Fourier Transform Parseval's).** Suppose $x(t), y(t) \in L^2(\mathbb{R})$; $w(t)$ is a window function; and let $X_w(\mu, \omega)$ and $Y_w(\mu, \omega)$ be the STFTs of $x(t)$ and $y(t)$, respectively, based on windowing with $w(t)$. Then

$$2\pi \|w\|_2^2 \langle x, y \rangle = \int_{-\infty}^{\infty} \int_{-\infty}^{\infty} X_w(\mu, \omega) \overline{Y_w(\mu, \omega)} \, d\omega d\mu = \langle X_w, Y_w \rangle_{L^2(\mathbb{R}^2)} . \tag{10.45}$$

***Proof:*** Similar to Gabor transform (exercise). ■

**Theorem (Short-Time Fourier Transform Plancherel's).** Suppose $\sigma > 0$; $x(t) \in L^2(\mathbb{R})$; $w(t)$ is a window function; and let $X_w(\mu, \omega)$ be the STFT of $x(t)$. Then

$$\|x\|_2 = \sqrt{2\pi} \frac{\|X_g(\mu, \omega)\|_{2, L^2(\mathbb{R}^2)}}{\|g\|_2} . \tag{10.46}$$

***Proof:*** Exercise. ■

**Theorem (Inverse Short-Time Fourier Transform).** Suppose $x(t) \in L^2(\mathbb{R})$, $w(t)$ is a window function, and let $X_w(\mu, \omega)$ be the STFT of $x(t)$. Then for all $a \in \mathbb{R}$, if $x(t)$ is continuous at $a$, then

$$x(a) = \frac{1}{(2\pi\|w\|_2^2)} \int_{-\infty}^{\infty} X_w(\mu, \omega) w(a) e^{j\omega a} d\omega d\mu . \tag{10.47}$$

***Proof:*** Apply a limit argument to the Parseval formula, as with the Gabor transform (exercise). ■

### 10.2.4 Time-Frequency Localization

How precisely we can locate the frequency values within a signal using the short-time Fourier transform? Section 10.1.5 showed how the Gaussian window width dramatically affects the transform coefficients. Indeed, an improperly chosen window width—determined by the standard deviation $\sigma$—can render the transform information useless for intepreting signal evolution through time. The reason is not too hard to grasp. By narrowing the window, we obtain a more precise time frame in which frequencies of interest occur. But if we calculate the transform from discrete samples, then we cannot shrink $\sigma$ too far; eventually the number of samples within the window are too few to compute the discrete signal frequencies. This is, of course, the threshold governed by the Nyquist rate. As $\sigma$ decreases, then, the Gabor transform gains time-domain resolution, but it loses frequency-domain resolution at the same time.

***10.2.4.1 Window Location and Size.*** To study the tradeoffs between time and frequency-domain resolution requires first of all a standard for measuring a signal's width or extent. The standard deviation of the enclosing Gaussian is a natural choice for the Gabor elementary function, $y(t) = g_{\mu,\sigma}(t)\exp(j\omega t)$. Recalling the Gaussian or normal distribution from the probability theory tutorial in Section 1.8, the probability that a normally distributed random variable has a value within one standard deviation of the mean $\mu$ is approximately 68%. That is, the area under the bell curve from $\mu - \sigma$ to $\mu + \sigma$ is about 0.68, whereas the total underlying area is unity. Thus, we propose $2\sigma$ for the "width" of $y(t)$, rather than a single standard deviation. Now, the standard deviation for a normally distributed random variable with density function $g_{\mu,\sigma}(t)$ is

$$\sigma = \left[ \int_{-\infty}^{\infty} (t-\mu)^2 g_{\mu,\sigma}(t) dt \right]^{\frac{1}{2}} . \tag{10.48}$$

Can we extend this scheme to a general $x(t) \in L^2(\mathbb{R})$ which we propose to Gabor transform? The answer is, unfortunately, no; we do know that there are signals that have finite energy without being integrable. The canonical example in signal processing is $\text{sinc}(t) = \sin(t)/t$. It is square-integrable, because $\text{sinc}^2(t)$ decays like $t^{-2}$ at

infinity. However, $\text{sinc}(t) \notin L^1(\mathbb{R})$, because, for instance, its Fourier transform is a square pulse, which is not continuous. Another problem is that the second moment integral (10.48) must also be valid. The following definition accounts for both difficulties, but we need a preliminary lemma.

**Lemma.** If $x(t)$ is a window function, then $t^{1/2}x(t) \in L^2(\mathbb{R})$.

***Proof:*** This turns out to be a consequence—through the Schwarz inequality—of the square integrability of $x(t)$ and $tx(t)$. We leave this as an exercise. ■

**Definition (Center and Radius).** If $x(t)$ is a window function, then the *center* $C_x$ and the *radius* $\rho_x$ for $x(t)$ are given by

$$C_x = \frac{1}{\|x\|_2^2} \int_{-\infty}^{\infty} t|x(t)|^2 \, dt \tag{10.49a}$$

and

$$\rho_x = \left[ \frac{1}{\|x\|_2^2} \int_{-\infty}^{\infty} (t - C_x)^2 |x(t)|^2 \, dt \right]^{\frac{1}{2}}, \tag{10.49b}$$

respectively. The *diameter* or *width* of a windowing function $x(t)$ is $\Delta_x = 2\rho_x$.

*Remark.* The lemma assures us that the integral (10.49a) exists.

The more highly concentrated a signal $x(t)$ is about its center $C_x$, the smaller is its radius $\rho_x$. Let us consider a few examples of window functions before stating some of their basic properties.

**Examples (Window Functions).** Any Gaussian, $g(t) = A\exp(-Bt^2)$ is a window function as we already showed. All of the standard window functions of Table 10.2 are also window functions. The B-spline functions $\beta_n(t)$ are also window functions, and, for $n \geq 1$, $B_n(\omega)$ is a window function.

Now let us work out a few basic properties of window center and radius.

**Lemma (Window Translation and Modulation).** Suppose $x(t)$ is a window function and $y(t) = x(t + t_0)$. Then:

(a) $C_y = C_x - t_0$.
(b) If $X = \mathcal{F}x$ and $Y = \mathcal{F}y$ are the Fourier transforms of $x$ and $y$, respectively, and $X$ and $Y$ are window functions, then $C_X = C_Y$.
(c) $\rho_y = \rho_x$.
(d) If $y(t) = \exp(-jC_X t)x(t + C_x)$ and $X = \mathcal{F}x$ and $Y = \mathcal{F}y$ are window functions, then $C_y = C_Y = 0$ and $\rho_y = \rho_x$.

***Proof:*** By the Shifting and Modulation Properties of the Fourier transform (exercises). ■

**Lemma (Radius of Derivative).** Suppose $x(t) \in L^2(\mathbb{R})$ and is differentiable. If $x'(t) \notin L^2(\mathbb{R})$, then $\rho_X = \infty$.

***Proof:*** Use Parseval's theorem for the radial Fourier transform and the formula for $\mathcal{F}[x'(t)](\omega)$. (exercise). ■

***10.2.4.2 Uncertainty Principle.*** The next theorem is the classic Heisenberg Uncertainty Principle[4] for the Fourier transform [20, 21]. The theorem says as a signal becomes more concentrated about its time-domain center, it becomes more dispersed about its frequency domain center. Recent tutorials on the Uncertainty Principle include [22, 23].

**Theorem (Heisenberg Uncertainty).** Suppose $x(t) \in L^2(\mathbb{R})$, $X(\omega) = \mathcal{F}[x](\omega)$ is the radial Fourier transform of $x(t)$. Then $\rho_x \rho_X \geq \frac{1}{2}$.

***Proof:*** We prove the Uncertainty Principle in two steps:

- First, for the happy circumstance that $x(t)$ obeys a special limit condition at infinity:

$$\lim_{t \to \infty} \sqrt{|t|}|x(t)| = 0; \tag{10.50}$$

  this condition does not necessarily hold for a square-integrable signal, of course; we could have $x(t) > \varepsilon > 0$ on some set $S$ of measure zero, for example.
- Then, for the general case by writing $x(t)$ as a limit of such continuous, piecewise smooth signals.

Note that we may assume that $x(t)$ is a window function; otherwise, $\rho_x = \infty$, so that $\rho_x \rho_X \geq 1/2$. We assume $X(\omega)$ is a window function as well, since otherwise $\rho_X = \infty$ with the same consequence. In either exceptional case, we are done. The Window Translation and Modulation Lemma allows the further simplifying assumption that $C_x = C_X = 0$. Therefore,

$$\begin{aligned} \rho_x^2 \rho_{\mathcal{F}x}^2 &= \left[\frac{1}{\|x\|_2^2} \int_{-\infty}^{\infty} t^2 |x(t)|^2 dt\right]\left[\frac{1}{\|X\|_2^2} \int_{-\infty}^{\infty} \omega^2 |X(\omega)|^2 d\omega\right] \\ &= \frac{1}{\|X\|_2^2 \|x\|_2^2}\left[\int_{-\infty}^{\infty} |tx(t)|^2 dt\right]\left[\int_{-\infty}^{\infty} |\omega X(\omega)|^2 d\omega\right]. \end{aligned} \tag{10.51}$$

[4]Werner Heisenberg (1901–1976) discovered that the probable location of a particle trades off against its probable momentum. In 1927, Heisenberg showed that $\Delta p \Delta x \geq 2h$, where $\Delta p$ represents the width of a particle's momentum distribution, $\Delta x$ is the width of its position distribution, and $h$ is Planck's constant [W. Heisenberg, *Physical Properties of the Quantum Theory*, New York: Dover, 1949].

Using Plancherel's theorem and the radial Fourier transform derivative formula gives

$$\rho_x^2\rho_{\mathcal{F}x}^2 = \frac{\|x\|_2^{-4}}{2\pi}\left[\int_{-\infty}^{\infty}|tx(t)|^2dt\right]\left[\int_{-\infty}^{\infty}|\mathcal{F}[x'(t)](\omega)|^2d\omega\right]$$
$$= \frac{\|x\|_2^{-4}}{2\pi}\|tx(t)\|_2^2\|\mathcal{F}[x'(t)](\omega)\|_2^2. \tag{10.52}$$

That is,

$$\|x\|_2^4\rho_x^2\rho_{\mathcal{F}x}^2 = \frac{1}{2\pi}\|tx(t)\|_2^2\|x'(t)\|_2^2 2\pi = \|tx(t)\|_2^2\|x'(t)\|_2^2. \tag{10.53}$$

Invoking the Schwarz inequality, $\|x\|_2\|y\|_2 \geq \|xy\|_1$, on (10.53) gives

$$\|x\|_2^4\rho_x^2\rho_{\mathcal{F}x}^2 \geq \|tx(t)x'(t)\|_1^2 = \left[\int_{-\infty}^{\infty}|tx(t)||x'(t)|\,dt\right]^2 = \left[\int_{-\infty}^{\infty}|t\overline{x(t)}||x'(t)|\,dt\right]^2 \tag{10.54}$$

and, continuing our algebraic duties, we find that

$$\|x\|_2^4\rho_x^2\rho_{\mathcal{F}x}^2 \geq \left|\int_{-\infty}^{\infty}t\overline{x(t)}x'(t)dt\right|^2 = \left(|\langle x'(t), tx(t)\rangle|^2 \geq (\mathrm{Re}\langle x'(t), tx(t)\rangle)^2\right). \tag{10.55}$$

Now, we claim the following:

$$(\mathrm{Re}\langle x'(t), tx(t)\rangle) = -\frac{1}{2}\int_{-\infty}^{\infty}|x(t)|^2dt = -\frac{1}{2}\|x(t)\|^2. \tag{10.56}$$

The trick behind the strange looking (10.56) is integration by parts on the inner product integral:

$$\int_{-\infty}^{\infty}t\overline{x(t)}x'(t)\,dt = t\overline{x(t)}x(t)\Big|_{-\infty}^{\infty} - \int_{-\infty}^{\infty}x(t)[t\overline{x'(t)} + \overline{x(t)}]\,dt$$
$$= 0 - \int_{-\infty}^{\infty}x(t)[t\overline{x'(t)} + \overline{x(t)}]\,dt. \tag{10.57}$$

Note that we have invoked (10.50) to conclude that $t|x(t)|^2 \to 0$ as $|t| \to \infty$. Separating the bottom of (10.57) into two integrals gives

$$\int_{-\infty}^{\infty}t\overline{x(t)}x'(t)\,dt = -\int_{-\infty}^{\infty}|x(t)|^2dt - \overline{\int_{-\infty}^{\infty}t\overline{x(t)}x'(t)\,dt}. \tag{10.58}$$

After rearrangment, the claim (10.56) easily follows. We insert the result into the inequality (10.55), thereby finding

$$\|x\|_2^4 \rho_x^2 \rho_{\mathcal{F}x}^2 \geq \frac{\|x\|_2^4}{4} \tag{10.59}$$

and hence $\rho_x \rho_X \geq \frac{1}{2}$.

Let us proceed to the second step in the proof: removing the limit assumption (10.50) on the finite energy signal $x(t)$. We write $x(t)$ as the limit of a sequence of signals in the Schwarz space $S$ of infinitely continuously differentiable, rapidly decreasing signals [21]:

$$x(t) = \lim_{n \to \infty} x_n(t) . \tag{10.60}$$

We introduced the Schwarz space in Chapter 3 and know it to be dense in both $L^2(\mathbb{R})$ and $L^1(\mathbb{R})$. Since for all $x \in S$, we have $t|x(t)|^2 \to 0$ as $|t| \to \infty$, we have

$$\lim_{n \to \infty} \int_{-\infty}^{\infty} t\overline{x_n(t)} x_n'(t) dt = \lim_{n \to \infty} t\overline{x_n(t)} x_n(t) \Big|_{-\infty}^{\infty} - \lim_{n \to \infty} \int_{-\infty}^{\infty} x_n(t) [t\overline{x_n'(t)} + \overline{x_n(t)}] \, dt. \tag{10.61}$$

Because $x_n \in S$, which decreases faster than any polynomial, the integrands in (10.61) are absolutely integrable and we may interchange the integration and limit operations. Schwarz space elements are also continuous, so the first limit on the right-hand side of (10.61) is still zero. Thus,

$$\int_{-\infty}^{\infty} \lim_{n \to \infty} t\overline{x_n(t)} x_n'(t) \, dt = - \int_{-\infty}^{\infty} \lim_{n \to \infty} x(t) [t\overline{x_n'(t)} + \overline{x_n(t)}] \, dt . \tag{10.62}$$

But these limits are precisely (10.57). ■

The above proof follows Weyl's derivation [24], which he published in 1931.[5]

Thus, every windowed Fourier transform has a lower limit on its joint time-frequency resolution. If we work with a transform based on a window function $w(t)$ whose Fourier transform $W(\omega)$ is also a window function, then it makes sense to define the time-frequency resolution as the product $\rho_w \rho_W$. If we use a standard window function—a Hamming window, for example—whose Fourier transform is not itself a window function, then $\rho_W$ is infinite. The Uncertainty Principle tells us that this is a hard lower bound: $\rho_w \rho_W \geq 1/2$. As a practical consequence, smaller time-domain window sizes result in proportionally large frequency-domain window

[5]The interests of Hilbert's student, Hermann Weyl (1885–1955), ranged from quantum mechanics to number theory. He showed, for instance, that given an irrational number r, the fractional parts of $r$, $2r$, $3r$, ..., etc., lie uniformly distributed on the interval (0, 1).

sizes. As we attempt to better locate a signal oscillation, we suffer a corresponding loss of accuracy in estimating the precise frequency of the oscillation.

There are window functions that achieve the lower bound on time-frequency localization given by the Heisenberg Uncertainty Principle. The next section shows that the optimally localizing window is none other than the Gaussian.

***10.2.4.3 Optimally Localized Signals.*** The Gabor transform is the short-time Fourier transform with the smallest time-frequency resolution. We identify *time-frequency resolution* with the joint product of the time-domain and frequency-domain radius: $\rho_x \rho_X$. To derive this optimality claim, we review the Uncertainty Principle's proof. Our scrutiny shows that inequality arises with its use of the Schwarz inequality [21].

**Corollary (Optimal Time-Frequency Locality).** We have $\rho_x \rho_X = \frac{1}{2}$ if and only if $x(t) = ae^{-bt^2}$ for some $a \in \mathbb{C}$ and $b \geq 0$.

***Proof:*** We recall that $\|x\|_2 \|y\|_2 \geq \|xy\|_1$ always, and equality occurs if and only if $x = cy$ for some constant $c \in \mathbb{C}$. In the context of the proof, then, optimally small time-frequency locality coincides with the condition $x'(t) = ctx(t)$. Are there any $L^2(\mathbb{R})$ signals satisfying the above differential equation? It is a basic first-order differential equation, but before we note the solution, let us address two problems:

- Since the Uncertainty Principle deals with square-integrable signals $x(t)$, we understand this equality as occurring almost everywhere; that is, we require $x'(t) = ctx(t)$ except on some set of measure zero.
- Furthermore, the proof depends on the fact that we can represent a general $x(t) \in L^2(\mathbb{R})$ as the limit of a sequence $x(t) = \lim_{n \to \infty} x_n(t)$, where $x_n(t) \in S$, the Schwarz space of infinitely continuously differentiable, rapidly decreasing signals. We must therefore show that for any $x(t)$ satisfying the differential equation, which is an $L^2(\mathbb{R})$ limit of $x_n(t) \in S$, that

$$x'(t) = \lim_{n \to \infty} x_n'(t). \tag{10.63}$$

In the convenient Schwarz space, the second point is straightforward. Indeed, we recall that $x(t) = y'(t)$ in Lebesgue integration theory means

$$y(t) = \int_0^t x(s)ds + y(0) \tag{10.64}$$

almost everywhere. We have $x(t) - x(0) = \lim_{n \to \infty} [x_n(t) - x_n(0)]$, and the $x_n(t) \in S$ are infinitely continuously differentiable; thus,

$$x(t) - x(0) = \lim_{n \to \infty} \int_0^t x_n'(s)\, ds = \int_0^t x'(s)\, ds. \tag{10.65}$$

To solve the differential equation, note that $t^{-1}x'(t) = c\overline{x(t)}$, whereby

$$\{t^{-1}x'(t)\}' = \{c\overline{x(t)}\}' = c\overline{x'(t)} = c\bar{c}tx(t) = |c|^2 tx(t). \tag{10.66}$$

If we let $b = |c|^2$, then the solutions to this second-order differential equation are of the form $x(t) = ae^{-bt^2}$, where $a \in \mathbb{C}$ is a constant. ■

**Example (STFT based on a B-Spline Window).** Suppose we use a B-spline function $\beta(t) = \beta_n(t)$, where $n \geq 1$, to define a short-time Fourier transform. We know that $\omega B_n(\omega) \in L^2(\mathbb{R})$, so that $B_n(\omega)$ is indeed a window function. The Uncertainty Principle applies. The Gaussian is not a B-spline, however, and we know therefore that $\rho_\beta \rho_B > 1/2$.

## 10.3 DISCRETIZATION

The short-time Fourier transform can also be discretized. There are two possible approaches:

- To compose discrete sums from values of a discrete signal $x(n)$, which is covered in Section 10.3.1.
- To sample the ordinary analog STFT analysis equation of an analog signal $x_a(t)$—the far more interesting and challenging problem—introduced in Section 10.3.2 and further explored in the sequel.

The second approach is our main emphasis. Its successful development leads to a new structural decomposition of finite-energy analog signals. It was also a focus of Gabor's original paper 1, a preoccupation of a number of later signal analysts, and the wellspring of much of our later insight into the nature of mixed-domain signal interpretation. We shall in fact pursue this idea for the remainder of this chapter.

### 10.3.1 Transforming Discrete Signals

Working with discrete signals, we can forumulate a purely discrete theory of windowed Fourier transforms. The results are not difficult to develop, and it turns out that they follow directly from discrete Fourier theorems. We are thus content to explicate only the discrete STFT synthesis and energy conservation equations.

We begin with a discrete signal $x(n)$ having period $N > 0$, $x(n) = x(n + N)$. Alternatively, we may select $N$ samples $\{s(n): 0 \leq n < N\}$ from an arbitrary discrete signal $s(n)$ and consider the periodic extension $x(n) = s(n \bmod N)$. We require the discrete window function to be nonzero and have the same period as the signal to be transformed.

**Definition (Discrete Short-Time Fourier Transform).** Let $x(n)$ and $w(n)$ be discrete signals of period $N > 0$. Further suppose $w(n)$ is real and not identically zero

on $[0, N-1]$. Then the *discrete short-time Fourier transform* (or *discrete windowed fourier transform*) of $x(n)$ with respect to $w(n)$ is

$$X_w(m,k) = \sum_{n=0}^{N-1} x(n)w(n-m)e^{-2\pi jk\frac{n}{N}}. \tag{10.67}$$

The signal $w(n)$ is called the *windowing function* for the transform.

**Definition (Discrete Gabor Elementary Function).** Let $w(n)$ be a discrete signal of period $N > 0$, with $w(n)$ is not identically zero on $[0, N-1]$. Then the *discrete Gabor elementary function* or *discrete Gabor atom* of discrete frequency $k \in [0, N-1]$ and location $m \in [0, N-1]$ is $w_{m,k}(n) = w(n-m)\exp(2\pi jkn/N)$.

As with its analog world counterpart, the discrete STFT can be viewed in several ways. In particular, we may think of (10.67) as giving

- For each $m \in [0, N-1]$, the discrete Fourier transform (DFT) of $x(n)w(n-m)$;
- For each $k \in [0, N-1]$, the inner product on $[0, N-1]$ of $x(n)$ with the discrete GEF $w_{m,k}(n)$.

The following theorem gives the synthesis equation for the discrete STFT.

**Theorem (Inverse Discrete STFT).** Let $x(n)$ and be a discrete signal with period $N > 0$; let $X_w(m,k)$ be its discrete STFT with respect to the windowing function $w(n)$; and, finally, let $\|w\|_2$ be the $l^2$-norm of $w(n)$ restricted to the interval $[0, N-1]$: $\|w\|_2 = [w^2(0) + w^2(1) + \cdots + w^2(N-1)]^{1/2}$. Then,

$$x(n) = \frac{1}{N\|w\|_2^2}\sum_{m=0}^{N-1}\sum_{k=0}^{N-1} X_w(m,k)w(n-m)e^{2\pi jk\frac{n}{N}}. \tag{10.68}$$

***Proof:*** Substituting the definition of $X_w(m,k)$ into the double summation on the right-hand side of (10.68) gives

$$\sum_{m=0}^{N-1}\sum_{k=0}^{N-1}\sum_{p=0}^{N-1} x(p)w(p-m)e^{-2\pi jk\frac{p}{N}}w(n-m)e^{2\pi jk\frac{n}{N}}. \tag{10.69}$$

Rearrangment of the sums produces

$$\sum_{p=0}^{N-1} x(p)\sum_{m=0}^{N-1} w(p-m)w(n-m)\sum_{k=0}^{N-1} e^{2\pi jk\frac{(n-p)}{N}}. \tag{10.70}$$

Reciting what has become a familiar and fun argument, we note that the final sum in is zero unless $n = p$, in which case it is $N$. Therefore the entire triple summation is simply

$$Nx(n)\sum_{m=0}^{N-1} w(n-m)w(n-m) \;=\; Nx(n)\|w\|_2^2, \tag{10.71}$$

and the theorem follows. ■

**Theorem (Discrete STFT Parseval's).** Let $x(n)$ and be a discrete signal with period $N > 0$; let $X_w(m, k)$ be its discrete STFT with respect to the windowing function $w(n)$; and, finally, let $\|w\|_2$ be as in the previous theorem. Then,

$$\sum_{n=0}^{N-1} |x(n)|^2 \;=\; \frac{1}{N\|w\|_2^2}\sum_{m=0}^{N-1}\sum_{k=0}^{N-1} \left|X_w(m, k)\right|^2. \tag{10.72}$$

***Proof:*** Let us expand the double summation on the right-hand side of (10.72):

$$\sum_{m=0}^{N-1}\sum_{k=0}^{N-1}\left[\sum_{p=0}^{N-1} x(p)w(p-m)e^{-2\pi jk\frac{p}{N}}\right]\left[\sum_{q=0}^{N-1} \overline{x(q)}w(q-m)e^{2\pi jk\frac{q}{N}}\right]. \tag{10.73}$$

Interchanging the sums we find that (10.73) becomes

$$\sum_{p=0}^{N-1}\sum_{q=0}^{N-1} x(p)\overline{x(q)}\left[\sum_{m=0}^{N-1} w(p-m)w(q-m)\right]\left[\sum_{k=0}^{N-1} e^{2\pi jk\frac{(q-p)}{N}}\right]. \tag{10.74}$$

The final bracketed sum is either $N$ or 0, depending on whether $p = q$ or not, respectively. Since only the case $p = q$ contributes to the sum, we let $n = p = q$ and reduce the double summation on the left-hand side of (10.74) to a single sum over $n$:

$$N\sum_{n=0}^{N-1} x(n)\overline{x(n)}\left[\sum_{m=0}^{N-1} w(n-m)w(n-m)\right]. \tag{10.75}$$

Finally we see

$$N\|w\|_2^2\sum_{n=0}^{N-1} x(n)\overline{x(n)} \;=\; \sum_{m=0}^{N-1}\sum_{k=0}^{N-1} \left|X_w(m, k)\right|^2, \tag{10.76}$$

using the periodicity of $w(n)$. ■

### 10.3.2 Sampling the Short-Time Fourier Transform

Now let us turn to the deeper question of what happens we attempt to sample the STFT. We select a time-domain sampling interval $T > 0$ and a frequency-domain

sampling interval $\Omega > 0$. These remain fixed for the discrete transform, and a complex-valued function on pairs of integers results. It might appear that our endeavors here will not differ radically in method and results from the work we did earlier in discretizing the Fourier transform. Quite the opposite turns out to be the case: Discretization of the windowed Fourier transform opens the door to a wealth of intriguing problems in signal analysis.

For one thing, discretizing the transform provides us with a ready breakdown of the signal into time localized frequency components, or time-frequency atoms. Each atom represents a spot in time. Each atom represents a possible frequency component. And—depending on the nature of our atomic signal building blocks—there is a way to measure the quantity of that frequency resident in the signal in the vicinity a discrete time instant. This is a structural decomposition of the signal. Chapters 4 and 9 explored time- and frequency- domain signal analysis, respectively. Among their lessons is the usefulness of a structural decomposition of the signal for purposes of classification, recognition, and interpretation. Time-frequency transforms benefit signal analysis by providing an elegant, formal mathematical theory as well as a relational description of the signal.

Discretization places Gabor's original problem on the agenda [1]. He proposed to model communication signals using families of discretely indexed signal elements, which he called *logons*, but which nowadays are known by various other monikers—*Gabor elementary functions*, *Gabor atoms*, *windowed Fourier atoms*, and so on. Can families of the form $\{\exp(2\pi jnt)g(t - m)\colon m, n \in \mathbb{Z}\}$ provide an orthonormal basis for $L^2(\mathbb{R})$ signals? Their optimal joint time-frequency localization does recommend them, but neither Gabor nor any other signal analyst for decades after his suggestive 1946 paper could substantiate in theory what seemed so tantalizing for practice.

It was a negative answer to Gabor's insightful proposal that began to emerge in the 1980s, a decade marking a watershed of results in time-frequency and time-scale signal analysis. The rest of the chapter elaborates some of these apparently discouraging results for short-time Fourier methods. The next chapter suggests an alternative approach, motivated in part our understanding of the limitations inherent in atomic time-frequency signal decompositions. Chapter 11 does show that transformations that rely on signal scale instead—the wavelet transform in particular—may avoid the weaknesses of short-time Fourier techniques.

**Definition (Discretized Short-Time Fourier Transform).** Suppose that $X_w(\mu, \omega)$ is the STFT of $x(t) \in L^2(\mathbb{R})$ with respect to the window function $w(t)$. Given $T > 0$ and $\Omega > 0$, the *discretized short-time Fourier transform* is

$$X_w(m, n) = (X_w)_a(m\Omega, nT) = \int_{-\infty}^{\infty} x(t)w(t - mT)e^{-jn\Omega t}dt\,. \tag{10.77}$$

If distinguishing between the discrete and analog transform signals becomes a problem, then we can append a subscript $a$ to the analog form, as in (10.77). Note that

we are using the first discrete independent variable of $X_w(m, n)$ as the time index and are using the second variable as the frequency index.

### 10.3.3 Extracting Signal Structure

If we can find a sufficiently strong mathematical representation, then discretized short-time Fourier transforms provide an attractive means of describing signal structure. We have already covered the broad qualifications for such a represenation. It must be able to represent any candidate signal, for otherwise some inputs will avoid our decomposition method. The representation must also be stable, which, informally, means that changing the signal a little bit only perturbs the representation a little bit.

So, the question is, Can windowed Fourier atoms of the form

$$w_{m,\,n}(t) = e^{jn\Omega t} w(t - mT)\,, \tag{10.78}$$

where $T > 0$ and $T\Omega = 2\pi$, serve as a complete signal representation? The two practical alternatives are that the family $\{w_{m,n}(t)\colon m, n \in \mathbb{Z}\}$ constitutes either

- An orthonormal basis or
- A frame.

It is hoped that we can discover $\{w_{m,n}(t)\colon m, n \in \mathbb{Z}\}$ that make up an orthonormal basis. Then every square-integrable signal $x(t)$ has a expansion in terms of Fourier coefficients, easily calcuated as the inner products of $x(t)$ with the $w_{m,n}(t)$:

$$x(t) = \sum_{m,\,n \in \mathrm{Z}} \langle x(t), w_{m,\,n}(t)\rangle w_{m,\,n}(t). \tag{10.79}$$

If we fail to find such a basis, then computing the expansion coefficients (10.79) becomes problematic. Lack of a basis encumbers our signal analysis too. While we might be able to decompose a candidate signal $x(t)$ into a linear combination of atoms, $x(t) = \Sigma c_{m,n} w_{m,n}(t)$, we do not necessarily know the uniqueness of the expansion coefficients $c_{m,n}$ for representing $x(t)$. So the utility of the expansion coefficients as indicators of some signal component's presence or the lack thereof is very much compromised.

Should a basis not be available, we could search for a frame representation of $L^2(\mathbb{R})$ signals using the Gabor atoms (10.118). After all, we know from Chapter 3 that frame coefficients can characterize the source signal $x(t)$, and they support numerically stable reconstructions. This may be a good redoubt.

***10.3.3.1 Discrete Time-Frequency Plane.*** Toward building a structural interpretation of a signal, we can place the expansion coefficients $c_{m,n}$ into an array. Thus, for a fixed frequency $n\Omega$, the rows of the array, $\{c_{m,n}\colon m \in \mathbb{Z}\}$, indicate the relative weight of frequency $n\Omega$ inside signal $x(t)$ at all time instants $mT$. Similarly, the columns record the frequencies at a given time instant. Refer to Figure 10.9.

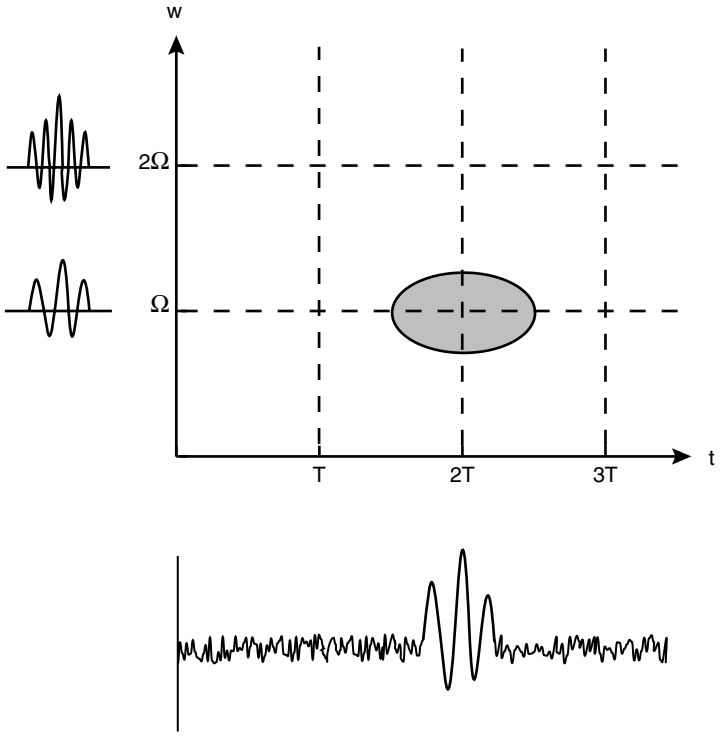


**Fig. 10.9.** Discretized STFT coefficients arranged in a rectangular grid.

Notice that upon discretizing the STFT we have a mathmatical signal transform that resolves a signal into finite regions of the time-frequency plane. The Fourier series of Chapter 5, in contrast, can only furnish time-frequency regions of infinite time- domain extent. When we covered discrete Fourier theory in Chapter 7, we studied the sampling theorem by which a band-limited analog signal can be reconstructed from sufficiently dense discrete samples. The sampling theorem too implies a partition of the time-frequency plane, except that its regions have an infinite frequency-domain extent. The STFT therefore marks a theoretical advance within our signal analytic understanding.

As a relational structure, this partition of the time-frequency plane is quite simple. Each region has the same size as its neighbors. We can, however, adjust the size of the regions to be smaller or larger in time or frequency by dilating our windowing function. The Uncertainty Principle imposes the constraint that the area of the STFT regions be no smaller than that given by the Gabor transform. Signal analysis applications based on STFT methods generally search the corresponding time-frequency mesh in order to understand signal content.

Let us consider some examples of how the time-frequency decomposition structure presents itself in applications.

Figure 10.10 illustrates a time-frequency mesh that contains a linear chirp and what is apparently a tone. Chirp signal energy concentration is fairly constant and can

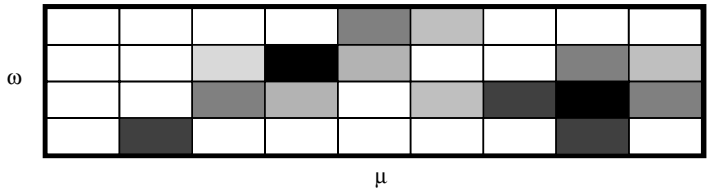


**Fig. 10.10.** Schematic representation of a signal with two components: a linear chirp and an isolated tone.

be tracked as a rising line over time. Tone signal energy concentration remains at a fixed frequency. Clicks or pops are characterized by a narrow time-domain extent and an extended, more or less uniform distribution of signal energy over a wide range of frequencies—a vertical linear structure. A sinusoidal tone is a horizontal linear structure. These ideas are only schematic, but they convey some of the signal varieties that are amenable to time-frequency analysis.

Let us now consider a speech analysis application. We have considered speech signal interpretation already in Chapters 4 and 9. In fact, in Chapter 9 we saw that many speech recognition systems have been developed using the basic technique of windowing the Fourier transform. If $x(t)$ is a speech signal, for example, then looking for a large percentage of signal energy in a pair of frequencies might indicate the presence of a vowel phoneme. Or, a broad dispersion of signal energy in a range of high frequencies could mark a velar fricative. Time-frequency signal decomposition offers a complete picture of the speech waveform. Figure 10.11 shows a contour diagram of the energies in a speech fragment.

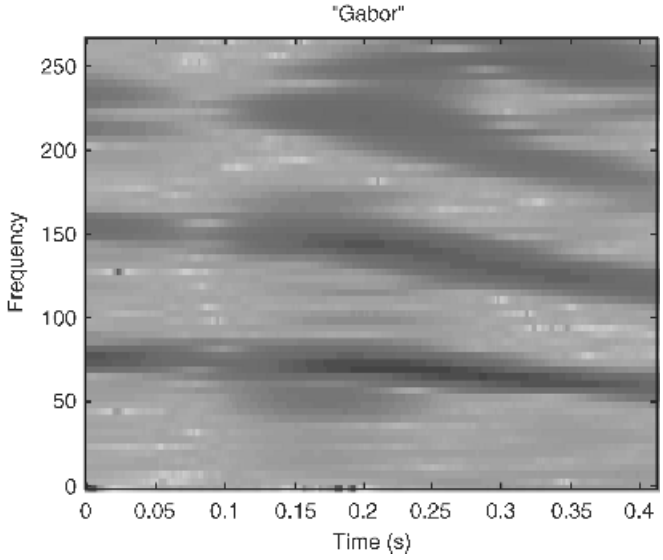


**Fig. 10.11.** The time-frequency decomposition of the word "Gabor." Lines indicate signal energy contours. Note that the two syllables can be segmented in time according to the distribution of signal energy along the frequency axis.

***10.3.3.2 Identifying Significant Local Frequency Components.*** Many of the filtering, enhancement, and thresholding techniques we applied in time-domain signal analysis can help us find localized signal frequency components. For instance, we might use a threshold to indicate a significant frequency component. Furthermore, we might calculate the total amount of energy among all time-frequency cells at a certain time instant and count the number that contain say a majority of the energy. Such quantities can be assembled into feature vectors, for example. All of the methods we employed in Chapter 4 for thresholding signals apply equally well to thresholding values in the two-dimensional time-frequency plane. Indeed, this is an elementary instance of image analysis, and with it, our work in interpreting signal content begins to take advantage of techniques in image processing and computer vision.

### 10.3.4 A Fundamental Limitation

We have observed that the windowed Fourier transform provides an elegant and natural description of signal structure—a two-dimensional array, easily searched along time or frequency axes. With other decomposition techniques, especially those revolving around signal scale, structures may assume the form of a tree or some more general graph. Traversing graph structures consumes computer time. So even though our derived structures may be far simpler than the time-domain signal, we are still concerned to make the graphs sparse and conclude our exhaustive search as quickly as possible. Hence the problem before us is, How large can we choose the time and frequency sampling intervals, $T$ and $\Omega$, so that we still build a family of windowed Fourier atoms that provide an orthonormal basis or exact frame structure?

***10.3.4.1 Nyquist Density.*** Our question directly concerns the power of short-time Fourier transforms for signal interpretation. Gabor studied the case $T\Omega = 2\pi$, suggesting that the Fourier expansion coefficients could be used to encode a signal for efficient transmission. Note too that for this case the time-domain sampling interval is $T = 2\pi/\Omega$. If a signal $x(t)$ has bandwidth $\Omega$, then its highest frequency component is $\Omega/2$ radians per second, or $F_{\max} = (\Omega/2)/(2\pi) = \Omega/(4\pi)$ hertz. By the Shannon–Nyquist sampling theorem, it can be reconstructed from discrete samples taken at intervals sampled at a rate not less than $F = T^{-1} = 2F_{\max} = \Omega/(2\pi)$ hertz. We offer the formal definition.

**Definition (Time-Frequency, Nyquist Densities).** Let $x(t)$ have bandwidth $\Omega$ and be sampled at intervals $T > 0$. Then we define its *time-frequency density* to be $(T\Omega)^{-1}$. The *Nyquist density* is $(2\pi)^{-1}$.

In other words, Gabor's concern was to set the time- and frequency-domain sampling intervals so that $T\Omega = 2\pi$—that is, to sample at the Nyquist density. This is equivalent to time sampling at the largest interval allowable, by the sampling theorem, for analog signal reconstruction from discrete samples. Gabor proposed families of windowed Fourier atoms, separated from one another at the Nyquist

limit $T = 2\pi\Omega^{-1}$. Our problem is to characterize Gabor's proposal for each of the three cases:

(i) $T\Omega < 2\pi$, when the sampling interval is less than the Nyquist frequency or, equivalently, when the time-frequency density exceeds the Nyquist density.
(ii) $T\Omega = 2\pi$, the original proposal of Gabor.
(iii) $T\Omega > 2\pi$.

***10.3.4.2 Too Sparse: $T\Omega > 2\pi$.*** Gabor's proposal to represent signals using sums of windowed Fourier atoms does not in fact succeed for the sparse case, $T\Omega > 2\pi$. This case occurs when the time- domain sampling interval exceeds the maximum allowable for reconstructing an analog signal of bandwidth $\Omega$ by its discrete samples at times $mT$, $m \in \mathbb{Z}$. That is, families of Gabor atoms $\{w_{m,n}(t) = \exp(jn\Omega)w(t - mT)$: $m, n \in \mathbb{Z}\}$ cannot be a frame when $(T\Omega)^{-1}$ is less than the Nyquist density.

Using the Zak transform, introduced in Chapter 8, this result can be shown for the case where $(2\pi)^{-1}T\Omega$ is rational and exceeds unity. We will only consider a far simpler case: $\Omega = 2\pi$ and $T = 2$. We recount the following results from Ref. 12.

**Lemma.** Let $w(t) \in L^2(\mathbb{R})$; $w_{m,n}(t) = e^{jn\Omega t}w(t - mT)$, for $m, n \in \mathbb{Z}$; $\Omega = 2\pi$; and $T = 2$. Then there is an $x(t) \in L^2(\mathbb{R})$ such that $\|x\|_2 \neq 0$ and $\langle x(t), w_{m,n}(t)\rangle = 0$ for all $m, n \in \mathbb{Z}$.

***Proof:*** Let $t \in [0, 1)$ and define

$$x(t + k) = (-1)^k \overline{w(t - k - 1)}, \tag{10.80}$$

where $k \in \mathbb{Z}$. It is easily shown (exercise) that

(i) $x \in L^2(\mathbb{R})$.
(ii) $\|x\|_2 = \|w\|_2$.
(iii) $\|x\|_2 \neq 0$.

We contend that $\langle x(t), w_{m,n}(t)\rangle = 0$ for all $m, n \in \mathbb{Z}$. Breaking up the inner product integral reveals

$$\begin{aligned}\langle x(t), w_{m,n}(t)\rangle &= \int_{-\infty}^{\infty} x(t)\overline{e^{jn\Omega t}w(t - 2m)}\, dt \\ &= \int_{0}^{1} e^{-jn\Omega t} \sum_{k=-\infty}^{\infty} x(t + k)\overline{w(k + t - 2m)}\, dt\end{aligned} \tag{10.81}$$

But inserting (10.80), we observe that

$$\sum_{k=-\infty}^{\infty} x(t + k)\overline{w(k + t - 2m)} = \sum_{k=-\infty}^{\infty} (-1)^k \overline{w(t - k - 1)}\,\overline{w(t + k - 2m)}. \tag{10.82}$$

On the right-hand side of (10.82) consider a summand,

$$(-1)^k \overline{w(t-k-1)}\,\overline{w(t+k-2m)}\,, \tag{10.83a}$$

for some $k \in \mathbb{Z}$. Let $i = 2m - k - 1$ and compare the term

$$(-1)^i \overline{w(t-i-m)}\,\overline{w(t+i-2m)}\,. \tag{10.83b}$$

The trick is that

$$(-1)^i \overline{w(t-i-m)}\,\overline{w(t+i-2m)} = (-1)^{-k-1} \overline{w(t-2m+k)}\,\overline{w(t-k-1)}\,, \tag{10.84}$$

which is the additive inverse of (10.83a). The upshot is that every summand in is complemented by its additive inverse also inside the summation; the sum is precisely zero! All inner products (10.81) are zero, and we have constructed a nontrivial $x(t)$ in the orthogonal complement of $\{w_{m,n}(t)\colon m, n \in \mathbb{Z}\}$. ■

Now we can prove the theorem. Recall that a frame generalizes the notion of an orthogonal basis, yet provides stable signal reconstruction and complete signal representation. We introduced frame theory in Section 3.3.4.

**Theorem.** Let $w(t) \in L^2(\mathbb{R})$; $w_{m,n}(t) = e^{jn\Omega t} w(t - mT)$, for $m, n \in \mathbb{Z}$; $\Omega = 2\pi$; and $T = 2$. Then $\{w_{m,n}(t)\colon m, n \in \mathbb{Z}\}$ cannot be a frame.

***Proof:*** Let $x(t)$ be given by the lemma: nontrivial and orthogonal to all of the $w_{m,n}(t)$. If the $\{w_{m,n}(t)\colon m, n \in \mathbb{Z}\}$ were a frame, then by the definition of frame, there exist $A > 0$ and $B > 0$ such that

$$A\|y\|^2 \le \sum_{m,\, n\, =\, -\infty}^{\infty} \left|\langle y, w_n \rangle\right|^2 \le B\|y\| \tag{10.85}$$

for all $y(t) \in L^2(\mathbb{R})$. The frame condition must hold for the lemma's $x(t)$ as well, but since $\langle x(t), w_{m,n}(t)\rangle = 0$ for all $m, n \in \mathbb{Z}$, we have a contradiction. ■

*Remark.* So there are no frames of windowed Fourier atoms, $w_{m,n}(t) = e^{jn\Omega t} w(t - mT)$, when the frequency- and time-domain sampling intervals are $\Omega = 2\pi$; and $T = 2$, respectively. This is perhaps not too surprising a result, given the Shannon–Nyquist sampling theorem.

We have shown our result for only a particular instance, $\Omega = 2\pi$ and $T = 2$, of the case $T\Omega > 2\pi$. An interesting, but somewhat technical, Zak transform application extends this same argument whenever $T\Omega > 2\pi$ and $T\Omega$ is a rational multiple of $2\pi$ [25]. Using advanced mathematical methods well beyond our present scope, it has been shown that whenever the time-frequency sampling is too sparse—whether either $T$ and $\Omega$ are rational or irrational—then there are no frames of windowed Fourier atoms [26].

### 10.3.5 Frames of Windowed Fourier Atoms

Now let us consider another possibility: $T\Omega < 2\pi$. This is the dense time-frequency sampling case. Now, from a classic construction [27], it can be shown that we can build frames from windowed Fourier atoms when $T\Omega < 2\pi$. Here, we adapt the presentation in Ref. 12 to our own notation and show that collections of Gabor atoms $\{w_{m,n}(t) = \exp(\, jn\Omega)w(t - mT)\colon m, n \in \mathbb{Z}\}$ can be a frame when $(T\Omega)^{-1}$ exceeds the Nyquist density, $(2\pi)^{-1}$.

**Theorem.** Let $w(t) \in L^2(\mathbb{R})$; let $w_{m,n}(t) = e^{\,jn\Omega t}w(t - mT)$, for $m, n \in \mathbb{Z}$; $T\Omega < 2\pi$; and suppose that $[-\pi/\Omega, \pi/\Omega] \supset \text{Support}(w)$. Then for any $x(t) \in L^2(\mathbb{R})$,

$$\sum_{m,\,n\,=\,-\infty}^{\infty} \left|\langle x, w_{m,\,n}\rangle\right|^2 = \frac{2\pi}{\Omega}\int_{-\infty}^{\infty} |x(t)|^2\left(\sum_{k\,=\,-\infty}^{\infty} |w(t - kT)|^2\right) dt\,. \tag{10.86}$$

***Proof:*** Let us expand the sum on the left-hand side of (10.86) as sums over $2\pi/\Omega$-wide intervals:

$$\sum_{m,\,n\,=\,-\infty}^{\infty} \left|\langle x, w_{m,\,n}\rangle\right|^2 = \sum_{m,\,n\,=\,-\infty}^{\infty}\left|\int_0^{\frac{2\pi}{\Omega}} e^{jn\Omega t}\sum_{k\,=\,-\infty}^{\infty} x\left(t + \frac{2\pi k}{\Omega}\right)\overline{w\left(t + \frac{2\pi k}{\Omega} - mT\right)}\right|^2 dt. \tag{10.87}$$

Notice that the integral in (10.87) is a constant multiple of a Fourier series coefficient. The functions $\sqrt{\frac{\Omega}{2\pi}}e^{jn\Omega t} = e_n(t)$ are an orthonormal basis for the Hilbert space $H = L^2[0, 2\pi/\Omega]$, and we know therefore that $\|y\|_2^2 = \sum_n \left|\langle y, e_n\rangle\right|^2$ for any square-integrable $y(t)$ in $H$. (This is in fact a Parseval result for $H$, and its roots extend back to our very early algebraic result from abstract Banach spaces—Bessel's inequality.) Thus, for each $m \in \mathbb{Z}$ we are able to replace the sum over $n \in \mathbb{Z}$ in (10.87) with the square of the $L^2[0, 2\pi/\Omega]$ norm of the sum in the integrand:

$$\sum_{m,\,n\,=\,-\infty}^{\infty} \left|\langle x, w_{m,\,n}\rangle\right|^2 = \frac{2\pi}{\Omega}\sum_{m\,=\,-\infty}^{\infty}\int_0^{\frac{2\pi}{\Omega}}\left|\sum_{k\,=\,-\infty}^{\infty} x\left(t + \frac{2\pi k}{\Omega}\right)\overline{w\left(t + \frac{2\pi k}{\Omega} - mT\right)}\right|^2 dt\,. \tag{10.88}$$

Next, observe that for any $m$ all of the summands over $k$ inside the integral are zero except for possibly one. This is due to the choice of support for the window function $w(t)$. The right-hand side of  simplifies, and we see

$$\sum_{m,\,n\,=\,-\infty}^{\infty} \left|\langle x, w_{m,\,n}\rangle\right|^2 = \frac{2\pi}{\Omega}\sum_{m,\,k\,=\,-\infty}^{\infty}\int_0^{\frac{2\pi}{\Omega}}\left|x\left(t + \frac{2\pi k}{\Omega}\right)\overline{w\left(t + \frac{2\pi k}{\Omega} - mT\right)}\right|^2 dt. \tag{10.89}$$

We can now reassemble the separate finite integrals to one over the entire real line:

$$\sum_{m,\,n\,=\,-\infty}^{\infty} \left|\langle x, w_{m,\,n}\rangle\right|^2 = \frac{2\pi}{\Omega} \int_{-\infty}^{\infty} |x(t)|^2 \left( \sum_{k\,=\,-\infty}^{\infty} |w(t-kT)|^2 \right) dt\,. \tag{10.90}$$

■

The term in parentheses inside the integral (10.90) is crucial. If we can show that there are constants $A$, $B > 0$ such that $A$ bounds this term below and $B$ bounds this term above, then we will have found frame bounds and shown that the windowed Fourier atoms $\{w_{m,n}(t) = \exp(jn\Omega)w(t - mT)\colon m, n \in \mathbb{Z}\}$ do comprise a frame. The following corollary imposes a reasonable technical condition on the window function $w(t)$ [27], namely that the window function be continuous and positive on some interval about $t = 0$.

**Corollary.** Let $w(t) \in L^2(\mathbb{R})$ be as in the theorem. Further suppose that $w(t)$ is continuous and that there are $\varepsilon > 0$ and $1 > \delta > 0$ such that $|w(t)| > \varepsilon$ on $I = [-\delta\pi/\Omega, \delta\pi/\Omega]$. Then $\{w_{m,n}(t) = e^{jn\Omega t}w(t - mT)\colon m, n \in \mathbb{Z}\}$ are a frame.

$$\sum_{m,\,n\,=\,-\infty}^{\infty} \left|\langle x, w_{m,\,n}\rangle\right|^2 = \frac{2\pi}{\Omega} \int_{-\infty}^{\infty} |x(t)|^2 \left( \sum_{k\,=\,-\infty}^{\infty} |w(t-kT)|^2 \right) dt\,. \tag{10.91}$$

***Proof:*** Since

$$\sum_{m,\,n\,=\,-\infty}^{\infty} \left|\langle x, w_{m,\,n}\rangle\right|^2 = \frac{2\pi}{\Omega} \int_{-\infty}^{\infty} |x(t)|^2 \left( \sum_{k\,=\,-\infty}^{\infty} |w(t-kT)|^2 \right) dt, \tag{10.92}$$

by the theorem, we seek positive constants $\alpha$ and $\beta$ such that $\alpha < \Sigma|w(t - kT)|^2$ and $\Sigma|w(t - kT)|^2 < \beta$ for all $t$. Then we have

$$\frac{2\pi\alpha}{\Omega} \int_{-\infty}^{\infty} |x(t)|^2 dt \le \sum_{m,\,n\,=\,-\infty}^{\infty} \left|\langle x, w_{m,\,n}\rangle\right|^2 = \frac{2\pi\beta}{\Omega} \int_{-\infty}^{\infty} |x(t)|^2 dt\,, \tag{10.93}$$

so that $A = (2\pi\alpha)/\Omega$ and $B = (2\pi\beta)/\Omega$ constitute lower and upper frame bounds, respectively, for $\{w_{m,n}(t)\}$. By the assumption that $w(t)$ exceeds $\varepsilon > 0$ on the proper subinterval $I$, we can set $\alpha = \inf\{|w(t)|^2\colon t \in I\}$. Since $\alpha$ is the greatest lower bound of $|w(t)|^2$ on $I$, and $|w(t)| > \varepsilon$ on $I$, we know $\alpha \ge \varepsilon > 0$. The lower frame condition follows easily with bound $A = (2\pi\alpha)/\Omega$. To find the upper frame bound, we note that because the support of $w(t)$ is contained within the interval $[-\pi/\Omega, \pi/\Omega]$, only a finite number $K$ of terms in the sum $\Sigma|w(t - kT)|^2$ will be nonzero. Since $w(t)$ is continuous and supported on $[-\pi/\Omega, \pi/\Omega]$, we may let $M$ be its least upper bound; that is, $M = \|w\|_\infty$. We can then set $\beta = \sup\{\Sigma|w(t - kT)|^2 : t \in \mathbb{R}\} \le KM$, and with $B = (2\pi\beta)/\Omega$ we can verify the upper frame bound property. ■

*Remarks.* Recall from our general discussion of frames in Section 3.3.4 that the frame reconstruction algorithm is more efficient when the frame is tight. We can see in the theorem that finding $w(t)$ so that $\Sigma|w(t-kT)|^2$ is constant does provide us with a tight frame: $A = B = 2\pi(\Omega T)^{-1}$. In fact, it is fairly straightforward to concoct window functions $w(t)$ so that this expression is constant. Moreover, the construction method gives windows with compact support arbitrarily good smoothness. We refer the reader to the literature for details [12, 25, 27].

The result of the theorem (10.86) can be used to find examples of windowed Fourier frames from special window functions.

**Example.** Suppose $w(t) = (1 + t^2)^{-1}$. Then $w(t)$ is bounded and absolutely integrable. If $T > 0$, then $\Sigma|w(t-kT)|^2$ has an upper and lower bound. One can show (exercise) that $\{w_{m,n}(t) = e^{jn\Omega t}w(t-mT)\colon m, n \in \mathbb{Z}\}$ are a frame if we take $\Omega$ to be sufficiently small.

**Example.** Now let $w(t) = g_{\mu,\sigma}(t)$, the Gaussian with mean $\mu$ and standard deviation $\sigma$. Again, $\Sigma|g_{\mu,\sigma}(t-kT)|^2$ is bounded above and below when $T > 0$, and we can use the theorem's criterion for showing that Gabor frames exist for a sufficiently small frequency sampling interval.

Before summarizing our results in pursuit of Gabor's problem, let us note an important necessary condition of windowed Fourier frames [12].

**Theorem.** Suppose $w(t) \in L^2(\mathbb{R})$; $\Omega$, $T > 0$; and $\{w_{m,n}(t) = e^{jn\Omega t}w(t-mT)\colon m, n \in \mathbb{Z}\}$ constitute a frame with lower and upper bounds A and B, respectively. Then

$$A \le \frac{2\pi}{\Omega T}\|w\|_2^2 \le B. \tag{10.94}$$

***Proof:*** Exercise. ■

### 10.3.6 Status of Gabor's Problem

We can briefly summarize the status of our search for frames of windowed Fourier atoms. There are three cases, which depend on the time- and frequency-domain sampling intervals, $T$ and $\Omega$, respectively. Our present understanding is as follows:

(i) When $T\Omega < 2\pi$ the time-frequency density is higher than the Nyquist density, and we have just constructed frames of windowed Fourier atoms in this case.

(ii) When $T\Omega = 2\pi$ the atom are at Nyquist density exactly; this is the alternative proposed by Gabor, and our analysis of it is not yet complete.

(iii) Finally, when $T\Omega > 2\pi$ we have noted that windowed Fourier frames do not exist in this situation; we proved a simple instance, and the research literature—portions of which rely on advanced analysis—completely covers the remaining cases.

We will in fact devote a considerable portion of the remainder of this chapter to Gabor's dividing line case. The applicability of the short-time Fourier transform (STFT) when time-frequency localization is of paramount importance hangs on this question. This question also vexed signal processing investigators for a number of years; we are especially interested in fully understanding the impact of windowed Fourier transform discretization when $T\Omega = 2\pi$.

Before turning to this question, however, let us consider another approach to time-frequency signal decompositions.

## 10.4 QUADRATIC TIME-FREQUENCY TRANSFORMS

There are classes of time-frequency transforms that do not depend on a windowing function. Instead, the transform relation emerges out of the properties of the analyzed signal. The signal $x(t)$ enters the transform integral as a quadratic rather than as linear term, as it does in the windowed Fourier transform. This transform family is therefore generally known as the *quadratic* time-frequency transformations. Its principal members are the *Wigner–Ville transform* (WVT) and the closely related *ambiguity function*.

Now, transforming without a window function appears to be quite advantageous, since the resulting procedure eliminates the effect window selection imposes on the transform's behavior. The short-time Fourier transform mixes spectral properties of the analyzed signal $x(t)$ together with those of the window function $w(t)$. Blindly perusing coefficients, we do not know whether their large magnitude results from signal or window properties. On the other hand, we do not often blindly process transform coefficients. Rather, the window function is typically chosen to isolate signal features of expected frequency content and time- domain extent; in the more typical application then, choosing a window function may well be the best first step.

Although avoiding window effects may recommend quadratic transforms, there are some more important considerations. We shall explore three significant properties of these transforms. This transform family:

- More precisely resolves certain standard cases of time-varying frequencies than does the STFT;
- Enjoys special properties called *marginal conditions* that allow them to act as distribution functions for a signal's spectral content;
- Has the significant drawback that transformed signals exhibit certain artifacts called *cross-terms* that hamper higher-level interpretation.

This is in fact a very rich transform family. An entire book could be written about these transforms, and many treatments devote considerable space to these transforms [2, 6, 9]. By our brief sketch we hope that the reader will acquire a more balanced opinion of the windowed Fourier transforms and an interest in further exploring the theory and application of quadratic transforms.

### 10.4.1 Spectrogram

We can base a quadratic time-frequency transform on the STFT. This is in fact just the spectrogram, which we define as follows.

**Definition (Spectrogram).** Let $x(t) \in L^2(\mathbb{R})$ and let $w(t)$ be a window function. The *spectrogram with respect to w(t)*, written $X_{S,w}(\mu, \omega)$, is

$$X_{S,\,w}(\mu, \omega) \;=\; |X(\mu, \omega)|^2 \;=\; \left| \int_{-\infty}^{\infty} x(t) w(t-\mu) e^{-j\omega t} dt \right|^2 , \tag{10.95}$$

where $X_w(\mu, \omega)$, is the STFT of $x(t)$ with respect to $w(t)$.

Thus, the spectrogram of $x(t)$ is the squared magnitude of the STFT of $x(t)$ with respect to $w(t)$. The spectrogram is thus a natural generalization of the windowed Fourier methods we have been comfortable in using. However, despite the more intuitive feel, spectrograms are far from being the most popular quadratic time-frequency transforms. For one thing, $X_{S,w}$ relies on a window function. But it also has some other undesirable traits that have motivated signal theorists to search out other transform techniques. Among these better transforms is the the classic transform of Wigner and Ville which we introduce next; we shall assess the merits of the spectrogram in this context.

### 10.4.2 Wigner–Ville Distribution

The Wigner–Ville distribution (WVD) is the oldest time-frequency transform and the preeminent quadratic signal representation. In fact it dates to the early 1930s when E. Wigner[6] applied it in quantum mechanics [28]. The communication theorist J. Ville[7] introduced the transform to the signal processing community some 16 years later [29].

The transform has been widely studied for signal analysis applications [30, 31]. It has also found use as an important tool in computer vision [32]. The WVD has some distinct advantages over the more intuitive spectrogram. But it is not without its faults.

One difficulty in applying the WVD is the presence of so-called *cross-* or *interference terms* among the transform coefficients. Indeed, many research efforts in time-frequency theory have concentrated on avoiding or ameliorating the effects of cross-terms when using this type of tool. This problem is covered in the Section 10.4.3.

***10.4.2.1 Definition and Motivation.*** The Wigner–Ville distribution takes the Fourier transform of a product of the signal with its complex conjugate. Thus, it resembles the computation of the power spectral density.

[6]The Hungarian chemical engineer Eugene P. Wigner (1902–1996) immigrated to the United States to teach mathematics at Princeton University in 1930. He received the Nobel prize in 1963 for discoveries in atomic and elementary particle research.

[7]French communication researcher J. Ville developed the same transform as Wigner, but for the purposes of clarifying the concept of instantaneous frequency.

**Definition (Wigner–Ville Distribution).** If $x(t) \in L^2(\mathbb{R})$ is an analog signal, then its *Wigner–Ville distribution*, written $X_{\mathrm{WV}}(\mu, \omega)$, is the radial Fourier transform of the product $x(\mu + t/2)x^*(\mu - t/2)$:

$$X_{\mathrm{WV}}(\mu, \omega) = \int_{-\infty}^{\infty} x\left(\mu + \frac{t}{2}\right)\overline{x\left(\mu - \frac{t}{2}\right)}e^{-j\omega t}dt\,. \tag{10.96}$$

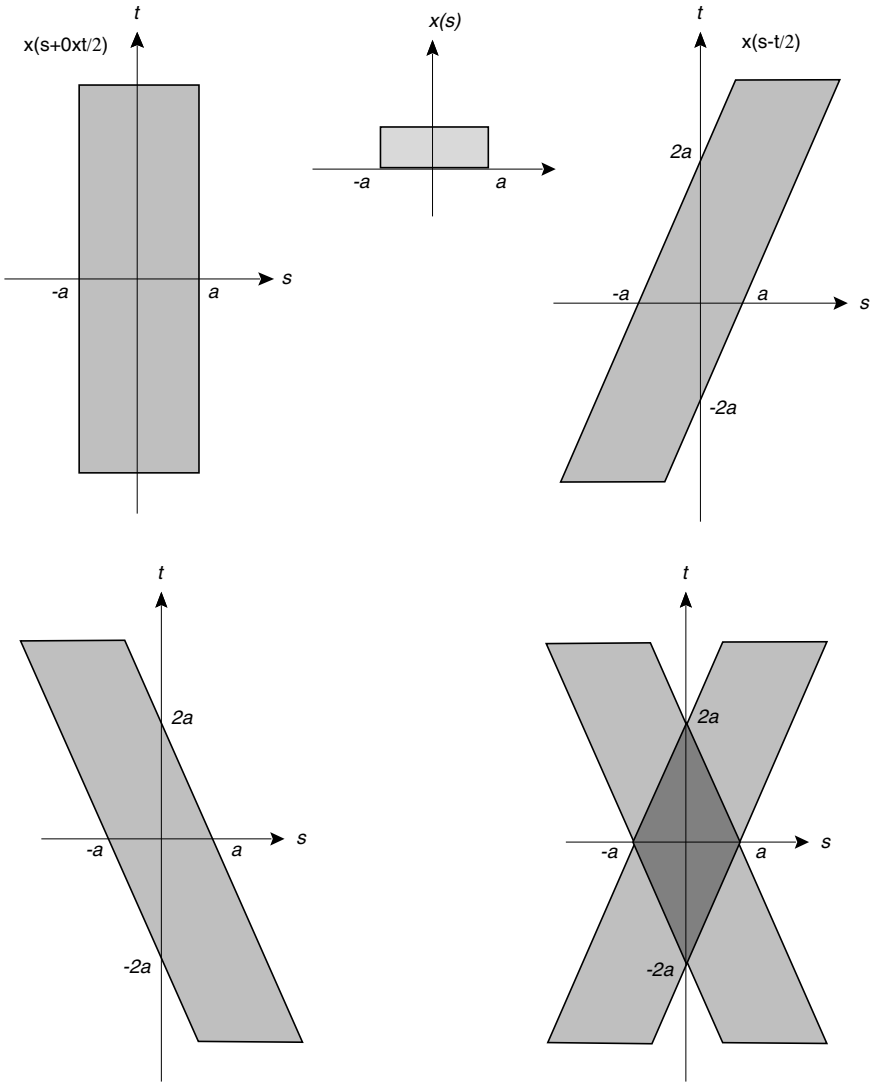


**Fig. 10.12.** Illustrating the support of $x(s + t/2)x^*(s - t/2)$ in the $(s, t)$ plane. Panel (a) shows the support of $x(s)$. We move to two dimensions in Panel (b), but show the support of the degenerate function $x(s + 0 \times (t/2))$. The support of $x(s - t/2)$ is the parallelpiped region (c) and the product $x(s + t/2)x^*(s - t/2)$ has support mainly within the diamond (d).

*Remark.* We observe that the integral (10.96) is well-defined. It is the Fourier transform of $x(\mu + t/2)x^*(\mu - t/2)$, which must be absolutely integrable. This follows because both factors are in $L^2(\mathbb{R})$, and the Schwarz inequality ensures that $\|x(\mu + t/2)\|_2 \, \|x^*(\mu - t/2)\|_2 \geq \|x(\mu + t/2)x^*(\mu - t/2)\|_1$. Of course, $L^1(\mathbb{R})$ signals have Fourier transforms.

No window function appears in the definition (10.96), but there is an easy way to understand how folding the source signal $x(t)$ over on itself accomplishes the required time localization. Imagining that a signal's support lies mainly within the interval $[-a, a]$, the local region implied by the WVD transform is a diamond, as shown in Figure 10.12.

***10.4.2.2 Properties.*** The properties of this transform are quite remarkable. To begin with, we can show that the Wigner–Ville distribution is *real-valued*.

**Proposition (Real-Valued).** Let $x(t) \in L^2(\mathbb{R})$ and $X_{\mathrm{WV}}(\mu, \omega)$ be its WVD. Then $X_{\mathrm{WV}}(\mu, \omega) \in \mathbb{R}$.

***Proof:*** We calculate the complex conjugate of (10.96) and make the change of integration variable $s = -t$.

$$\begin{aligned}\overline{X_{\mathrm{WV}}(\mu, \omega)} &= \int_{-\infty}^{\infty} \overline{x\left(\mu + \frac{t}{2}\right)} x\left(\mu - \frac{t}{2}\right) e^{j\omega t} dt \\ &= -\int_{\infty}^{-\infty} \overline{x\left(\mu - \frac{s}{2}\right)} x\left(\mu + \frac{s}{2}\right) e^{-j\omega s} \, ds = X_{\mathrm{WV}}(\mu, \omega). \end{aligned} \tag{10.97}$$

Because $X^*_{\mathrm{WV}}(\mu, \omega) = X_{\mathrm{WV}}(\mu, \omega)$, it must be real. ■

Already we see that the WVD's properties are quite unlike those of the Fourier transform or its time-limited versions. However, the time- and frequency-domain shifting properties are familiar, as the next proposition shows. Symmetry properties are covered in the exercises.

**Proposition (Time and Frequency Shift).** Let $x(t) \in L^2(\mathbb{R})$ and $X_{\mathrm{WV}}(\mu, \omega)$ be its WVD. Then

(a) If $s(t) = x(t - a)$, then $S_{\mathrm{WV}}(\mu, \omega) = X_{\mathrm{WV}}(\mu - a, \omega)$.
(b) If $y(t) = e^{j\theta t}x(t)$, then $Y_{\mathrm{WV}}(\mu, \omega) = X_{\mathrm{WV}}(\mu, \omega - \theta)$.

***Proof:*** Exercise. ■

The double product of $x(t)$ terms in the WVD integral, which is the "quadratic" factor, spoils the transform's linearity. This is easy to see for the scaling property of the linearity. We let $y(t) = ax(t)$, where a is a constant. Then $Y_{\mathrm{WV}}(\mu, \omega) = |a|^2 X_{\mathrm{WV}}(\mu, \omega)$.

Superposition also fails for the WVD. We use an auxiliary transform as part of the argument.

**Definition (Cross Wigner–Ville Distribution).** If $x(t), y(t) \in L^2(\mathbb{R})$ are analog signals, then the *Cross Wigner–Ville Distribution*, written $X_{\mathrm{WV},y}(\mu, \omega)$, is the radial Fourier transform of the product $x(\mu + t/2)y^*(\mu - t/2)$:

$$X_{\mathrm{WV},\,y}(\mu, \omega) = \int_{-\infty}^{\infty} x\left(\mu + \frac{t}{2}\right)\overline{y\left(\mu - \frac{t}{2}\right)}e^{-j\omega t}\,dt\,. \tag{10.98}$$

One can easily show that $X_{\mathrm{WV,y}}(\mu, \omega)$ is the complex conjugate of $Y_{\mathrm{WV},x}(\mu, \omega)$. If we set $s(t) = x(t) + y(t)$, then $S_{\mathrm{WV}}(\mu, \omega) = X_{\mathrm{WV}}(\mu, \omega) + Y_{\mathrm{WV}}(\mu, \omega) + 2\mathrm{Real}[X_{\mathrm{WV},y}(\mu, \omega)]$.

Thus, both component properties of linearity fail for the WVD. The failure of superposition is the more serious deficiency. This defect causes artifacts, called *cross-terms*, in the WVD transform coefficients. The presence of cross-terms leads to difficulties of automatic interpretation, and removing them by various alternative transformations has been a major research goal of the last several years.

The next theorem reveals an interesting symmetry between time and frequency domain representations for the WVD. Besides having an eerie similarity to the inverse Fourier relation, it is also useful in calculations involving the WVD.

**Theorem (Frequency-Domain Representation).** Let $x(t) \in L^2(\mathbb{R})$, let $X(\omega)$ be its Fourier transform, and $X_{\mathrm{WV}}(\mu, \omega)$ be its WVD. Then

$$X_{\mathrm{WV}}(\mu, \omega) = \frac{1}{2\pi}\int_{-\infty}^{\infty} X\left(\omega + \frac{\theta}{2}\right)\overline{X\left(\omega - \frac{\theta}{2}\right)}e^{j\theta\mu}\,d\theta\,. \tag{10.99}$$

***Proof:*** The key idea is to write $X_{\mathrm{WV}}(\mu, \omega)$ as an inner product,

$$X_{\mathrm{WV}}(\mu, \omega) = \left\langle x\left(\mu + \frac{t}{2}\right)e^{\frac{-j\omega t}{2}},\qquad x\left(\mu - \frac{t}{2}\right)e^{\frac{j\omega t}{2}}\right\rangle, \tag{10.100}$$

splitting the exponential between its two terms. We can then apply Parseval's theorem:

$$\begin{aligned} X_{\mathrm{WV}}(\mu, \omega) &= \frac{1}{2\pi}\left\langle \mathcal{F}x\left(\mu + \frac{t}{2}\right)e^{\frac{-j\omega t}{2}},\ \mathcal{F}x\left(\mu - \frac{t}{2}\right)e^{\frac{j\omega t}{2}}\right\rangle \\ &= \frac{1}{2\pi}\langle 2X(\omega + 2\phi)e^{j\mu(\omega + 2\phi)}, 2X(\omega - 2\phi)e^{j\mu(\omega - 2\phi)}\rangle. \end{aligned} \tag{10.101}$$

The final inner product in (10.101) simplifies to the integral

$$X_{\mathrm{WV}}(\mu, \omega) = \frac{4}{2\pi} \int_{-\infty}^{\infty} X(\omega + 2\phi)\overline{X(\omega - 2\phi)} e^{4j\phi\mu} d\phi\,, \tag{10.102}$$

whereupon the substitution $\theta = 4\phi$ gives (10.99). ■

**Corollary (Fourier Transform of WVD).** Let $x(t) \in L^2(\mathbb{R})$, let $X(\omega)$ be its Fourier transform, and $X_{\mathrm{WV}}(\mu, \omega)$ be its WVD. Then, with $\omega$ fixed and viewing $X_{\mathrm{WV}}(\mu, \omega)$ as a signal with independent time variable $\mu$, we have

$$\mathcal{F}[X_{\mathrm{WV}}(\mu, \omega)](\theta) = \int_{-\infty}^{\infty} X_{\mathrm{WV}}(\mu, \omega) e^{-j\mu\theta} d\mu = X\left(\omega + \frac{\theta}{2}\right)\overline{X\left(\omega - \frac{\theta}{2}\right)}. \tag{10.103}$$

***Proof:*** Apply the theorem to the WVD term in the integral (exercise).

Table 10.3 summarizes WVD properties. Some of the table's properties are left as exercises.

***10.4.2.3 Examples.*** Let us look at some WVD calculations on standard example signals. These examples are revealing, because they show how the WVD improves upon the frequency resolving capability of the STFT.

**TABLE 10.3. Wigner–Ville Distribution Properties**[a]

| Signal Expression | WVD or Property |
|---|---|
| $x(t)$ | $X_{\mathrm{WV}}(\mu, \omega)$ |
| $ax(t)$ | $\lvert a\rvert^2 X_{\mathrm{WV}}(\mu, \omega)$ |
| $x(t) + y(t)$ | $X_{\mathrm{WV}}(\mu, \omega) + Y_{\mathrm{WV}}(\mu, \omega) + 2\mathrm{Real}[X_{\mathrm{WV},y}(\mu, \omega)]$ |
| $x(t - a)$ | $X_{\mathrm{WV}}(\mu - a, \omega)$ |
| $x(t)\exp(j\theta t)$ | $X_{\mathrm{WV}}(\mu, \omega - \theta)$ |
| $x(t)\exp(j\theta t^2)$ | $X_{\mathrm{WV}}(\mu, \omega - 2\theta\mu)$ |
| $x(t/a)$, with $a > 0$ | $aX_{\mathrm{WV}}(\mu/a, a\omega)$ |
| $X_{\mathrm{wv}}(\mu, \omega) = \frac{1}{2\pi}\int_{-\infty}^{\infty} X\left(\omega + \frac{\theta}{2}\right)\overline{X\left(\omega - \frac{\theta}{2}\right)} e^{j\theta\mu} d\theta$ | Frequency-domain representation |
| $\int_{-\infty}^{\infty} X_{\mathrm{wv}}(\mu, \omega) e^{-j\mu\theta} d\mu = X\left(\omega + \frac{\theta}{2}\right)\overline{X\left(\omega - \frac{\theta}{2}\right)}$ | Fourier transform of WVD |

[a]In this table, $x(t)$ and $y(t)$ are square-integrable.

**Example (Dirac).** Let $x(t) = \delta(t - a)$. Then $X_{\mathrm{WV}}(\mu, \omega) = \delta(\mu - a)$. To verify this formula, we utilize the Frequency-Domain Representation Theorem. Then.

$$X_{\mathrm{WV}}(\mu, \omega) = \frac{1}{2\pi} \int_{-\infty}^{\infty} e^{-j\left(\omega + \frac{\theta}{2}\right)a} e^{j\left(\omega - \frac{\theta}{2}\right)a} e^{j\theta\mu} d\theta = \frac{1}{2\pi} \int_{-\infty}^{\infty} e^{j(\mu - a)} d\theta = \delta(\mu - a). \tag{10.104}$$

The interesting aspect of this example is that the WVD maps an impulse to an impulse. The time-frequency representation that the WVD provides is just as temporally localized as the original time-domain signal. In the $(\mu, \omega)$ plane, realm of the WVD, the signal $\delta(\mu - a)$ is a Dirac knife edge, infinitely high and infinitely narrow, parallel to the $\omega$-axis and passing through the point $\mu = a$. This stands in stark contrast to the STFT. The windowed Fourier transformation of the same Dirac impulse $x(t) = \delta(t - a)$ is $X_w(\mu, \omega) = w(a - \mu)e^{-j\omega a}$, an exponential modulated by the transform window $w(t)$ situated over the point $\mu = a$.

**Example (Sinusoid).** Let $x(t) = e^{jat}$. Then $X_{\mathrm{WV}}(\mu, \omega) = (2\pi)^{-1}\delta(\omega - a)$. This can be shown using the WVD properties (Table 10.3) or by direct computation as above.

**Example (Gaussian Pulse).** Now let $g(t) = g_{\alpha,\sigma}(t)$, the Gaussian of mean $\alpha$ and standard deviation $\sigma$. Then

$$G_{\mathrm{WV}}(\mu, \omega) = \frac{e^{-(\sigma\omega)^2}}{2\pi^{3/2}\sigma} e^{-\left(\frac{\mu - \alpha}{\sigma}\right)^2}. \tag{10.105}$$

Notice in this example that the WVD of a Gaussian pulse is always positive. The only signals $x(t)$ for which $X_{\mathrm{WV}}(\mu, \omega)$ is positive are linear chirps, $\exp(jbt^2 + jat)$, modulated by a Gaussian envelope Ref. [7].

**Example (Square Pulse).** Let $s(t) = u(t + 1) - u(t - 1)$, the square pulse supported on the interval $[-1, 1]$. Then

$$S_{\mathrm{WV}}(\mu, \omega) = \frac{2s(\mu)}{\omega} \sin(2\omega(1 - |\mu|)). \tag{10.106}$$

Thus, although the WVD is real-valued, its values can be negative.

These examples illustrate the trade offs between the windowed Fourier transforms and the WVD. There are still other time-frequency transforms, of course; Ref. 33 compares the frequency resolution efficiencies of several of them.

***10.4.2.4 Densities and Marginals.*** Now we turn to an important feature of the Wigner–Ville distribution, a set of properties that distinguish it from the

short-time Fourier transform, namely its density function-like character. What does this mean? In the case of the Fourier transform, we have been content to use fractions of signal energy as an indication that a frequency range is significant within a signal $x(t)$. Thus, the energy of $x(t)$ is $E_x$:

$$E_x^2 = \int_{-\infty}^{\infty} |x(t)|^2 \, dt = \|x\|_2^2 = \frac{1}{2\pi} \int_{-\infty}^{\infty} |X(\omega)|^2 \, d\omega = \frac{\|X\|_2^2}{2\pi}. \tag{10.107}$$

We may normalize $x(t)$ or $X(\omega)$ so that the have unit energy, or we may elect to use the normalized radial Fourier transform and equate time and frequency-domain energies. The exercises explore the use of the Hertz Fourier transform for quantifying energy distributions in both time and frequency-domains. In any case then, like a probability density function, the fraction of signal energy between $\omega_0$ and $\omega_1$ is given by

$$E_x^2[\omega_0, \omega_1] = \int_{\omega_0}^{\omega_1} |X(\omega)|^2 d\omega, \tag{10.108}$$

where we have normalized so that $\int_{-\infty}^{\infty} |X(\omega)|^2 \, d\omega = 1$.

Now, we are interested in transform representations of signals that have both a time- and a frequency-domain independent variable. Our question is whether such transforms can have joint density function behavior as well. For this to be the case, we should require that the signal transform assumes non-negative values and obey certain marginal integral conditions.

**Definition (Marginals).** The time-frequency transform $P(\mu, \omega)$ of $x(t) \in L^2(\mathbb{R})$ obeys the *marginal conditions* if

$$P(\mu, \omega) \geq 0, \tag{10.109a}$$

$$\frac{1}{2\pi} \int_{-\infty}^{\infty} P(\mu, \omega) \, d\omega = |x(t)|^2, \tag{10.109b}$$

$$\int_{-\infty}^{\infty} P(\mu, \omega) \, d\mu = |X(\omega)|^2, \tag{10.109c}$$

where $X(\omega)$ is the radial Fourier transform of $x(t)$.

(These conditions are somewhat imperfect, due to the scaling factor in (10.109b). We can escape the scaling by using a Hertz Fourier transform. All we really require is that the marginal integral with respect to one variable be proportional to the signal

energy with respect to the other variable; see the exercises.) The idea behind the definition is that $P(\mu, \omega)$ represents a relative amount of the signal per unit time and per unit frequency. Summing the distribution over frequency values should produce a relative amount of signal per unit time. Finally, summing over time should produce a signal strength per unit frequency.

The interpretation of the WVD as a kind of probability density function seems to gain steam from the fact that its values are real; we have already seen from the example of the square pulse, however, that the values can be negative. In contrast, the spectrogram, because it is a squared norm, is always non-negative. However, the WVD does satisfy marginal conditions, which the spectrogram does not.

**Theorem (Marginals).** Let $x(t) \in L^2(\mathbb{R})$, let $X(\omega)$ be its Fourier transform, and let $X_{\mathrm{WV}}(\mu, \omega)$ be its WVD. Then

$$\int_{-\infty}^{\infty} X_{\mathrm{WV}}(\mu, \omega)\, d\omega = 2\pi |x(\mu)|^2, \tag{10.110a}$$

$$\int_{-\infty}^{\infty} X_{\mathrm{WV}}(\mu, \omega)\, d\mu = |X(\omega)|^2. \tag{10.110b}$$

***Proof:*** We can directly evaluate the integral (10.110a) as follows:

$$\int_{-\infty}^{\infty} X_{\mathrm{WV}}(\mu, \omega)\, d\omega = \int_{-\infty}^{\infty}\int_{-\infty}^{\infty} x\left(\mu + \frac{t}{2}\right)\overline{x\left(\mu - \frac{t}{2}\right)} e^{-j\omega t}\, dt\, d\omega. \tag{10.111}$$

Interchanging the order of integration on the right-hand side of (10.111) gives

$$\begin{aligned}\int_{-\infty}^{\infty} x\left(\mu + \frac{t}{2}\right)\overline{x\left(\mu - \frac{t}{2}\right)} \int_{-\infty}^{\infty} e^{-j\omega t}\, d\omega\, dt &= 2\pi \int_{-\infty}^{\infty} x\left(\mu + \frac{t}{2}\right)\overline{x\left(\mu - \frac{t}{2}\right)} \delta(t)\, d\omega\, dt \\ &= 2\pi x\left(\mu + \frac{t}{2}\right)\overline{x\left(\mu - \frac{t}{2}\right)}\Bigg|_{t=0} \\ &= 2\pi x(\mu)\overline{x(\mu)} = 2\pi |x(\mu)|^2. \end{aligned} \tag{10.112}$$

We leave the second marginal as an exercise. ■

Thus, we have shown that the WVD obeys a marginal condition akin to that of a joint probability density function. It is possible to show that employing a Hertz formulation of the WVD produces perfect marginal conditions for the transform. Unfortunately, the spectrogram fails the marginals, precisely because of the window function (exercises).

### 10.4.3 Ambiguity Function

Another quadratic time-frequency signal representation is the ambiguity function. Its formulation is much like the WVD, except that it swaps the time and integration variables in the defining Fourier integral.

**Definition (Ambiguity Function).** If $x(t) \in L^2(\mathbb{R})$ is an analog signal, then its *ambiguity function*, written $X_{\mathrm{AF}}(\mu, \omega)$, is the radial Fourier transform of the product $x(t + \mu/2)x^*(t - \mu/2)$:

$$X_{\mathrm{AF}}(\mu, \omega) = \int_{-\infty}^{\infty} x\left(t + \frac{\mu}{2}\right)\overline{x\left(t - \frac{\mu}{2}\right)}e^{-j\omega t}\,dt. \tag{10.113}$$

The following result relates the ambiguity function to the WVD.

**Theorem (Ambiguity Function Characterization).** Let $x(t) \in L^2(\mathrm{R})$ be an analog signal, $X_{\mathrm{AF}}(\mu, \omega)$ its ambiguity function, and $X_{\mathrm{WV}}(\mu, \omega)$ its Wigner–Ville distribution. Then,

$$X_{\mathrm{AF}}(\mu, \omega) = \int_{-\infty}^{\infty}\int_{-\infty}^{\infty} X_{\mathrm{WV}}(\nu, \theta)e^{-j(\nu\omega + \mu\theta)}\,d\nu\,d\theta. \tag{10.114}$$

***Proof:*** Let us evaluate the integral on the right-hand side of (10.114) by splitting up the exponential into two one-dimensional Fourier transforms. Then the corollary to the Frequency-Domain Representation Theorem [(10.103) applies.

$$\int_{-\infty}^{\infty}\int_{-\infty}^{\infty} X_{\mathrm{WV}}(\nu, \theta)e^{-j(\nu\omega + \mu\theta)}\,d\nu\,d\theta = \int_{-\infty}^{\infty} X\left(\omega + \frac{\theta}{2}\right)\overline{X\left(\omega - \frac{\theta}{2}\right)}e^{-j\mu\theta}\,d\theta. \tag{10.115}$$

Writing the integral on the right-hand side of (10.115) as an inner product and invoking Parseval's formula, we find

$$\int_{-\infty}^{\infty} X\left(\omega + \frac{\theta}{2}\right)\overline{X\left(\omega - \frac{\theta}{2}\right)}e^{-j\mu\theta}\,d\theta = \int_{-\infty}^{\infty} x\left(t + \frac{\mu}{2}\right)\overline{x\left(t - \frac{\mu}{2}\right)}e^{-j\omega t}\,dt. \tag{10.116}$$

But the last integral above is $X_{\mathrm{AF}}(\mu, \omega)$. ■

*Remark.* Notice that the ambiguity function characterization (10.114) shows that $X_{\mathrm{AF}}(\mu, \omega)$ is the two-dimensional Fourier transform of $X_{\mathrm{WV}}(\mu, \omega)$.

### 10.4.4 Cross-Term Problems

While the WVD does have several advantages over the spectrogram—among them superior frequency-domain resolution, satisfaction of the marginals, and independence of a windowing function—it does have the misfortune of interference terms.

**Fig. 10.13.** An example of the presence of cross-terms in the WVD. The original signal is a chirp, first rising in frequency and then falling. High-energy coefficients appear beneath the main arc of energy in the transform plane, yet the time-domain signal contains no such tones. Higher-level interpretation routines are beset with the problem of separating such artifacts from genuine features of the signal's time evolution.

The cross-terms represent time-frequency domain energy in locations where it is not present in the original signal (Figure 10.13).

Cross-terms in WVD coefficients are, generally speaking, oscillatory in nature. As such, their effect on applications can be mitigated if not removed by filtering in the $(\mu, \omega)$ plane. The *quid pro quo* is some loss of frequency resolution [9]. The principal approach to removing these oscillatory components is through frequency domain filtering. Thus, one manipulates the Fourier transform of $X_{\mathrm{WV}}(\mu, \omega)$—the ambiguity function $X_{\mathrm{AF}}(\mu, \omega)$. Several such methods are compared in Ref. 34. Modification of the ambiguity plane image, a two-dimensional undertaking, is outside our present scope, however.

Although they are in general tolerable, WVD interferences can be extreme in some cases. For example, for each pair of energy concentrations in the time-frequency plane, a possible cross-term region is created. Thus, if there are $N$ significant temporal-spectral components of $x(t)$, then $X_{\mathrm{WV}}(\mu, \omega)$ will have $N \times (N-1)$ interference term regions. This combinatorial explosion presents nasty problems for higher-level interpretation algorithms. Furthermore, by the algebraic nature of their origin, cross-term amplitudes can conceivably be double the magnitudes of their source pair of time-frequency energy modes. So how then can a high-level algorithm distinguish meaningful events from meaningless interferences?

### 10.4.5 Kernel Construction Method

Many of the latest time-frequency signal analysis research efforts have revolved around the problem of finding density-like distributions that obey the marginal conditions, but avoid cross-term effects.

The principal strategy is to introduce a third term into the defining transform integral [35].

**Definition (Kernel-Based or Cohen's Class of Transforms).** If $x(t) \in L^2(\mathbb{R})$ is an analog signal, then its *Cohen Class Transform* with respect to $K$, written $X_K(\mu, \omega)$, is

$$X_K(\mu, \omega) = \int_{-\infty}^{\infty}\int_{-\infty}^{\infty}\int_{-\infty}^{\infty} K(\theta, t)e^{j\theta(s-\mu)}x\left(s+\frac{t}{2}\right)\overline{x\left(s-\frac{t}{2}\right)}e^{-j\omega t}dtdsd\theta\,. \quad (10.117)$$

The kernel term can be thought of as smoothing the interferences. It is also possible to show that almost all time-frequency transforms, assuming a suitable choice of the kernel function, belong to the Cohen Class [7, 9].

Why resort to such triple integrals for basic one-dimensional signal representation? The spectrogram does not obey the marginals, so signal theorists sought a solution amongst transforms such as the WVD. Hope for a quadratic transform, however, was dashed by Wigner's theorem [36]. This result states that a quadratic time-frequency transform cannot obey the marginal conditions (10.109a)–(10.109c). Pursuing these very interesting ideas would require quite a bit of multidimensional transform development and take us far afield, however.

We return to the STFT family to answer conclusively the question Gabor posed: Can a critically sampled set of windowed Fourier atoms fully support representation and analysis?

## 10.5 THE BALIAN–LOW THEOREM

This section concludes the chapter by proving a famous result in time-frequency transform theory: the Balian–Low theorem. The theorem applies to the entire class of time-frequency (or windowed-Fourier) transforms. Balian–Low answers a question posed by discretizing the short-time Fourier transform: Can windowed Fourier atoms of the form

$$w_{m,n}(t) = e^{jn\Omega t}w(t-mT)\,, \quad (10.118)$$

where $T > 0$ and $T\Omega = 2\pi$ serve as a complete signal representation? We desire good time and frequency localization; we stipulate, therefore, that both $w(t)$ and its Fourier transform $W(\omega)$ are window functions. The two practical alternatives are that $\{w_{m,n}(t)\colon m, n \in \mathbb{Z}\}$ constitutes either

- An orthonormal basis or
- A frame.

It is hoped that we can discover $\{w_{m,n}(t)\colon m, n \in \mathbb{Z}\}$ that make up an orthonormal basis. Then every square-integrable signal $x(t)$ has a expansion in terms of Fourier coefficients, easily calcuated as the inner products of $x(t)$ with the $w_{m,n}(t)$:

$$x(t) = \sum_{m,n\in\mathrm{Z}} \langle x(t), w_{m,n}(t)\rangle w_{m,n}(t). \quad (10.119)$$

If we fail to find such a basis, then computing the expansion coefficients (10.119) becomes problematic. Lack of a basis encumbers our signal analysis too. While we might be able to decompose a candidate signal $x(t)$ into a linear combination of atoms, $x(t) = \Sigma c_{m,n} w_{m,n}(t)$, we do not necessarily know the uniqueness of the expansion coefficients $c_{m,n}$ for representing $x(t)$. So the utility of the expansion coefficients as indicators of some signal component's presence or the lack thereof is very much compromised.

Should a basis not be available, we could search for a frame representation of $L^2(\mathbb{R})$ signals using the Gabor atoms (10.118). After all, frame coefficients can characterize the source signal $x(t)$, and they support numerically stable reconstructions. This may be a good redoubt.

In either case, orthonormal basis or frame, we can build a structural interpretation of finite-energy signals x(t). The Balian–Low theorem dashes our hopes—both of them. We cover the theorem for the easier-to-prove case of orthonormal bases, first. Then we turn to Balian–Low's rejection of frames. To prove that no such frames exist, we need a special tool, namely the Zak transform. Frames were covered in Section 3.3.5, and the Zak transform was introduced at the end of Chapter 8.

### 10.5.1 Orthonormal Basis Decomposition

The Balian–Low theorem answers Gabor's original problem of finding well-localized signal representations using time-frequency atoms [25, 37–40]. It is also a negative result, for it shows the impossibility of finding well-localized, orthonormal decompositions based on windowed Fourier atoms when $T\Omega = 2\pi$.

We begin with a lemma. It is simple, but it allows us to reduce the proof of the theorem for all possible samplings $T\Omega = 2\pi$, to the specific case of $T = 1$ and $\Omega = 2\pi$.

**Lemma.** If $T > 0$, then the map $H(x(t)) = T^{1/2} x(Tt)$ is unitary on $L^2(\mathbb{R})$; that is,

(i) H is onto;

(ii) H preserves inner products, $\langle Hx, Hy \rangle = \langle x, y \rangle$.

***Proof:*** For (i), let $y \in L^2(\mathbb{R})$ and choose $x(t) = T^{-1/2} y(t/T)$. Then $(Hx)(t) = y(t)$. For (ii) we change variables, $s = Tt$, in the inner product integral:

$$\langle Hx, Hy \rangle = \int_{-\infty}^{\infty} (Hx)(t)\overline{(Hy)(t)}\, dt = T \int_{-\infty}^{\infty} x(Tt)\overline{y(Tt)}\, dt = T \int_{-\infty}^{\infty} \frac{x(s)\overline{y(s)}}{T}\, ds = \langle x, y \rangle \tag{10.120}$$

This completes the proof. ■

Now we can prove the result of Balian and Low for the orthonormal basis situation.

**Theorem (Balian–Low for Orthonormal Bases).** Let $T\Omega = 2\pi$, let $w(t) \in L^2(\mathbb{R})$, and let the collection of windowed Fourier atoms $\{w_{m,n}(t)\colon m, n \in \mathbb{Z}\}$ be given by (10.118). If $\{w_{m,n}(t)\colon m, n \in \mathbb{Z}\}$ is an orthonormal basis for $L^2(\mathbb{R})$, then either

(i) $w(t)$ is not a window function:

$$\int_{-\infty}^{\infty} t^2 |w(t)|^2 dt = \|tw(t)\|_2^2 = \infty, \quad \text{or} \tag{10.121}$$

(ii) $W(\omega)$ is not a window function:

$$\int_{-\infty}^{\infty} \omega^2 |W(\omega)|^2 d\omega = \|\omega W(\omega)\|_2^2 = \infty. \tag{10.122}$$

***Proof:*** It is sufficient to prove the theorem for the special case $T = 1$ and $\Omega = 2\pi$. We know from the lemma that the scaling map $H(x(t)) = T^{1/2}x(Tt)$ is unitary on $L^2(\mathbb{R})$. If we examine its effect on atoms, we find

$$\begin{aligned} H(w_{m,n}(t)) &= \sqrt{T} w_{m,n}(Tt) = \sqrt{T} e^{jn\Omega Tt} w(Tt - mT) \\ &= e^{2\pi jnt} \sqrt{T} w(T(t-m)) = e^{2\pi jnt} (Hw)(t-m). \end{aligned} \tag{10.123}$$

The map $H$ takes basis elements $w_{m,n}(t)$ with time and frequency sampling intervals $T$ and $\Omega$, respectively, to basis elements with corresponding sampling intervals 1 and $2\pi$. So it suffices to prove the theorem for this special case—that is, for the image of the set $\{w_{m,n}(t)\colon m, n \in \mathbb{Z}\}$ under $H$.

We note that the derivative $w'(t) \in L^2(\mathbb{R})$ if and only if $W(\omega)$ is a window function. We can check this relationship of differentiation to the window condition on $W(\omega)$ as follows:

$$\|w'(t)\|_2^2 = \frac{1}{2\pi} \|\mathcal{F}w'\|_2^2 = \frac{1}{2\pi} \int_{-\infty}^{\infty} |j\omega W(\omega)|^2 d\omega = \frac{1}{2\pi} \int_{-\infty}^{\infty} \omega^2 |W(\omega)|^2 d\omega. \tag{10.124}$$

Let us assume that both $w(t)$ and $W(\omega)$ are window functions. From (10.124) this is equivalent to assuming that $tw(t)$ and $w'(t)$ are square-integrable. Our goal is to show that this leads to a contradiction.

From the assumption, we can calculate the pair of inner products $\langle tw(t), -jw'(t)\rangle$ and $\langle -jw'(t), tw(t)\rangle$. Since $\{w_{m,n}(t)\colon m, n \in \mathbb{Z}\}$ is an orthonormal basis for $L^2(\mathbb{R})$, we can expand both inner products as follows:

$$\langle tw(t), -jw'(t)\rangle = \sum_{m,n \in \mathbb{Z}} \langle tw(t), w_{m,n}(t)\rangle \langle w_{m,n}(t), -jw'(t)\rangle, \tag{10.125a}$$

and

$$\langle -jw'(t), tw(t)\rangle = \sum_{m,\, n \in \mathrm{Z}} \langle -jw'(t), w_{m,\,n}(t)\rangle \langle w_{m,\,n}(t), tw(t)\rangle. \tag{10.125b}$$

Let us attend to the first inner product in the summations of (10.125a). We compute

$$\begin{aligned}\langle tw(t), w_{m,\,n}(t)\rangle &= \int_{-\infty}^{\infty} tw(t)\overline{e^{2\pi jnt} w(t-m)}\, dt \\ &= \int_{-\infty}^{\infty} (s+m)w(s+m)e^{-2\pi jns}\overline{w(s)}\, ds,\end{aligned} \tag{10.126}$$

where $s = t - m$. Since $w_{-m,-n}(t) = \exp(-2\pi jnt)w(t + m)$, we can write the final integral in (10.126) as a sum,

$$\langle tw(t), w_{m,\,n}(t)\rangle = \int_{-\infty}^{\infty} sw(s+m)e^{-2\pi jns}\overline{w(s)}\, ds + m\int_{-\infty}^{\infty} w_{-m,\,-n}(s)\overline{w(s)}\, ds. \tag{10.127}$$

The final term in (10.127) is zero. It is clearly so if $m = 0$, and if $m \neq 0$, then it is $m\langle w_{-m,-n}(t),\ w(t)\rangle$. But by the orthogonality of the $\{w_{m,\,n}(t)\}$, of which $w_{0,0}(t) = w(t)$, we get $\langle w_{-m,-n}(t),\ w(t)\rangle = 0$. Thus,

$$\langle tw(t), w_{m,\,n}(t)\rangle = \int_{-\infty}^{\infty} sw(s+m)e^{-2\pi jns}\overline{w(s)}\, ds = \langle w_{-m,\,-n}(s), sw(s)\rangle. \tag{10.128}$$

Now we can rewrite the inner product (10.125a) like this:

$$\langle tw(t), -jw'(t)\rangle = \sum_{m,\, n \in \mathrm{Z}} \langle w_{-m,\,-n}(t), tw(t)\rangle \langle w_{m,\,n}(t), -jw'(t)\rangle. \tag{10.129}$$

Let us now divert our attention to the second inner product expansion (10.125b). We try the same strategy, expand the first inner product in the summation, and use the orthogonality of the $\{w_{m,n}(t)\}$ to simplify.

$$\langle -jw'(t), w_{m,\,n}(t)\rangle = -j\int_{-\infty}^{\infty} w'(t)e^{-2\pi jnt}\overline{w(t-m)}\, dt. \tag{10.130}$$

Integration by parts gives

$$j\langle -jw'(t), w_{m,\,n}(t)\rangle = w(t)\overline{w(t-m)}e^{-2\pi jnt}\Big|_{-\infty}^{\infty} - I_1(m,n) + I_2(m,n), \tag{10.131}$$

where $I_1(m, n)$ and $I_2(m, n)$ are the integrals

$$I_1(m, n) = -\int_{-\infty}^{\infty} (e^{-2\pi jnt} w(t) \overline{w'(t-m)}\, dt) \tag{10.132a}$$

and

$$I_2(m, n) = 2\pi jn \int_{-\infty}^{\infty} (e^{-2\pi jnt} w(t) \overline{w(t-m)}\, dt). \tag{10.132b}$$

Since $w(t) \in L^2(\mathbb{R})$, the first term on the right-hand side of (10.131) must be zero. The second integral (10.132b) is zero also. To see this, note that

$$I_2(m, n) = 2\pi jn \int_{-\infty}^{\infty} w(t) \overline{w(t-m) e^{j2\pi nt}} dt = 2\pi n \langle w(t), w_{m,-n}(t) \rangle . \tag{10.133}$$

But the final term in (10.133) is zero; either $n = 0$ or $\langle w(t), w_{m,-n}(t) \rangle = 0$ by orthogonality of the $\{w_{m,n}(t)\}$. Thus,

$$\langle -jw'(t), w_{m,n}(t) \rangle = jI_1(m, n) = j \int_{-\infty}^{\infty} w(t) e^{-2\pi jnt} \overline{w'(t-m)}\, dt . \tag{10.134}$$

Letting $s = t - m$ to change integration variables in (10.134) gives

$$\langle -jw'(t), w_{m,n}(t) \rangle = \int_{-\infty}^{\infty} w(s+m) e^{-2\pi jnt} \overline{[-jw'(s)]}\, ds = \langle w_{-m,-n}(t), -jw'(t) \rangle . \tag{10.135}$$

Thanks to this last result (10.135) we can rewrite the inner product (10.125b) as follows:

$$\langle -jw'(t), tw(t) \rangle = \sum_{m,n \in \mathrm{Z}} \langle w_{-m,-n}(t), -jw'(t) \rangle \langle w_{m,n}(t), tw(t) \rangle . \tag{10.136}$$

Reversing the order of summation in (10.136) produces

$$\langle -jw'(t), tw(t) \rangle = \sum_{m,n \in \mathrm{Z}} \langle w_{m,n}(t), -jw'(t) \rangle \langle w_{-m,-n}(t), tw(t) \rangle . \tag{10.137}$$

This is nothing else but the summation in (10.129); in other words, we have shown that $tw(t)$ and $-jw'(t)$ commute under the inner product relation:

$$\langle tw(t), -jw'(t) \rangle = \langle -jw'(t), tw(t) \rangle. \tag{10.138}$$

Contradiction looms. Indeed, computing the integral on the left-hand side of (10.138), we can integrate by parts to find

$$\int_{-\infty}^{\infty} tw(t)\overline{[-jw'(t)]}dt = jtw(t)\overline{w(t)}\Big|_{-\infty}^{\infty} - j\int_{-\infty}^{\infty} \overline{w(t)}\{w(t) + tw'(t)\}\, dt. \qquad (10.139)$$

Again, $|w(t)|^2 \to 0$ as $t \to \infty$, because w(t) $\in L^2(\mathbb{R})$. This means

$$j\langle tw(t), -jw'(t)\rangle = \int_{-\infty}^{\infty} \overline{w(t)}w(t)\, dt - \int_{-\infty}^{\infty} \overline{tw(t)}w'(t)\, dt = \|w\|_2^2 + \langle -jw'(t), w(t)\rangle. \qquad (10.140)$$

Of course, $\|w\| = \|w_{0,0}\| = 1$ by orthogonality of $\{w_{m,n}\}$, and this contradicts (10.138). ■

To illustrate the Balian–Low theorem, we consider two examples of orthonormal bases for $L^2(\mathbb{R})$.

**Example (Fourier Basis).** For the first example, we try $w(t) = u(t) - u(t-1)$, where $u(t)$ is the unit step signal, as the window function. Then the family $\{w_{m,n}(t) = \exp(2\pi jnt)w(t-m)\colon m, n \in \mathbb{Z}\}$ is an orthonormal basis for $L^2(\mathbb{R})$. In fact, for any fixed $m_0 \in \mathbb{Z}$, we can represent a general signal $x(t)$ restricted to $[m_0, m_0 + 1]$ by its Fourier series. And the collection of all such Fourier series suffices to construct $x(t)$. Orthogonality follows, of course, from the orthogonality of the exponentials on unit intervals. What does Balian–Low say? Either $w(t)$ or its Fourier transform $W(\omega)$ must not be a window function. Indeed the Fourier transform of $w(t)$ is a sinc function, its Fourier transform decays like $\omega^{-1}$, and $\|\omega W(\omega)\|_2 = \infty$. So although $w(t)$ is well-localized in time, it is poorly localized in frequency.

**Example (Shannon Basis).** This example takes the other extreme. We now let $w(t) = \mathrm{sinc}(\pi t) = (\pi t)^{-1}\sin(\pi t)$. Then, once again, $\{w_{m,n}(t) = \exp(2\pi jnt)w(t-m)\colon m, n \in \mathbb{Z}\}$ is an orthonormal basis for $L^2(\mathbb{R})$. Although the Fourier transform of this signal is a window function, a square pulse, we now find $tw(t) \notin L^2(\mathbb{R})$.

We might yet hope to find an exact frame representation, having shown now that no orthonomal basis of Gabor elementary functions, or more general windowed Fourier atoms, can exist of the case of $T\Omega = 2\pi$. Orthonormality is, after all, an extremely strict constraint. And we understand that exact frames can support complete and stable signal representation for analysis purposes. Unfortunately, the looser requirement—that the windowed Fourier decomposition set should form an exact frame—is also impossible. The next section covers this more involved proof.

### 10.5.2 Frame Decomposition

The most elegant and accesible proof of the Balian–Low theorem for frames relies uses the notion of a signal's Zak transform.

***10.5.2.1 Zak Transform Preliminaries.*** Recall from Chapter 8 that the Zak transform maps an analog signal $x(t)$ to a two-dimensional function having independent variables in both time and frequency. In this sense, it resembles the Gabor transform; however, it looks through no window function, and, much like the discrete-time Fourier transform, it is the limit of an infinite sum involving discrete samples of $x(t)$. With parameter $a = 1$, we define

$$(\mathcal{Z}x)(s, \omega) = \sum_{k=-\infty}^{\infty} x(s-k)e^{2\pi j\omega k}. \tag{10.141}$$

The Zak transform's properties make it a particularly effective tool for studying frames based on windowed Fourier atoms. Reviews concerning the Zak transform, frames, and windowed Fourier expansions include Refs. 41 and 42.

The Zak transform is a unitary map from $L^2(\mathbb{R})$ to $L^2(S)$, where $S$ is the unit square $[0, 1] \times [0, 1]$. The set of two-dimensional exponentials $\{e_{m,n}(t) = \exp(2\pi jmt)\exp(2\pi jnt)\colon m, n \in \mathbb{Z}\}$ is a basis for $L^2(S)$. Because of this unitary map, the Zak transform converts questions about frames in $L^2(\mathbb{R})$ into questions about frames in $L^2(S)$, where the answers are generally easier to find. The next proposition shows that Zak transforming a Gabor atom is equivalent to a modulation operation.

**Proposition (Modulation).** Let $w(t) \in L^2(\mathbb{R})$; let $w_{m,n}(t) = \exp(2\pi jnt)w(t-m)$ for $m, n \in \mathbb{Z}$; and let $\mathcal{Z}\colon L^2(\mathbb{R}) \to L^2(S)$ be the Zak transform, where $S$ is the unit square $[0, 1] \times [0, 1]$. Then

$$(\mathcal{Z}w_{m,n})(s, \omega) = e^{2\pi jns}e^{-2\pi j\omega m}(\mathcal{Z}w)(s, \omega). \tag{10.142}$$

***Proof:*** We compute

$$\begin{aligned}(\mathcal{Z}w_{m,n})(s, \omega) &= \sum_{k=-\infty}^{\infty} e^{2\pi j\omega k}e^{2\pi jns}e^{-2\pi jnk}w(s-k-m) \\ &= e^{2\pi jns}\sum_{k=-\infty}^{\infty} e^{2\pi j\omega k}w(s-k-m)\end{aligned} \tag{10.143}$$

and find

$$\begin{aligned}(\mathcal{Z}w_{m,n})(s, \omega) &= e^{2\pi jns}e^{-2\pi j\omega m}\sum_{k=-\infty}^{\infty} e^{2\pi j\omega(k+m)}w(s-(k+m)) \\ &= (\mathcal{Z}w)(s, \omega)e^{2\pi jns}e^{-2\pi j\omega m}\end{aligned} \tag{10.144}$$

as required. ■

**Proposition (Norms).** If $w(t) \in L^2(\mathbb{R})$; $w_{m,n}(t) = \exp(2\pi jnt)w(t - m)$ for $m, n \in \mathbb{Z}$; and $\mathcal{Z}$: $L^2(\mathbb{R}) \to L^2(S)$ is the Zak transform, where $S$ is the unit square $[0, 1] \times [0, 1]$, then

$$\sum_{m,\, n \in \mathbb{Z}} \left|\langle x, w_{m,\, n}\rangle\right|^2 = \left\|(\mathcal{Z}x)(s, \omega)(\mathcal{Z}w)(s, \omega)\right\|^2. \tag{10.145}$$

***Proof:*** From the transform's unitary property and the previous proposition, the sum in (10.145) expands as follows:

$$\begin{aligned}\sum_{m,\, n \in \mathbb{Z}} \left|\langle x, w_{m,\, n}\rangle\right|^2 &= \sum_{m,\, n \in \mathrm{Z}} \left|\langle \mathcal{Z}x, \mathcal{Z}w_{m,\, n}\rangle\right|^2 \\ &= \sum_{m,\, n \in \mathbb{Z}} \left|\int_0^1\int_0^1 e^{-2\pi jns} e^{2\pi j\omega m} (\mathcal{Z}x)(s, \omega)\overline{(\mathcal{Z}w)(s, \omega)}\, ds d\omega\right|^2.\end{aligned} \tag{10.146}$$

The two-dimensional exponentials are an orthonormal basis for $L^2(S)$. Hence, the Bessel relation for Hilbert spaces implies that the final sum in is in fact

$$\sum_{m,\, n \in \mathbb{Z}} \left|\langle x, w_{m,\, n}\rangle\right|^2 = \int_0^1\int_0^1 \left|(\mathcal{Z}x)(s, \omega)\right|^2 \left|(\mathcal{Z}w)(s, \omega)\right|^2 ds d\omega. \tag{10.147}$$

as desired. ■

The theorem below uses the ideas on Lebesgue measure and integration from Chapter 3.

**Theorem (Bounds).** Let $w(t) \in L^2(\mathbb{R})$ and suppose $\{w_{m,n}(t) = e^{2\pi jnt}w(t - m)$: $m, n \in \mathbb{Z}\}$ is a frame, with lower and upper bounds $A$ and $B$, respectively. Then for almost all $s$ and $\omega$ we have

$$A \le \left|(\mathcal{Z}w)(s, \omega)\right|^2 \le B. \tag{10.148}$$

***Proof:*** The frame property implies

$$0 < A\|x\|^2 \le \sum_{m,\, n \in \mathrm{Z}} \left|\langle x, w_{m,\, n}\rangle\right|^2 \le B\|x\|^2 < \infty \tag{10.149}$$

for any $x(t) \in L^2(\mathbb{R})$. By the previous proposition,

$$0 < A\|x\|^2 \le \int_0^1\int_0^1 \left|(\mathcal{Z}x)(s, \omega)\right|^2 \left|(\mathcal{Z}w)(s, \omega)\right|^2 ds d\omega \le B\|x\|^2 < \infty \tag{10.150}$$

must hold for all finite energy $x(t)$ as well. We argue that this entails

$$0 < A \leq \int_0^1 \int_0^1 |(\mathcal{Z}w)(s, \omega)|^2 \, ds d\omega \leq B < \infty . \tag{10.151}$$

To see this, let us suppose that, for example, $|(\mathcal{Z}w)(s, \omega)|^2 < A$ on some subset $R \subseteq S$ with positive measure: $\mu(R) > 0$. Let $v(s, \omega)$ be the characteristic function on $S$ and set $y = \mathcal{Z}^{-1}v$; since $\mathcal{Z}$ is unitary, $\|y(t)\|^2 = \|v(s, \omega)\|^2 = \mu(R)$. Consequently,

$$\begin{aligned} A\mu(R) = A\|y\|^2 &< \int_0^1 \int_0^1 |(\mathcal{Z}y)(s, \omega)|^2 |(\mathcal{Z}w)(s, \omega)|^2 \, ds d\omega \\ &= \int_0^1 \int_0^1 |v(s, \omega)|^2 |(\mathrm{Z}w)(s, \omega)|^2 ds d\omega. \end{aligned} \tag{10.152}$$

Now, because $v(s, \omega) = 1$ on $R \subseteq S$ and $v(s, \omega) = 0$ otherwise, this last integral becomes

$$\int_0^1 \int_0^1 |v(s, \omega)|^2 |(\mathcal{Z}w)(s, \omega)|^2 \, ds d\omega = \int_R \int |(\mathcal{Z}w)(s, \omega)|^2 \, ds d\omega < \int_R \int A \, ds d\omega = A\mu(R). \tag{10.153}$$

Together, (10.152) and (10.153) produce a contradiction. By a similar argument, so does the assumption $B < |(\mathcal{Z}w)(s, \omega)|^2$. Showing this last step is left as an exercise, which finishes the proof. ■

The next two propositions characterize time- and frequency-domain window functions as having differentiable derivatives of their Zak transforms.

**Lemma (Window Function).** If $x(t) \in L^2(\mathbb{R})$, and $x(t)$ is a window function, then

$$\mathcal{Z}(tx(t))(s, \omega) = s(\mathcal{Z}x)(s, \omega) + \frac{j}{2\pi}\left[\frac{\partial}{\partial \omega}(\mathcal{Z}x)(s, \omega)\right]. \tag{10.154}$$

***Proof:*** Applying the Zak transform (10.141) to $y(t) = tx(t)$, this is straightforward:

$$\begin{aligned} (\mathcal{Z}y)(s, \omega) &= \sum_{k=-\infty}^{\infty} (s-k)x(s-k)e^{2\pi j \omega k} \\ &= s \sum_{k=-\infty}^{\infty} x(s-k)e^{2\pi j \omega k} - \sum_{k=-\infty}^{\infty} kx(s-k)e^{2\pi j \omega k}. \end{aligned} \tag{10.155}$$

The first summation on the bottom of (10.155) is $s(\mathcal{Z}x)(s, \omega)$. Partial differentiation of $(\mathcal{Z}x)(s, \omega)$ with respect to $\omega$ gives

$$\frac{\partial}{\partial \omega}(\mathcal{Z}x)(s, \omega) = \sum_{k=-\infty}^{\infty} 2\pi j k e^{2\pi j k \omega} x(s-k), \tag{10.156}$$

and algebraic manipulation accounts for the second summation in (10.155). ■

**Proposition (Window Function Characterization).** Let $x(t) \in L^2(\mathbb{R})$ and $\mathcal{Z}$ be the Zak transform $\mathcal{Z}$: $L^2(\mathbb{R}) \to L^2(S)$, where $S$ is the unit square $[0, 1] \times [0, 1]$. Then $x(t)$ is a window function if and only if

$$\frac{\partial}{\partial \omega}(\mathcal{Z}x)(s, \omega) \in L^2[S]. \tag{10.157}$$

***Proof:*** If $x(t)$ is a window function, then the Window Function Lemma applies and (10.154) holds. Since $s(\mathcal{Z}x)(s, \omega) \in L^2(\mathbb{R})$, necessarily (10.157) holds. Conversely, suppose (10.157). Because both of the final two sums in (10.155) are in $L^2(S)$, so is their sum. Following equalities backwards in (10.155), we thereby find that

$$\sum_{k=-\infty}^{\infty} (s-k)x(s-k)e^{2\pi j \omega k} \in L^2(S). \tag{10.158}$$

But (10.158) is none other than the Zak transform expansion for $tx(t)$. Thus, $x(t)$ is a window function. ■

**Lemma (Derivative).** If $x(t), x'(t) \in L^2(\mathbb{R})$, then

$$\mathcal{Z}(x'(t))(s, \omega) = \frac{\partial}{\partial s}(\mathcal{Z}x)(s, \omega). \tag{10.159}$$

***Proof:*** By differentiating the Zak transform sum (exercise). ■

**Proposition (Derivative Characterization).** Let $x(t) \in L^2(\mathbb{R})$, let $X(\omega)$ be its radial Fourier transform, and let $\mathcal{Z}$ be the Zak transform $\mathcal{Z}$: $L^2(\mathbb{R}) \to L^2(S)$, where $S$ is the unit square $[0, 1] \times [0, 1]$. Then $X(\omega)$ is a window function if and only if

$$\frac{\partial}{\partial s}(\mathcal{Z}x)(s, \omega) \in L^2[S]. \tag{10.160}$$

***Proof:*** The Fourier transform of $x'(t)$ is $j\omega X(\omega)$, so $x'(t) \in L^2(\mathbb{R})$ if and only if $\omega X(\omega) \in L^2(\mathbb{R})$; that is, $X(\omega)$ is a window function. Invoking the Derivative Lemma completes the proof (exercise). ■

The proof of the general Balian–Low theorem for frames uses the above Zak transform properties. The bounds theorem, however, implies a weaker version of the theorem, recapitulated from Ref. 13, where it is attributed to Yves Meyer.

**Theorem (Meyer).** Let $w$: $\mathbb{R} \to \mathbb{R}$ be continuous and suppose there are $\varepsilon > 0$ and $C > 0$ such that

$$|w(t)| \leq \frac{C}{(1 + |t|)^{1+\varepsilon}}. \tag{10.161}$$

Then $\{w_{m,n}(t) = e^{2\pi jnt} w(t - m)\colon m, n \in \mathbb{Z}\}$ cannot be a frame.

***Proof:*** Since $|w(t)|$ is dominated by $C(1 + |t|)^{-1-\varepsilon}$, its Zak transform sum converges. Moreover, it must converge to a continuous function in $L^2(S)$, where $S$ is the unit square $[0, 1] \times [0, 1]$. For the sake of contradiction, now suppose that $\{w_{m,n}(t) = e^{2\pi jnt} w(t - m)\colon m, n \in \mathbb{Z}\}$ constitute an $L^2(\mathbb{R})$ frame with lower and upper bounds $A$ and $B$, respectively. Since $w(t)$ has a Zak transform, the bounds theorem (10.148) entails $0 < A \leq |(\mathcal{Z}w)(s, \omega)|$ for almost all $(s, \omega) \in S$. But $(\mathcal{Z}w)(s, \omega)$ is continuous, and therefore $|(\mathcal{Z}w)(s, \omega)| \neq 0$ for all $(s, \omega) \in S$.

The trick is to define, for each $s \in [0, 1]$, the curve, $\zeta_s$: $[0, 1] \to \mathbb{C}$:

$$\zeta_s(\omega) = \frac{(\mathcal{Z}w)(s, \omega)}{(\mathcal{Z}w)(0, \omega)}. \tag{10.162}$$

Note that $\zeta_0(\omega) = 1$. Since $(\mathcal{Z}w)(s + 1, \omega) = e^{2\pi j\omega}(\mathcal{Z}w)(s, \omega)$, it follows as well that $\zeta_1(\omega) = e^{2\pi j\omega}$ for all $\omega \in [0, 1]$. But we cannot continuously map the horizontal line segment defined by $\zeta_0(\omega)$ to the unit circle defined by $\zeta_1(\omega)$ unless at some $r \in (0, 1)$ and some $\omega_0 \in [0, 1]$ we have $\zeta_r(\omega_0) = 0$. But then $(\mathcal{Z}w)(r, \omega_0) = 0$, which contradicts the fact that $(\mathcal{Z}w)(s, \omega) \neq 0$ for all $(s, \omega) \in S$. Indeed, $\{w_{m,n}(t)\colon m, n \in \mathbb{Z}\}$ cannot be a frame. ■

The next section proves the general Balian–Low theorem. We have already shown the result for orthonormal bases and for frames deriving from continuous window functions with a sufficient decay rate. In the general theorem, the window function assumption is much weaker: the windowing function $w(t)$ of $\{w_{m,n}(t)\colon m, n \in \mathbb{Z}\}$ need only have finite energy.

***10.5.2.2 General Balian–Low Theorem.*** The idea of a frame generalizes the notion of an orthonormal basis. We introduced frames along with the theory of Hilbert spaces of analog signals in Section 3.3.4. Signal analysis using atomic signal models is possible with frames in the sense that such a decomposition:

- Uniquely represents candidate signals;
- Reconstructs a candidate signal in a numerically stable way from its decomposition coefficients.

Frame theory has classic beginnings—Ref. 43–45, for example—and numerous recent texts and papers cover its relationship to mixed-domain signal analysis [27, 42, 46].

We begin with two lemmas on applying the Zak transform to dual frame elements. Recall from basic frame theory (Section 3.3.4.3) that if $F = \{f_n(t)\colon m, n \in \mathbb{Z}\}$ is a frame in a Hilbert space $H$, then the associated *frame operator* $\mathcal{T}\colon H \to l^2(\mathbb{Z})$ is defined by

$$\mathcal{T}(x)(n) = \langle x, f_n \rangle . \tag{10.163}$$

Frame operator $\mathcal{T}$ is linear; it is bounded; and, in particular, if $B$ is the upper frame bound, then $\|\mathcal{T}(\mathrm{x})\|^2 \leq B\|\mathrm{x}\|^2$. Associated to $\mathcal{T}$ is the operator $S\colon l^2(\mathbb{Z}) \to H$ defined for $y(n) \in l^2(\mathbb{Z})$ by

$$\mathcal{S}(y) = \sum_{n=-\infty}^{\infty} y(n) f_n . \tag{10.164}$$

In fact, we showed that $S$ is the Hilbert space *adjoint operator* of $\mathcal{T}$: $S = \mathcal{T}^*$. The composition $\mathcal{T}^*\mathcal{T}$ happens to be an invertible map $\mathcal{T}^*\mathcal{T}\colon L^2(\mathbb{R}) \to L^2(\mathbb{R})$ given by

$$(\mathcal{T}^*\mathcal{T})(x) = \sum_{n=-\infty}^{\infty} \langle x, f_n \rangle f_n . \tag{10.165}$$

We can thus define the *dual frame* to $F$ by applying the inverse of $\mathcal{T}^*\mathcal{T}$ to frame elements:

$$\tilde{F} = \left\{ (\mathcal{T}^*\mathcal{T})^{-1}(f_n) \right\}_{n \in \mathrm{Z}} . \tag{10.166}$$

The dual frame idea is key in signal analysis applications. If the dual frame elements are given by $\tilde{f}_n = (\mathcal{T}^*\mathcal{T})^{-1} f_n$, then we have a reconstruction formula for $x(t)$ from both frame and dual frame elements:

$$x(t) = \sum_{n=-\infty}^{\infty} \langle x(t), f_n(t) \rangle \tilde{f}_n(t) \tag{10.167a}$$

and

$$x(t) = \sum_{n=-\infty}^{\infty} \langle x(t), \tilde{f}_n(t) \rangle f_n(t) . \tag{10.167b}$$

If $x(t), y(t) \in H$, then these formulas imply

$$\langle x(t), y(t) \rangle = \sum_{n=-\infty}^{\infty} \langle x(t), f_n(t) \rangle \langle \tilde{f}_n(t), y(t) \rangle \tag{10.168a}$$

and

$$\langle x(t), y(t)\rangle = \sum_{n=-\infty}^{\infty} \langle x(t), \tilde{f}_n(t)\rangle \langle f_n(t), y(t)\rangle . \tag{10.168b}$$

Our theory now combines frame and Zak transform concepts. We are also exploiting several different Hilbert spaces: $L^2(\mathbb{R})$, $L^2([0, 1] \times [0, 1])$, and $l^2(\mathbb{Z})$. Note that although we have formulated these properties for frame elements indexed by a single integral variable, we can specify a one-to-one correspondence between integers and their pairs, $k \leftrightarrow (m, n)$. Our families of windowed Fourier atoms $\{w_{m,n}(t)$: $m, n \in \mathbb{Z}\}$ are doubly indexed, and we thus rewrite (10.163) through (10.166) accordingly. The next lemma shows the relationship between the Zak transform and the frame operator.

**Lemma.** Let $w(t) \in L^2(\mathbb{R})$; let $F = \{w_{m,n}(t) = \exp(2\pi jnt)w(t - m)$: $m, n \in \mathbb{Z}\}$ be a frame; let $\mathcal{T}$ be the associated frame operator; and let $\mathcal{Z}$: $L^2(\mathbb{R}) \to L^2(S)$ be the Zak transform, where $S$ is the unit square $[0, 1] \times [0, 1]$. If $x \in L^2(\mathbb{R})$ and $\mathcal{Z}x = y \in L^2(S)$, then $[\mathcal{Z}(\mathcal{T}^*\mathcal{T})\mathcal{Z}^{-1}]y = |\mathcal{Z}w|^2 y$.

***Proof:*** We have $[\mathcal{Z}(\mathcal{T}^*\mathcal{T})\mathcal{Z}^{-1}]y = [\mathcal{Z}(\mathcal{T}^*\mathcal{T})]x$. Since $(\mathcal{T}^*\mathcal{T})x = \Sigma\langle x, w_{m,n}\rangle w_{m,n}$, we have

$$[\mathcal{Z}(\mathcal{T}^*\mathcal{T})\mathcal{Z}^{-1}]y = \sum_{m,n\in \mathrm{Z}} \langle x, w_{m,n}\rangle \mathcal{Z}w_{m,n} = \sum_{m,n\in \mathrm{Z}} \langle \mathcal{Z}x, \mathcal{Z}w_{m,n}\rangle \mathcal{Z}w_{m,n}. \tag{10.169}$$

But

$$\sum\langle \mathcal{Z}x, \mathcal{Z}w_{m,n}\rangle \mathcal{Z}w_{m,n} = \sum\langle y, e^{2\pi jns}e^{-2\pi j\omega m}\mathcal{Z}w\rangle e^{2\pi jns}e^{-2\pi j\omega m}\mathcal{Z}w, \tag{10.170}$$

by the Modulation Proposition in the previous section. Manipulating the inner product on the right-hand side of (10.170) gives

$$\sum\langle \mathcal{Z}x, \mathcal{Z}w_{m,n}\rangle \mathcal{Z}w_{m,n} = \sum\langle y\overline{\mathcal{Z}w}\mathcal{Z}w, e^{2\pi jns}e^{-2\pi j\omega m}\rangle e^{2\pi jns}e^{-2\pi \mathrm{j}\omega m}. \tag{10.171}$$

Now, $\overline{\mathcal{Z}w}\mathcal{Z}w = |\mathcal{Z}w|^2$, and since the two-dimensional exponentials $e^{2\pi jns}e^{-2\pi j\omega m}$ are an orthonormal basis for $L^2(S)$, the last expression is precisely $|\mathcal{Z}w|^2 y$. ■

**Lemma (Dual Frame).** Let $w(t) \in L^2(\mathbb{R})$, let $F = \{w_{m,n}(t) = e^{2\pi jnt}w(t - m)$: $m, n \in \mathbb{Z}\}$ be a frame, and let $\mathcal{T}$ be the frame operator on F. Further, let

$$\tilde{w}_{m,n} = (\mathcal{T}^*\mathcal{T})^{-1} w_{m,n} \tag{10.172}$$

be the dual frame elements for $F$ and $\mathcal{Z}$: $L^2(\mathbb{R}) \to L^2(S)$ be the Zak transform, where $S$ is the unit square $[0, 1] \times [0, 1]$. Then

$$(\mathcal{Z}\tilde{w}_{m,n})(s,\omega) = \frac{(\mathcal{Z}w_{m,n})(s,\omega)}{|(\mathcal{Z}w)(s,\omega)|^2} = \frac{e^{2\pi jns}e^{-2\pi j\omega m}}{\overline{(\mathcal{Z}w)(s,\omega)}}. \tag{10.173}$$

***Proof:*** By the previous lemma, if $\mathcal{Z}w_{m,n} = y \in L^2(S)$, then $[\mathcal{Z}(\mathcal{T}^*\mathcal{T})\mathcal{Z}^{-1}]y = |\mathcal{Z}w|^2 y$. By definition of the dual frame, $\tilde{w}_{m,n} = (\mathcal{T}^*\mathcal{T})^{-1}w_{m,n}$. Fiddling with operators shows

$$\mathcal{Z}\tilde{w}_{m,n} = \mathcal{Z}(\mathcal{T}^*\mathcal{T})^{-1}w_{m,n} = \mathcal{Z}(\mathcal{T}^*\mathcal{T})^{-1}\mathcal{Z}^{-1}y = |\mathcal{Z}w|^2 y = |\mathcal{Z}w|^2 \mathcal{Z}w_{m,n}. \tag{10.174}$$

The Bounds Theorem justifies division by $|\mathcal{Z}w|^2$ in (10.174), and (10.173) follows from the Modulation Proposition. ■

These tools allow us to extend the Balian–Low theorem to frames.

**Theorem (Balian–Low for Frames).** Let $T\Omega = 2\pi$, $w(t) \in L^2(\mathbb{R})$, and let $W = \mathcal{F}w$ be the Fourier transform of $w$. If the collection of windowed Fourier atoms $F = \{w_{m,n}(t) = e^{\Omega jnt}w(t - mT)\colon m, n \in \mathbb{Z}\}$ is a frame, then—once again—either

(i) $w(t)$ is not a window function:

$$\int_{-\infty}^{\infty} t^2|w(t)|^2\,dt = \|tw(t)\|_2^2 = \infty, \quad \text{or} \tag{10.175}$$

(ii) $W(\omega)$ is not a window function:

$$\int_{-\infty}^{\infty} \omega^2|W(\omega)|^2\,d\omega = \|\omega W(\omega)\|_2^2 = \infty. \tag{10.176}$$

***Proof:*** By a scaling argument, such as we used in proving the theorem for orthonormal bases in Section 10.6.1, it suffices to prove the theorem for $T = 1$ and $\Omega = 2\pi$. Let us suppose that both $tw(t)$ and $\omega W(\omega)$ are square-integrable and seek a contradiction.

Let $\mathcal{Z} : L^2(\mathbb{R}) \to L^2(S)$ be the Zak transform, where $S = [0, 1] \times [0, 1]$, and $\tilde{w} = (\mathcal{T}^*\mathcal{T})^{-1}w$, where $\mathcal{T}$ is the frame operator for $F$. We claim that

$$t\tilde{w}(t) \in L^2(\mathbb{R}) \tag{10.177a}$$

and

$$\frac{d}{dt}\tilde{w}(t) \in L^2(\mathbb{R}). \tag{10.177b}$$

Indeed, from the assumption that $tw(t) \in L^2(\mathbb{R})$, the Window Function Characterization Proposition (10.157) implies $\frac{\partial}{\partial \omega}(\mathcal{Z}w)(s, \omega) \in L^2[S]$. Likewise, supposing $\omega W(\omega) \in L^2(\mathbb{R})$ gives $\frac{\partial}{\partial s}(\mathcal{Z}w)(s, \omega) \in L^2[S]$ via the Derivative Characterization Proposition. But extracting derivatives is straightforward using the Dual Frame Lemma (10.173) with $m = n = 0$. Thus, $w_{m,n}(t) = w(t)$, and we calculate

$$\frac{\partial}{\partial s}(\mathcal{Z}\tilde{w})(s, \omega) = \frac{\partial}{\partial s}\frac{(\mathcal{Z}w)(s, \omega)}{|(\mathcal{Z}w)(s, \omega)|^2} = \frac{\partial}{\partial s}\frac{1}{\overline{(\mathcal{Z}w)(s, \omega)}} = \frac{-\frac{\partial}{\partial s}\overline{(\mathcal{Z}w)(s, \omega)}}{\overline{(\mathcal{Z}w)(s, \omega)}^2} \quad (10.178a)$$

and

$$\frac{\partial}{\partial \omega}(\mathcal{Z}\tilde{w})(s, \omega) = \frac{\partial}{\partial \omega}\frac{(\mathcal{Z}w)(s, \omega)}{|(\mathcal{Z}w)(s, \omega)|^2} = \frac{\partial}{\partial \omega}\frac{1}{\overline{(\mathcal{Z}w)(s, \omega)}} = \frac{-\frac{\partial}{\partial s}\overline{(\mathcal{Z}w)(s, \omega)}}{\overline{(\mathcal{Z}w)(s, \omega)}^2}. \quad (10.178b)$$

Denominators are nonzero almost everywhere in (10.178a) and (10.178b) by the Bounds Theorem on the Zak transform. That is, the expressions on the right-hand sides of (10.178a) and (10.178b) are in $L^2(S)$. Hence the partial derivatives $\frac{\partial}{\partial s}(\mathcal{Z}\tilde{w})(s, \omega)$ and $\frac{\partial}{\partial \omega}(\mathcal{Z}\tilde{w})(s, \omega)$ are in $L^2(S)$. Hence $t\tilde{w}(t) \in L^2(\mathbb{R})$ and $\tilde{w}'(t) \in L^2(\mathbb{R})$ by the Window Function and Derivative Characterization Propositions, respectively.

Now—working toward a contradiction along the same lines we used for the case of orthonormal bases—we claim that

$$\langle \tilde{w}, w_{m,n} \rangle = \langle w, \tilde{w}_{m,n} \rangle = \begin{cases} 1 & \text{if } m = n = 0 \\ 0 & \text{otherwise.} \end{cases} \quad (10.179)$$

To justify the claim, we apply the unitary Zak transform to the inner products of (10.179) and use (10.173) once more:

$$\begin{aligned} \langle w, \tilde{w}_{m,n} \rangle &= \langle Zw, Z\tilde{w}_{m,n} \rangle = \int_0^1\int_0^1 (Zw)(s, \omega)\overline{(Z\tilde{w}_{m,n})(s, \omega)}\, ds d\omega \\ &= \int_0^1\int_0^1 (Zw)(s, \omega)\frac{e^{-2\pi jns}e^{2\pi j\omega m}}{(\mathcal{Z}w)(s, \omega)}\, ds d\omega. \end{aligned} \quad (10.180)$$

Consequently,

$$\langle w, \tilde{w}_{m,n} \rangle = \int_0^1\int_0^1 e^{-2\pi jns}e^{2\pi j\omega m}\, ds d\omega, \quad (10.181)$$

which will be unity when $m = n = 0$ and zero otherwise by the orthogonality of the dual exponentials on the unit square. Showing the same result for $\langle \tilde{w}, w_{m,n} \rangle$ is left as an exercise.

Our next claim is that

$$\langle tw(t), \tilde{w}'(t) \rangle = -\langle w'(t), t\tilde{w}(t) \rangle . \tag{10.182}$$

Recalling the reconstruction formula for frames (10.167a) and (10.167b), we write

$$\langle tw(t), \tilde{w}'(t) \rangle = \sum_{m,n=-\infty}^{\infty} \langle tw(t), \tilde{w}_{m,n}(t) \rangle \langle w_{m,n}(t), \tilde{w}'(t) \rangle \tag{10.183}$$

and work on inner products within the sum. We compute the first by expanding the inner product integral and using (10.179) (exercise):

$$\langle tw(t), \tilde{w}_{m,n}(t) \rangle = \langle w_{-m,-n}(t), t\tilde{w}(t) \rangle . \tag{10.184}$$

The second inner product in the sum of (10.183) involves integration by parts, and here the proof has much of the uncertainty principle's flavor.

$$\langle w_{m,n}(t), \tilde{w}'(t) \rangle = \int_{-\infty}^{\infty} e^{2\pi jnt} w(t-m) \overline{\tilde{w}'(t)} \, dt . \tag{10.185}$$

It follows, upon integrating by parts, that

$$\begin{aligned} \langle w_{m,n}(t), \tilde{w}'(t) \rangle = {} & e^{2\pi jnt} w(t-m) \overline{\tilde{w}(t)} \Big|_{-\infty}^{\infty} - \int_{-\infty}^{\infty} e^{2\pi jnt} w'(t-m) \overline{\tilde{w}(t)} \, dt \\ & - \int_{-\infty}^{\infty} 2\pi jn e^{2\pi jnt} w(t-m) \overline{\tilde{w}(t)} \, dt . \end{aligned} \tag{10.186}$$

The first term on the right-hand side of (10.186) is zero. The inner product in the third term, $2\pi jn \langle w_{m,n}(t), \tilde{w}(t) \rangle$, is zero unless $m = n = 0$, as we proved above, and, thanks to the $2\pi jn$ factor, the entire term is necessarily zero. Changing the integration variable in the remaining term produces

$$\langle w_{m,n}(t), \tilde{w}'(t) \rangle = -\int_{-\infty}^{\infty} e^{2\pi jnt} w'(t-m) \overline{\tilde{w}(t)} \, dt = -\langle w'(t), \tilde{w}_{-m,-n}(t) \rangle . \tag{10.187}$$

Substituting (10.184) and (10.187) into (10.183) and reversing the summation, we discover

$$\langle tw(t), \tilde{w}'(t) \rangle = -\sum_{m,n=-\infty}^{\infty} \langle w'(t), \tilde{w}_{m,n}(t) \rangle \langle w_{m,n}(t), t\tilde{w}(t) \rangle = -\langle w'(t), t\tilde{w}(t) \rangle . \tag{10.188}$$

Is this last equality plausible? We claim that it is not, that it leads to a contradiction, and that, therefore, our assumption that $w(t)$ and $W(\omega)$ are both window functions is false. To verify this final claim, let us work the integration by parts on the inner product on the left-hand side of (10.188):

$$\langle tw(t), \tilde{w}'(t)\rangle = \int_{-\infty}^{\infty} tw(t)\overline{\tilde{w}'(t)}\, dt = -\int_{-\infty}^{\infty} w(t)\overline{\tilde{w}(t)}\, dt - \int_{-\infty}^{\infty} w'(t)\overline{t\tilde{w}(t)}\, dt\,. \tag{10.189}$$

The integrals on the right-hand side of (10.189) are inner products, so that

$$\langle tw(t), \tilde{w}'(t)\rangle = -\langle w(t), \tilde{w}(t)\rangle - \langle w'(t), t\tilde{w}(t)\rangle\,. \tag{10.190}$$

But we know $\langle tw(t), \tilde{w}'(t)\rangle = -\langle w'(t), t\tilde{w}(t)\rangle$ by (10.188) and $\langle w(t), \tilde{w}(t)\rangle = 1$ by (10.179). This exposes the contradiction and finishes the proof. ■

*Remark.* Integration by parts for $x, y \in L^2(\mathbb{R})$, $\int x'y = xy| - \int xy'$, generally presupposes that $x'y, xy' \in L^1(\mathbb{R})$. Using a limit argument, however, we can make only the additional assumptions that the derivatives $x'$ and $y'$ are square-integrable [12, 13]. We can specify $x_n \to x$ and $y_n \to y$, where $\{x_n\}$ and $\{y_n\}$ are Schwarz space elements, for example.

### 10.5.3 Avoiding the Balian–Low Trap

Let us add a final footnote to the saga of Gabor's problem. It is possible to escape the negative conclusion of the Balian–Low theorem only by giving up on some of its suppositions. One of these suppositions is the exponential term in the windowed Fourier atoms. This is something that probably seems quite natural given all the work we have done with signal transforms with the complex exponential at their heart. The idea is to extract orthonormal bases with good time-frequency localization by using *sines and cosines* instead [12].

## 10.6 SUMMARY

The Gabor transform is the most accessible mixed-domain transform tool. It is a representative of a broader class of short-time (or windowed) Fourier transforms (STFT). These transforms invoke a tiling of the time-frequency plane with regions of equal size. The Gabor transform tiles have the minimal area. Tilings of the time-frequency plane are a powerful technique for discovering signal structure, and, developing wavelet theory in the next chapter, we will explore the concept further. In point of fact, equally sized tiles can be a difficulty when analyzing signals that contain feature of different extents and transients; the wavelet transform has time-frequency tiles of varying size, and it was first developed as a transient-capable alternative to the Gabor transform.

Thus, there are some practical and theoretical limitations to the Gabor transform and the STFT in general:

- The size of the signal structures that must be analyzed becomes problematic when the time-domain window has already been fixed for the transform analysis.
- Computationally, the method does not support frames based on windowed Fourier atoms unless the time-frequency density is sufficiently dense.

Natural and synthetic signals have time-limited frequency components. One of the important observations from Chapter 9's study of frequency-domain signal analysis is that standard Fourier transform tools sometimes do a poor job of identifying these localized oscillations. Our principal approach was to trim the source signal $x(t)$ with a symmetric, decaying window function. This technique time-limits, or windows, a signal before calculating its spectrum. There are many variants, depending on the window's shape. Windowing furnishes better estimates of a signal's spectrum, because it restricts the signal values to those over which the relevant oscillatory waveform features should appear.

The short-time Fourier transform extends this idea of signal windowing to a full transform. It lays out the frequency content of a signal according to the time that the oscillatory components appear. Discretized, the windowed Fourier transform presents a complete structural description of a signal. In Chapters 4 and 9, such constructions were at best ad hoc. Now we can produce a full graphical representation of signal frequency components and the time of their occurrence. Moreover, a rich mathematical theory supports the application of this structural tool.

Of the many feasible window shapes upon which we can found a time-limited Fourier transformation, the one which uses a Gaussian window is the Gabor transform. It is the most natural of the various STFTs, and we introduced it to lead off the chapter. The Gabor transform's Gaussian window function has optimal time and frequency locality—a result of the classic Heisenberg Uncertainty Principle.

Applications generally use the squared norm of the transformed signal, called the spectrogram. We discovered, moreover, that spectrogram performance is satisfactory for many signal analysis tasks. In particular, it has seen wide and largely successful application in speech recognition. It has been the basis for many applications that need time-limited descriptions of signal spectra. The spectrogram of the signal $x(t)$ relative to the window function $w(t)$ is the squared magnitude of the Fourier transform of the product: $|\mathcal{F}[s(t)]|^2 = |\mathcal{F}[x(t)w(t)]|^2$. This is a nonnegative real value. Applications can therefore compare or threshold spectrogram values in order to decide whether one frequency is more significant than another or whether an individual frequency is significant, respectively. With the spectrogram, of course, the application design may need to search through possible time locations as well as through possible frequency ranges when seeking local spectral components. That is, Fourier applications tend to be one-dimensional, in contrast to short-time Fourier applications, which are inherently two-dimensional in nature.

Virtuous in their locality, short-time Fourier transform methods improve upon the necessarily global Fourier transform, but they are not without their problems. The previous chapter found the spectrogram adequate for many important signal analysis tasks. It can perform poorly, however, when signals contain sharply varying frequencies, such as chirps, transients, or unconstrained frequency modulation. This behavior is mitigated in the short-time Fourier transform, but not completely removed. There is still the problem of selecting a window for the transform operation. And there is the fundamental limitation for discrete methods that the Balian-Low theorem enforces. Since their critically sampled collections cannot be frames, and hence cannot provide stable signal reconstruction, we are led to hope that the signal universe is made up of more than just windowed Fourier atoms.

### 10.6.1 Historical Notes

A recent history of time-frequency analysis by one of the principal contributors to the discipline, L. Cohen, is Ref. 47. It includes an extensive bibliography.

The original time-frequency signal analysis technique is the Wigner–Ville distribution. E. Wigner proposed it for application to quantum mechanics [28]. J. Ville used it to explicate the notion of instantaneous frequency for communication theory purposes [29]. The WVD does not rely on a separate window function for generating the transform, using instead a bilinear term involving the original signal. This independence from window selection is at once its strength and weakness. The WVD and its more modern variants have been widely studied and are quite powerful; under certain conditions these transforms are optimal detectors for frequency-modulated signals [48]. It has been used as the cornerstone of a complete approach to biological and computer vision, for example [32].

The WVD has come under critical scrutiny because of the problematic cross-terms that the transform produces [7]. Some conferences have witnessed spirited debates over this transform's strengths and weaknesses. There are a variety of approaches for reducing cross-term effects, and a number of researchers were already investigating them in the early 1980s. The main line of attack was given by P. Flandrin in 1984 [49].

The general theory of quadratic kernel-based transforms is due to L. Cohen [35]. He introduced the *Cohen class* of distributions for applications in quantum mechanics—an area that has stimulated many original contributions to time-frequency signal theory. Later, Wigner published the result that quadratic time-frequency representations, such as his namesake distribution, cannot be simultaneously non-negative and obey the Marginal Conditions.

The Gabor transform is the most easily accessible time-frequency transform, and this is due to the analytic tractability of the Gaussian window function. Gabor's 1946 paper studied sets of signal atoms—Gabor elementary functions—with optimal joint resolution in the time and frequency domains. Gabor applied the theory to acoustics [19] and communication theory [1]. Gabor's conjecture—that optimally localized time-frequency atoms of spatial and spectral sampling intervals satisfying $T\Omega = 2\pi$ could be a foundation for signal analysis—was seriously

undermined by the Balian–Low theorem. Such windowed Fourier atoms cannot comprise a frame; their signal reconstruction behavior is therefore unstable. Nevertheless, Gabor methods remain the mostly widely applied time-frequency transform.

Researchers in diverse areas—communications theory, speech recognition, seismic signal interpretation, image analysis, and vision research—have had a keen interest in the Gabor transform for many years. One surprise, in fact, issued from investigations into the behavior of neurons in the visual cortex of animals. Research showed that individual neurons respond to certain visual stimuli in ways that resemble the shapes of the real and imaginary parts of GEFs. Chapter 12 outlines these discoveries and provide references to the literature.

We now know from frame theory, largely developed by I. Daubechies and her coworkers [12, 25, 27] that frames of windowed Fourier atoms are possible for sufficiently dense time-frequency samplings. For many years, investigators pondered how to expand a signal with elementary functions based on a particular window function, such as the Gaussian. Sparse samplings preclude windowed Fourier frames, and at the Nyquist density they are only possible given poor time-frequency localization. Therefore, decomposing signals with windowed Fourier atoms was a major problem. The first solution was in fact given many years after Gabor's paper, by M. Bastianns [50, 51] using the Zak transform. Another strategy for finding expansion coefficients relied upon a neural network for their approximation [52]. Only recently have efficient algorithms for calculating the decomposition coefficients been disclosed [53].

The correct proof of the Balian–Low theorem eluded researchers for a number of years. The result was given independently by Balian [37] and Low [38]. Their proofs both contained the same technical gap, which was corrected several years later for the specific case of orthonormal bases [39] and later extended to frames [25, 40]. It is a hard-won result. Further research in this area produced a workaround for the Balian–Low theorem: Use sinusoids instead of exponentials for the atomic decomposition! Some examples of this approach are [54, 55].

### 10.6.2 Resources

Readers will find the following resources handy for working with time-frequency transforms:

- The Matlab and Mathematica commercial software packages, which we have used to generate many of the figures.
- The Time-Frequency ToolBox (TFTB), available over the web from CNRS in France; this public-domain software package, based on Matlab, contains a variety of tools for performing STFT, WVD, and other time-frequency signal transforms. We have used it for replicating the WVD analysis of the speech sample "Gabor."
- The small, but very educational, demonstration tool bundled with the treatise [8], the Joint Time-Frequency Analysis (JTFA) package. We have used JTFA to illustrate a number of STFT and WVD concepts in this chapter.

### 10.6.3 Looking Forward

Time-frequency transforms are problematic in certain applications, especially those with transients or local frequency information that defies any *a priori* demarcation of its frequency- and time-domain boundaries. Quadratic methods have better spectral resolution, but interference terms are sometimes hard to overcome. Finally, the Balian–Low theorem enforces a fundamental limitation on the joint time-frequency resolution capability of the windowed Fourier transforms.

This situation led to the discovery of another mixed-domain signal analysis tool—the wavelet transform, one of the great discoveries of mathematical analysis in the twentieth century. As we have already indicated, the wavelet transform uses a signal scale variable instead of a frequency variable in its tranform relation. This renders it better able to handle transient signal behavior, without completely giving up frequency selectivity. Readers seeking a popular introduction to wavelet theory, a review of the basic equations, and fascinating historical background will find Ref. 56 useful. A more mathematical treatment focusing on applications is Ref. 57. The next chapter introduces wavelets, and the final chapter covers both time-frequency and time-scale applications.

## REFERENCES


1. D3. Gabor, Theory of communication, *Journal of the Institute of Electrical Engineers*, vol. 93, pp. 429–457, 1946.
2. F. Hlawatsch and G. F. Boudreaux-Bartels, Linear and quadratic time-frequency signal representations, *IEEE SP Magazine*, pp. 21–67, April 1992.
3. L. Cohen, Introduction: A primer on time-frequency analysis, in *Time-Frequency Signal Analysis*, B. Boashash, ed., Melbourne: Longman Cheshire, pp. 3–42, 1992.
4. S. Qian and D. Chen, Joint time-frequency analysis, *IEEE Signal Processing Magazine*, pp. 52–67, March 1999.
5. H. G. Feichtinger and T. Strohmer, eds., *Gabor Analysis and Algorithms: Theory and Applications*, Boston: Birkhäuser, 1998.
6. B. Boashash, ed., *Time-Frequency Signal Analysis*, Melbourne: Longman Cheshire, 1992.
7. L. Cohen, *Time-Frequency Analysis*, Englewood Cliffs, NJ: Prentice-Hall, 1995.
8. S. Qian and D. Chen, *Joint Time-Frequency Analysis: Methods and Applications*, Englewood Cliffs, NJ: Prentice-Hall, 1996.
9. P. Flandrin, *Time-Frequency/Time-Scale Analysis*, San Diego, CA: Academic Press, 1999.
10. C. K. Chui, *An Introduction to Wavelets*, San Diego, CA: Academic Press, 1992.
11. S. Mallat, *A Wavelet Tour of Signal Processing*, San Diego, CA: Academic Press, 1998.
12. I. Daubechies, *Ten Lectures on Wavelets*, Philadelphia: Society for Industrial and Applied Mathematics, 1992.
13. E. Hernandez and G. Weiss, *A First Course on Wavelets*, Boca Raton, FL: CRC Press, 1996.
14. J. H. Ahlberg, E. N. Nilson, and J. L. Walsh, *The Theory of Splines and Their Applications*, New York: Academic Press, 1967.

15. R. H. Bartels, J. C. Beatty, and B. A. Barsky, *Splines for Use in Computer Graphics*, Los Altos, CA: Morgan Kaufmann, 1987.
16. M. Unser, A. Aldroubi, and M. Eden, B-spline signal processing: Part I—theory, *IEEE Transactions on Signal Processing*, vol. 41, no. 2, pp. 821–833, February 1993.
17. M. Unser, A. Aldroubi, and M. Eden, B-spline signal processing: Part II— efficient design and applications, *IEEE Transactions on Signal Processing*, vol. 41, no. 2, pp. 834–848, February 1993.
18. M. Unser, Splines: A perfect fit for signal and image processing, *IEEE Signal Processing Magazine*, vol. 16, no. 6, pp. 22–38, November 1999.
19. D. Gabor, Acoustical quanta and the theory of hearing, *Nature*, vol. 159, no. 4044, pp. 591–594, May 1947.
20. G. B. Folland, *Fourier Analysis and Its Applications*, Pacific Grove, CA: Wadsworth, 1992.
21. H. Dym and H. P. McKean, *Fourier Series and Integrals*, New York: Academic, 1972.
22. J. J. Benedetto, Uncertainty principle inequalities and spectrum estimation, in *Recent Advances in Fourier Analysis and Its Applications*, J. S. Byrnes and J. F. Byrnes, eds., Dordrecht: Kluwer, pp. 143–182, 1990.
23. G. B. Folland and A. Sitaram, The uncertainty principle: A mathematical survey, *Journal of Fourier Analysis and Applications*, vol. 3, pp. 207–238, 1997.
24. H. Weyl, *The Theory of Groups and Quantum Mechanics*, New York: Dutton, 1931; also, New York: Dover, 1950.
25. I. Daubechies, The wavelet transform, time-frequency localization and signal analysis, *IEEE Transactions on Information Theory*, vol. 36, no. 5, pp. 961–1005, September 1990.
26. M. A. Rieffel, Von Neumann algebras associated with pairs of lattices in Lie groups, *Mathematische Annalen*, vol. 257, pp. 403–418, 1981.
27. I. Daubechies, A. Grossmann, and Y. Meyer, Painless nonorthogonal expansions, *Journal of Mathematical Physics*, vol. 27, no. 5, pp. 1271–1283, May 1986.
28. E. Wigner, On the quantum correction for thermodynamic equilibrium, *Physical Review*, vol. 40, pp. 749–759, 1932.
29. J. Ville, Théorie et applications de la notion de signal analytique, *Cables et Transmission*, vol. 2A, pp. 61–74, 1948.
30. F. Hlawatsch and P. Flandrin, The interference structure of the Wigner distribution and related time-frequency signal representations, in *The Wigner Distribution—Theory and Applications in Signal Processing*, W. F. G. Mecklenbrauker, ed., Amsterdam: Elsevier, 1993.
31. T. A. C. M. Claasen and W. F. G. Mecklenbrauker, The Wigner distribution—a tool for time-frequency signal analysis; part I: Continuous-time signals, *Philips Journal of Research*, vol. 35, no. 3, pp. 217–250, 1980.
32. H. Wechsler, *Computational Vision*, San Diego, CA: Academic Press, 1990.
33. B. Boashash, Time-frequency signal analysis, in S. Haykin, ed., *Advances in Spectrum Estimation*, Prentice-Hall, 1990.
34. F. Hlawatsch, T. G. Manickam, R. L. Urbanke, and W. Jones, Smoothed pseudo-Wigner distribution, Choi–Williams distribution, and cone-kernel representation: ambiguity-domain analysis and experimental comparison, *Signal Processing*, vol. 43, pp. 149–168, 1995.

35. L. Cohen, Generalized phase-space distribution functions, *Journal of Mathematical Physics*, vol. 7. pp. 781–786, 1966.

36. E. Wigner, Quantum-mechanical distribution functions revisited, in *Perspectives in Quantum Theory*, W. Yourgrau and A. van der Merwe, eds., New York: Dover, 1971.

37. R. Balian, Un principe d'incertitude fort en theorie du signal ou en mecanique quantique, *C.R. Acad. Sci. Paris*, vol. 292, series 2, pp. 1357–1362, 1981.

38. F. Low, Complete sets of wave packets, in *A Passion for Physics—Essays in Honor of Geoffrey Chew*, C. DeTar, ed., Singapore: World Scientific, pp. 17–22, 1985.

39. G. Battle, Heisenberg proof of the Balian–Low theorem, *Letters on Mathematical Physics*, vol. 15, pp. 175–177, 1988.

40. I. Daubechies and A. J. E. M. Jannsen, Two theorems on lattice expansions, *IEEE Transactions on Information Theory*, vol. 39, no. 1, pp. 3–6, January 1993.

41. A. J. E. M. Janssen, The Zak transform: A signal transform for sampled time-continuous signals, *Philips Journal of Research*, vol. 43, no. 1, pp. 23–69, 1988.

42. C. E. Heil and D. F. Walnut, Continuous and discrete wavelet transforms, *SIAM Review*, vol. 31, pp. 628–666, December 1989.

43. B. Sz-Nagy, Expansion theorems of Paley–Wiener type, *Duke Mathematical Journal*, vol. 14, pp. 975–978, 1947.

44. R. J. Duffin and A. C. Schaeffer, A class of nonharmonic Fourier series, *Transactions of the American Mathematical Society*, vol. 72, pp. 341–366, 1952.

45. R. M. Young, *An Introduction to Nonharmonic Fourier Series*, New York: Academic Press, 1980.

46. Y. Meyer, *Wavelets and Operators*, Cambridge: Cambridge University Press, 1992.

47. L. Cohen, Time-frequency analysis, in L. Atlas and P. Duhamel, Recent developments in the core of digital signal processing, *IEEE Signal Processing Magazine*, vol. 16, no. 1, pp. 22–28, January 1999.

48. B. Barkat and B. Boashash, Adaptive window in the PWVD for IF estimation of FM signals in additive Gaussian noise, *Proceedings of the ICASSP*, vol. 3, pp. 1317–1320, 1999.

49. P. Flandrin, Some features of time-frequency representations of multi-component signals, *IEEE International Conference on Acoustics, Speech and Signal Processing*, ICASSP-84, San Diego, CA, pp. 41.B.4.1–41B.4.4, 1984.

50. M. Bastiaans, Gabor's expansion of a signal into gaussian elementary signals, *Optical Engineering*, vol. 20, no. 4, pp. 594–598, July 1981.

51. M. Bastiaans, On the sliding-window representation in digital signal processing, *IEEE Transactions on Acoustics, Speech, and Signal Processing*, vol. ASSP-33, pp. 868–873, August 1985.

52. J. Daugman, Complete discrete 2-D Gabor transforms by neural networks for image analysis and compression, *IEEE Transactions on Acoustics, Speech, and Signal Processing*, vol. 36, July 1988.

53. J. Yao, Complete Gabor transformation for signal representation, *IEEE Transactions on Image Processing*, vol. 2, no. 2, pp. 152–159, April 1993.

54. I. Daubechies, A simple Wilson orthonormal basis with exponential decay, *SIAM Journal of Mathematical Analysis*, vol. 22, pp. 554–572, 1991.

55. H. Malvar, Lapped transforms for efficient transform/subband coding, *IEEE Transactions on Acoustics, Speech, and Signal Processing*, vol. 38, pp. 969–978, 1990.

56. B. B. Hubbard, *The World According to Wavelets*, Wellesley, MA: A. K. Peters, 1996.
57. Y. Meyer, *Wavelets: Algorithms and Applications*, Philadelphia: SIAM, 1993.

## PROBLEMS

**1.** Suppose that $\mu, \sigma \in \mathbb{R}$, $\sigma > 0$; and $g(t) = g_{\mu,\sigma}(t)$ is the Gaussian signal with mean $\mu$ and standard deviation $\sigma$. Find the Gabor transform with respect to $g_{0,4}(t)$ of the following signals:
**(a)** $x(t) = \exp(6\pi jt)$
**(b)** $y(t) = \exp(-5\pi jt)$
**(c)** $z(t) = x(t) + y(t)$
**(d)** $\exp(j\omega_0 t)$
**(e)** $\sin(6\pi t)$
**(f)** $\cos(5\pi t)$

**2.** Using the notation of the first problem, find the Gabor transform with respect to $g_{0,1}(t)$ of the following signals:
**(a)** $x(t) = \delta(t)$, the Dirac delta
**(b)** $y(t) = \delta(t - 5)$
**(c)** $s(t) = x(t) + y(t)$
**(d)** $z(t) = \delta(t - r)$, where $r \in \mathbb{R}$

**3.** Using the notation of the first problem, find the Gabor transform with respect to $g_{0,1}(t)$ of the following signals:
**(a)** $x(t) = g_{2,4}(t)$
**(b)** $y(t) = g_{2,4}(t)\exp(6\pi jt)$
**(c)** $z(t) = g_{-2,4}(t)\cos(6\pi t)$
**(d)** $s(t) = g_{-2,4}(t)\sin(6\pi t)$

**4.** Let $x(t) = \exp(j\Omega t^2)$ be a linear chirp signal and $g(t) = g_{0,\sigma}(t)$ be the zero-mean Gaussian with standard deviation $\sigma > 0$.
**(a)** Find the Gabor transform $X_g(\mu, \omega)$ of $x(t)$.
**(b)** Show that the frequency at which $|X_g(\mu, \omega)|$ reaches a maximum value for $\mu = T$ is $\Omega_{\max} = 2T\Omega$.
**(c)** Let $\phi(t) = \Omega t^2$, so that $\phi(t)$ is the phase of the signal $x(t)$; show that the instaneous frequency of $x(t)$, $d\phi/dt$ evaluated at $t = T$, is precisely $\Omega_{\max}$ of part (b).

**5.** Suppose that $x(t)$ is an analog signal; $\mu, \sigma \in \mathbb{R}$, $\sigma > 0$; and $g(t) = g_{\mu,\sigma}(t)$ is the Gaussian signal with mean $\mu$ and standard deviation $\sigma$. Show the following:
**(a)** $g(t) \in L^2(\mathbb{R})$.
**(b)** If $x(t) \in L^2(\mathbb{R})$, then $x(t)g(t) \in L^2(\mathbb{R})$ and the Gabor transform of $x(t)$, $X_g(\mu, \omega)$ exists.

**(c)** Show that if $x(t) \in L^2(\mathbb{R})$, then its Gabor transform with respect to the window function $g(t)$ is the inner product of $x(t)$ and the Gabor elementary function $g(t)\exp(j\omega t)$.

**(d)** Find the norm of $g(t)$ in $L^2(\mathbb{R})$: $\|g(t)\|_2$.

**6.** With the notation of Problem 1, show the following:

**(a)** If $x(t) \in L^1(\mathbb{R})$, then $x(t)g(t) \in L^1(\mathbb{R})$ also.

**(b)** If $x(t) \in L^1(\mathbb{R})$, then $X_g(\mu, \omega)$ exists.

**(c)** Find an upper bound for $\|X_g(\mu, \omega)\|_1$, the $L^1(\mathbb{R})$ norm of $X_g(\mu, \omega)$.

**7.** Let $y(t) = g(t)\exp(j\omega_0 t)$, using the notation of Problem 1.

**(a)** Write the sinusoidal signal, $\sin(\omega_0 t)$, as a sum of exponentials and sketch its spectrum using Dirac delta functions.

**(b)** Using the Sifting Property of the Dirac delta, calculate $Y(\omega)$.

**(c)** Sketch the magnitude spectrum $|Y(\omega)|$ and the phase spectrum $\arg[Y(\omega)]$.

**8.** If $w(t)$ is a window function and $v(t) = w(t + t_0)$. Define the center $C_w$ and radius of $\rho_w$ of $w(t)$ by

$$C_w = \frac{1}{\|w\|_2^2} \int_{-\infty}^{\infty} t|w(t)|^2 dt, \tag{10.191}$$

$$\rho_w = \left[\frac{1}{\|w\|_2^2} \int_{-\infty}^{\infty} (t - C_w)^2 |w(t)|^2 dt\right]^{\frac{1}{2}}. \tag{10.192}$$

**(a)** Show that $v(t)$ is a window function also.

**(b)** Show $C_v = C_w - t_0$.

**(c)** If $W = \mathcal{F}w$ and $V = \mathcal{F}v$ are the Fourier transforms of $w$ and $v$, respectively, and $W$ and $V$ are window functions, then $C_W = C_V$.

**(d)** $\rho_v = \rho_w$.

**(e)** If $x(t) = \exp(-jC_W t)w(t + C_w)$, then $C_x = C_X = 0$ and $\rho_x = \rho_w$.

**9.** Let $w(t)$ be a window function. Show the following:

**(a)** $s(t) = (1 + |t|)^{-1} \in L^2(\mathbb{R})$.

**(b)** $v(t) = (1 + |t|)w(t) \in L^2(\mathbb{R})$.

**(c)** Use the Schwarz inequality for analog Hilbert spaces (Chapter 3) and the previous two results to show that $w(t) \in L^1(\mathbb{R})$.

**(d)** Again using the Schwarz inequality, show that $t^{1/2}w(t) \in L^2(\mathbb{R})$.

**10.** This problem explores how our definitons of center and radius accord with the mean and standard deviation of a Gaussian pulse.

**(a)** Calculate the center and radius of $g(t) = g_{\mu,\sigma}(t)$, the Gaussian with mean $\mu$ and standard deviation $\sigma$. For instance, for $\rho_x$ we find

$$\int_{-\infty}^{\infty} t|g(t)|^2 dt = \int_{-\infty}^{\infty} \frac{t}{\sigma^2 2\pi} e^{-\frac{(t-\mu)^2}{\sigma^2}} dt. \tag{10.193}$$

**(b)** Calculate the center and radius of the other standard window functions: the rectangular, triangular, Hanning, Hamming, and Blackman windows.

**(c)** Calculate the center and radius of the $B$-spline windows, $\beta_n(t)$.

**11.** Let $w(t) \in L^2(\mathbb{R})$ and define the signal $x(t)$ by

$$x(t+k) = (-1)^k \overline{w(t-k-1)}, \tag{10.194}$$

where $t \in [0, 1)$ and $k \in \mathbb{Z}$. Show the following:

**(a)** $x \in L^2(\mathbb{R})$

**(b)** $\|x\|_2 = \|w\|_2$

**(c)** $\|x\|_2 \neq 0$

**12.** Let $x(t) \in L^2(\mathbb{R})$, and $x'(t) \notin L^2(\mathbb{R})$. Show that $\rho_X = \infty$. [*Hint*: Use Parseval's theorem for the radial Fourier transform and the formula for $\mathcal{F}[x'(t)](\omega)$.]

**13.** Consider the two-dimensional $L^2(\mathbb{R}^2)$ signals $x(s, t)$, or *images*, that satisfy

$$\int_{-\infty}^{\infty}\int_{-\infty}^{-\infty} |x(s,t)|^2 \, ds\,dt < \infty. \tag{10.195}$$

**(a)** Show that $L^2(\mathbb{R}^2)$ is a vector space: it is closed under sums and scalar multiplication, and each element has an additive inverse.

**(b)** What is the zero element of $L^2(\mathbb{R}^2)$? Is it unique? Explain how to rectify this difficulty by establishing equivalence classes of images $[x] = \{y \in L^2(\mathbb{R}^2)$: $x(s, t) = y(s, t)$ for almost all $(s, t) \in \mathbb{R}^2\}$. Define vector addition of equivalence classes by $[x] + [y] = [z]$, where $z = x + y$. Define scalar multiplication analogously. Show that this definition makes sense.

**(c)** Define a norm on $L^2(\mathbb{R}^2)$ by

$$\left[\int_{-\infty}^{\infty}\int_{-\infty}^{-\infty} |x(s,t)|^2 \, ds\,dt\right]^{\frac{1}{2}} = \|x\|_{2,\,L^2(\mathbb{R}^2)}. \tag{10.196}$$

Show that $\|x\|$ in (10.196) is indeed a norm: $\|x\| > 0$, unless $x(t)$ is zero almost everywhere; $\|ax\| = |a| \cdot \|x\|$; and $\|x\| + \|y\| \geq \|x + y\|$.

**(d)** Show that $L^2(\mathbb{R}^2)$ with norm (10.196) is a Banach space; that is, every Cauchy sequence of finite-energy images converges to a finite energy image.

**(e)** If $x(s, t)$ and $y(s, t)$ are in $L^2(\mathbb{R}^2)$, then we define their inner product by

$$\langle x, y\rangle_{L^2(\mathbb{R}^2)} = \int_{-\infty}^{\infty}\int_{-\infty}^{-\infty} x(s, t)\overline{y(s, t)}\, ds dt\,. \tag{10.197}$$

Show that $\langle x, y\rangle$ is an inner product space: $\langle x + y, z\rangle = \langle x, y\rangle + \langle x, z\rangle$; $\langle ax, y\rangle = a\langle x, y\rangle$; $\langle x, x\rangle \geq 0$; $\langle x, x\rangle = 0$ if and only if $x(t) = 0$ almost everywhere; and $\langle x, y\rangle = \overline{\langle y, x\rangle}$;

**(f)** Show that $L^2(\mathbb{R}^2)$ is a Hilbert space.

**14.** Prove the Parseval theorem for the short-time Fourier transform. Suppose $x(t)$, $y(t) \in L^2(\mathbb{R})$; suppose $w(t)$ is a window function; and let $X_w(\mu, \omega)$ and $Y_w(\mu, \omega)$ be the STFTs of $x(t)$ and $y(t)$, respectively, based on windowing with $w(t)$. Then

$$2\pi\|w\|_2^2\langle x, y\rangle = \int_{-\infty}^{\infty}\int_{-\infty}^{\infty} X_w(\mu, \omega)\overline{Y_w(\mu, \omega)}\, d\omega d\mu = \langle X_w, Y_w\rangle_{L^2(\mathbb{R}^2)}\,. \tag{10.198}$$

**15.** Prove the Plancherel formula for the short-time Fourier transform. Let $x(t) \in L^2(\mathbb{R})$, let $w(t)$ be a window function, and let $X_w(\mu, \omega)$ be the STFT of $x(t)$. Then

$$\|x\|_2 = \sqrt{2\pi}\frac{\|X_g(\mu, \omega)\|_{2, L^2(\mathrm{R}^2)}}{\|g\|_2}\,. \tag{10.199}$$

**16.** Prove the inversion formula for the short-time Fourier transform. Suppose $x(t) \in L^2(\mathbb{R})$, suppose $w(t)$ is a window function, and let $X_w(\mu, \omega)$ be the STFT of $x(t)$. Then for all $a \in \mathbb{R}$, if $x(t)$ is continuous at $a$, then

$$x(a) = \frac{1}{(2\pi\|w\|_2^2)}\int_{-\infty}^{\infty} X_w(\mu, \omega)w(a)e^{j\omega a}\, d\omega d\mu\,. \tag{10.200}$$

**17.** Provide an example of a signal $x(t) \in L^2(\mathbb{R})$ that fails to satisfy the special condition we assumed in the first part of the Uncertainty Principle's proof:

$$\lim_{t \to \infty} \sqrt{|t|}\,|x(t)| = 0\,; \tag{10.201}$$

[*Hint*: Define $x(t)$ so that $x(n) = \varepsilon > 0$ on the integers $\mathbb{Z}$.]

**18.** Restate and prove the Uncertainty Principle for the Hertz Fourier transform:

$$X(\omega) = \int_{-\infty}^{\infty} x(t)e^{-2\pi j\omega t}\, dt\,. \tag{10.202}$$

**19.** Let us derive a one-dimensional form of Heisenberg's Uncertainty Principle. Following the quantum mechanical viewpoint, we assume that the position and momentum describe the state of an electron, and a probability density function $|\phi(x)|^2$ governs its position. The probability that the particle is on the closed real interval $a \le x \le b$ is

$$\int_a^b |\phi(x)|^2 dx, \tag{10.203}$$

where we must have $\|\phi(x)\|_2 = 1$ so that $\phi$ is indeed a density. Define a momentum state function $\psi(\omega)$ as follows:

$$\psi(\omega) = \frac{\Phi\left(\frac{\omega}{h}\right)}{\sqrt{2\pi h}}, \tag{10.204}$$

where $\Phi(\omega)$ is the radial Fourier transform of $\phi(x)$, and $h$ is a constant (Planck's).

**(a)** Show that $\|\psi(\omega)\|_2 = 1$, so that $\psi$ is a density also.

**(b)** Let $\Delta_\phi = 2\rho_\phi$ and $\Delta_\psi = 2\rho_\psi$ be the diameters of $\phi$ and $\psi$, respectively, where $\rho$ is the radius (10.192). Show that $\Delta_\phi \Delta_\psi \ge 2h$.

**20.** Suppose we are interested in time-frequency localization and thus require a short-time Fourier transform based on a window function $w(t)$ such that $W(\omega)$ is also a window function.

**(a)** Which of the standard window functions, if any, in Table 10.2 supports this requirement?

**(b)** Show that a Gaussian works.

**(c)** Show that any B-spline $\beta_n(t)$ of order $n \ge 1$ works too.

**21.** This problem explores the idea of changing the window width normalization for the Gabor transform. We defined the Gabor transform for an arbitrary Gaussian window $g_{0,\sigma}(t)$ of zero mean and arbitrary standard deviation $\sigma > 0$:

$$X_g(\mu, \omega) = \frac{1}{\sigma\sqrt{2\pi}} \int_{-\infty}^{\infty} x(t) e^{-\frac{(t-\mu)^2}{2\sigma^2}} e^{-j\omega t} dt. \tag{10.205}$$

**(a)** Suppose we are Gabor transforming with a window function $g(t)$ with $\|g(t)\|_1 = 1$, where $\|\cdot\|_1$ is the norm in the Banach space of absolutely integrable signals $L^1(\mathbb{R})$. What form do the following Gabor tranform properties take in this case: the inverse theorem, the Plancherel theorem, and the Parseval theorem?

**(b)** Suppose instead that we have used a Gaussian $g(t)$ with $\|g(t)\|_2 = 1$. Now what form do these same properties take?

**22.** Try to prove the bounds theorem for windowed Fourier frames without resorting to Zak transform results. Let $w(t) \in L^2(\mathbb{R})$ and its windowed Fourier

atoms $\{w_{m,n}(t) = e^{jn\Omega t}w(t - mT)$: $m, n \in \mathbb{Z}\}$, constitute a frame. Show that $A \leq \frac{2\pi}{\Omega T}\|w\|_2^2 \leq B$, where $A$ and $B$ are the lower and upper frame bounds, respectively.

**23.** Suppose we select the following window function: $w(t) = (1 + t^2)^{-1}$.

**(a)** Show that $w(t)$ is bounded (in $L^\infty(\mathbb{R})$) and absolutely integrable (in $L^1(\mathbb{R})$).

**(b)** Let $T > 0$ be the time-domain sampling interval for discretizing the STFT with respect to $w(t)$. Show that $\Sigma|w(t - kT)|^2$ has an upper and lower bound.

**(c)** Show that we can find a frequency-domain sampling interval $\Omega > 0$ such that $\{w_{m,n}(t) = e^{jn\Omega t}w(t - mT)$: $m, n \in \mathbb{Z}\}$ are a frame. How small must $\Omega$ be?

**(d)** Repeat the above steps for the Gaussian window $w(t) = g_{\mu,\sigma}(t)$, the Gaussian with mean $\mu$, and standard deviation $\sigma$.

**24.** Let $x(t) \in L^2(\mathbb{R})$ and $X_{\mathrm{WV}}(\mu, \omega)$ be its Wigner–Ville distribution. Show the following:

**(a)** If $s(t) = x(t - a)$, then $S_{\mathrm{WV}}(\mu, \omega) = X_{\mathrm{WV}}(\mu - a, \omega)$.

**(b)** If $y(t) = e^{j\theta t}x(t)$, then $Y_{\mathrm{WV}}(\mu, \omega) = X_{\mathrm{WV}}(\mu, \omega - \theta)$.

**(c)** If $y(t) = ax(t)$, then $Y_{\mathrm{WV}}(\mu, \omega) = |a|^2 X_{\mathrm{WV}}(\mu, \omega)$.

**(d)** If $y(t) = x(t/a)$ and $a > 0$, then $Y_{\mathrm{WV}}(\mu, \omega) = aX_{\mathrm{WV}}(\mu/a, a\omega)$.

**(e)** If $y(t) = \exp(j\theta t^2)x(t)$, then $Y_{\mathrm{WV}}(\mu, \omega) = X_{\mathrm{WV}}(\mu, \omega - 2\theta\mu)$.

**25.** Let $x(t) \in L^2(\mathbb{R})$, $X(\omega)$ be its Fourier transform, and $X_{\mathrm{WV}}(\mu, \omega)$ be its WVD. Show the following symmetry properties:

**(a)** If $x(t)$ is real-valued and $X_{\mathrm{WV}}(\mu, \omega) = X_{\mathrm{WV}}(\mu, -\omega)$, then $X(\omega)$ is even: $X(\omega) = X(-\omega)$.

**(b)** If $X_{\mathrm{WV}}(-\mu, \omega) = X_{\mathrm{WV}}(\mu, \omega)$ and $X(\omega)$ is real-valued, then $x(t)$ is even.

**26.** Let $x(t) \in L^2(\mathbb{R})$, $w(t)$ be a window function, and let $X_{S,w}(\mu, \omega)$ be the spectrogram of $x(t)$ with respect to $w(t)$. Develop a table of properties for $X_{S,w}(\mu, \omega)$ analogous to Table 10.3.

**27.** Let $x(t)$ and $y(t)$ be finite energy analog signals and let $X_{\mathrm{WV},y}(\mu, \omega)$ be the cross Wigner–Ville distribution of $x(t)$ with respect to $y$:

$$X_{\mathrm{WV},\,y}(\mu, \omega) = \int_{-\infty}^{\infty} x\left(\mu + \frac{t}{2}\right)\overline{y\left(\mu - \frac{t}{2}\right)}e^{-j\omega t}\,dt. \tag{10.206}$$

**(a)** Show that $[X_{\mathrm{WV},y}(\mu, \omega)]^* = Y_{\mathrm{WV},x}(\mu, \omega)$.

**(b)** If $s(t) = x(t) + y(t)$, show then that $S_{\mathrm{WV}}(\mu, \omega) = X_{\mathrm{WV}}(\mu, \omega) + Y_{\mathrm{WV}}(\mu, \omega) + 2\mathrm{Real}[X_{\mathrm{WV},y}(\mu, \omega)]$.

**(c)** What is the relation between the cross Wigner–Ville distribution and the short-time Fourier transform?

**28.** Suppose $x(t) = e^{jat}$. Show that $X_{\mathrm{WV}}(\mu, \omega) = (2\pi)^{-1}\delta(\omega - a)$.

**29.** Let $g(t) = g_{\alpha,\sigma}(t)$, the Gaussian of mean $\alpha$ and standard deviation $\sigma > 0$. Show that

$$X_{WV}(\mu, \omega) = \frac{e^{-(\sigma\omega)^2}}{2\pi^{3/2}\sigma} e^{-\left(\frac{\mu-\alpha}{\sigma}\right)^2}. \tag{10.207}$$

**30.** Let $s(t) = u(t+1) - u(t-1)$. Show that

$$S_{\mathrm{WV}}(\mu, \omega) = \frac{2s(\mu)}{\omega} \sin(2\omega(1-|\mu|)). \tag{10.208}$$

**31.** Let $x(t) \in L^2(\mathbb{R})$, let $X(\omega)$ be its Fourier transform, and let $X_{\mathrm{WV}}(\mu, \omega)$ be its WVD. As a function of $\mu$, show that $X_{\mathrm{WV}}(\mu, \omega)$ has the following Fourier transform:

$$\mathcal{F}[X_{\mathrm{WV}}(\mu, \omega)](\theta) = \int_{-\infty}^{\infty} X_{\mathrm{WV}}(\mu, \omega) e^{-j\mu\theta} d\mu = X\left(\omega + \frac{\theta}{2}\right)\overline{X\left(\omega - \frac{\theta}{2}\right)}. \tag{10.209}$$

**32.** Complete the proof of the bounds theorem for windowed Fourier frames. Let $w(t) \in L^2(\mathbb{R})$ and suppose $\{w_{m,n}(t) = e^{2\pi jnt} w(t-m)\colon m, n \in \mathbb{Z}\}$ is a frame, with lower and upper bounds $A$ and $B$, respectively. Then for almost all $s$ and $\omega$ we have $|(\mathcal{Z}w)(s, \omega)|^2 \le B$, where $\mathcal{Z}w$ is the Zak transform (parameter $a = 1$) of $w$:

$$(\mathcal{Z}x)(s, \omega) = \sum_{k=-\infty}^{\infty} x(s-k) e^{2\pi j\omega k}. \tag{10.210}$$

**33.** Prove the Zak transform derivative lemma: if $x(t), x'(t) \in L^2(\mathbb{R})$, then

$$\mathcal{Z}(x'(t))(s, \omega) = \frac{\partial}{\partial s}(\mathcal{Z}x)(s, \omega). \tag{10.211}$$

Justify interchanging the summation and differentiation operations when differentiating the Zak transform sum with respect to $s$.

**34.** Complete the proof of the Zak transform derivative characterization. Let $x(t) \in L^2(\mathbb{R})$; $X(\omega) = \mathcal{F}[x(t)]$ be its Fourier transform; and $\mathcal{Z}$ be the Zak transform $\mathcal{Z}$: $L^2(\mathbb{R}) \to L^2(S)$, where $S$ is the unit square $[0, 1] \times [0, 1]$. Then the following are equivalent:

**(a)** $X(\omega)$ is a window function.

**(b)** $x'(t) \in L^2(\mathbb{R})$.

**(c)** $\frac{\partial}{\partial s}(\mathcal{Z}x)(s, \omega) \in L^2[S]$.

**35.** Let $w(t) \in L^2(\mathbb{R})$; $F = \{w_{m,n}(t) = e^{\Omega jnt} w(t - mT)\colon m, n \in \mathbb{Z}\}$ be a frame; let $\mathcal{Z}\colon L^2(\mathbb{R}) \to L^2(S)$ be the Zak transform, where $S = [0, 1] \times [0, 1]$; and let $\tilde{w} = (\mathcal{T}^*\mathcal{T})^{-1} w = \mathrm{S}^{-1} w$, where $\mathcal{T}$ is the frame operator for $F$. If $k \in \mathbb{Z}$, show that

**(a)** Translations by $k$ and the operator $\mathcal{S}$ commute:

$$(\mathcal{S}w)(t-k) = \mathcal{S}(w(t-k)). \tag{10.212}$$

**(b)** Modulations are also commutative under $S$ transformation:

$$e^{2\pi jkt}(\mathcal{S}w(t)) = \mathcal{S}(e^{2\pi jkt}w(t)). \tag{10.213}$$

**(c)** $((\mathcal{T}^*\mathcal{T})^{-1}w)_{m,n} = (\mathcal{T}^*\mathcal{T})^{-1}(w_{m,n})$.

**(d)** $\langle \tilde{w}, w_{m,n} \rangle = \begin{cases} 1 & \text{if } m = n = 0, \\ 0 & \text{otherwise.} \end{cases}$

**(e)** Show that

$$\langle tw(t), \tilde{w}_{m,n}(t) \rangle = \langle w_{-m,-n}(t), t\tilde{w}(t) \rangle. \tag{10.214}$$

by expanding the inner product integral.

**36.** Develop an experiment with either real or synthetic data showing that an improperly chosen STFT window width can render the transform information useless for intepreting signal evolution through time.

**37.** Develop an experiment with either real or synthetic data showing the presence of cross-terms in the WVD of a signal. Consider the analysis of a linear chirp signal. Devise an algorithm to estimate the rate of change in frequency over time. How do the WVD's cross terms affect this algorithm? Suppose that a quadratic chirp is given, and explore the same issues.

**38.** Obtain or generate signals have significant transient phenomena in addition to localized frequency components. Develop experiments comparing the STFT and the WVD for the purposes of analyzing such signals.

**39.** Define the following Hertz version of the spectrogram:

$$X_{S,w}(\mu, f) = \left| \int_{-\infty}^{\infty} x(t)w(t-\mu)e^{-2\pi jft}dt \right|^2. \tag{10.215}$$

**(a)** Show that

$$\int_{-\infty}^{\infty} X_{S,w}(\mu, f)df = \int_{-\infty}^{\infty} |s(t)w(t-\mu)|^2 dt. \tag{10.216}$$

**(b)** Also show

$$\int_{-\infty}^{\infty} X_{S,w}(\mu, f)d\mu = \int_{-\infty}^{\infty} |X(u)W(u-f)|^2 du. \tag{10.217}$$

**(c)** Show that the Hertz spectrogram does not satisfy the either the time or frequency marginal conditions.

**(d)** Define a Hertz version of the WVD.

**(e)** Show that the Hertz WVD satisfies the ideal Marginal Conditions.